A STUDY OF NEEDLE ICE EVENTS AT VANCOUVER, CANADA

1961 - 1968

by

Samuel I. Outcalt

A THESIS SUBMITTED IN PARTIAL FULFILMENT OF

THE REQUIREMENTS FOR THE DEGREE OF

DOCTOR OF PHILOSOPHY

to the department of

GEOGRAPHY

We accept this thesis as conforming to the

required standard

THE UNIVERSITY OF BRITISH COLUMBIA

April 1970

In presenting this thesis in partial fulfilment of the requirements for an advanced degree at the University of British Columbia, I agree that the Library shall make it freely available for reference and Study. I further agree that permission for extensive copying of this thesis for scholarly purposes may be granted by the Head of my Department or by his representatives. It is understood that copying or publication of this thesis for financial gain shall not be allowed without my written permission.

Department of Geography

The University of British Columbia
Vancouver 8, Canada

Date 9 March 70

Abstract

Prediction of needle ice events requires an understanding of energy and water transfer between the atmosphere and the soil. A project in southwestern British Columbia was conducted during 1961-1968 for the purposes of (1) constructing a general model of needle ice growth, (2) characterizing the processes which combine to produce ice needle events, and (3) explaining the variations in ice needle morphology.

The problem was approached by (1) comparing environmental conditions on event and non-event nights, (2) identifying the heat sinks which produce surface cooling and fusion, (3) determining the range of the variability in soil water and heat flow properties produced by changing soil water content, (4) statistically analyzing the event, non-event record, and (5) determining the time dependence of the components of the energy-water transfer system during needle ice growth.

Statistical and physical analysis demonstrated the overriding control of the thermal and evaporative heat sinks in needle ice growth and indicated that the equivalent radiant temperature of the night sky must drop below -15°C before a needle ice event is probable. Further, it was demonstrated that after ice crystals form at the surface the magnitude of the surface heat sink (equilibrium surface temperature) and the soil water content control the depth of the normally frozen soil cap above the needles and the spatial homogeneity of needle growth. The

statistical study of the event record produced a simple dew point-cloud cover empirical model for event prediction and a listing of favorable-unfavorable conditions for needle ice growth. A general model for needle ice growth was developed indicating the relationship between surface equilibrium temperature and soil water tension on the growth and the spatial temporal homogeneity of needle growth.

Contributions to general micrometeorology were made by demonstrating the utility of combined measurement of surface temperature soil water tension and soil heave in the analysis of soil structural evolution during diurnal freeze-thaw cycles. Specifically, the anomalous positive "bump" which frequently occurs in nocturnal surface temperature curves was shown to be coincident with a thermally driven flux of warm subsoil water toward the surface and a sudden increase in soil water tension was demonstrated to occur at the time when heave (ice segregation) began. Finally specific problems which appear both tractable and rewarding were formulated for future investigators.

ACKNOWLEDGEMENTS

The author wishes to acknowledge the assistance, aid and determination of the members of his committee. These members are:

Professor J. R. Mackay, Chairman	(Geography)
Dr. Jan DeVries	(Soil Science)
Dr. M. Miyake	(Oceanography)
Dr. J. V. Ross	(Geology)
Dr. V. C. Brink	(Plant Science)
Dr. G. R. Gates	(Geography)
Dr. W. H. Mathews	(Geology)

In addition valuable consultation was given by Dr. M. A. Melton (statistical analysis), Dr. P. J. Williams (Canadian National Research Council--soil physics), and Mr. J. W. Sayward (U.S. Cold Regions Research & Engineering Labs--soil physics).

Lastly Messrs. Don Pearce (Plant Science Field Station) and Wolfram Schmitt (Engineering Shops) for valuable assistance in equipment maintenance and design.

The author is indebted to the University and the National Research Council for providing funds for the project.

FRONTISPIECE. Needle ice in a backyard garden, Vancouver, British Columbia.

TABLE OF CONTENTS

CHAPTER PAGE

LIST OF TABLES

LIST OF FIGURES

NOTATION FOR PHYSICAL ARGUMENTS

(all units c.g.s. unless noted in text)

A	austausch coefficient
B	net radiation
C	volumetric heat capacity
E	volume of expelled water
F	fusion rate
K_{sv}	Sverdrup exchange coefficient
K	thermal conductivity
K_o	von Karman constant
L	sensible heat flux
P	pressure
S	soil heat flux
T	temperature
U	velocity
V	latent heat flux
a,m	regression parameters
e	vapor pressure
h	soil heave
q	specific humidity
r_c	critical pore radius
r_v	heat of vaporization
r_f	heat of fusion
t	elapsed time
x	volume fraction
z	distance from surface
z_o	roughness parameter
α	thermal diffusivity
δ	temperature range
ρ	density
σ	Stefan-Boltzman constant. & interfacial energy
Υ	soil water tension
ω	angular velocity

Subscripts:

a	air
0	surface
s	soil
10	distance from surface
i	initial value & ice
or	organic
m	mineral
w	water
f	frozen
x	critical value

CHAPTER I.

INTRODUCTION

The Problem

Definition. Needle ice, vertical filaments of ice approximately 1 $mm.^2$ in cross section and up to 8 cm. in length, are formed by the segregation of ice near the ground surface on calm clear "winter" evenings, from late October to early April, when the soil surface has initially been unfrozen (see Frontispiece). Segregation is the increase in water (ice) content in a soil layer produced by water migration to the freezing plane during ice formation (Jumikis, 1966). Needle ice is referred to in the European literature as Haarfrost, Haareis, Nedeleis, Stengeleis, Eisfilaments, Effloreszeneis, Barfrost etc... In the United States it is usually called mushfrost, ice filaments or ice columns. The Swedish term "pipkrake" has enjoyed wide international usage (Hamelin and Cook, 1967; Troll, 1944).

Background. The general climatological conditions, which lead to the growth of needle ice, have been understood since the late 1930's because of the exceptional investigations of a group of Japanese school girls (Fujita et. al., 1937), who noted the importance of the clear night sky as a major heat sink for the soil surface and recognized the necessity for unfrozen near-saturated soil conditions. The problem has, since that time, been studied quite extensively in a qualitative manner, but there have been only limited attempts to treat the total environment of needle ice growth from a quantitative viewpoint (Konko-Tatutaro et. al., 1957; Kinosita et. al., 1967).

Statement of Problem. It is the purpose of this thesis (1) to construct a general model for needle ice growth, (2) to gain a fundamental knowledge of the processes which combine to produce a needle ice event, and (3) to use this knowledge as a vehicle for the analysis of the morphology of needle ice growths and their associated geomorphic processes.

Uniqueness of this Study. The work reported in this study represents the most detailed field examination of natural needle ice growth known to the author. Special attention is devoted to the particular conditions of needle ice growth at the Point Grey Campus of the University of British Columbia in Vancouver where a unique record of needle ice events has been compiled from 1962 onward.

Importance of this Study. Needle ice formation and ablation are of interest to both soil and plant scientists because of the downslope, movement, ground patterning, and damage to plant materials which often accompany needle ice events. In addition to being an interesting variant of the more general segregation ice (frost heave) and frost warning applied research areas the theoretical implications of the study are also promising. Due to the restricted time scale and limited vertical dimensions of a needle ice event, it may be possible to gain some insight into quite similar, but less accessible, physical processes which have spatial and temporal dimensions many orders of magnitude larger than needle ice deposits. It is, therefore, considered that a detailed investigation of the phenomena of needle ice growth may yield numerous benefits through analogy. Lastly, an investigation of this type provides a trial arena for methods of instrumentation and analysis, which can be transferred to related phenomena.

Organization of Thesis

This thesis is designed to illustrate new information concerning the process and environment of needle ice growth.

The first chapter in the body of the manuscript, Chapter II., discusses the broad pattern of the needle ice event record and climatology of the study site at the University of British Columbia in conjunction with the interpretation soil temperature-time curves produced during nocturnal cooling. In Chapter III. the nature and relative magnitude of the heat sources, including radiation fog, and sinks available to the soil surface during needle ice growth will be examined. This information will establish the basic framework for further consideration of atmospheric processes during needle ice events. In a like manner, a similar framework is developed for the soil in Chapter IV. which reports the results of laboratory determinations of the particle size distribution, water retention and flow properties, and the thermal characteristics of the soil at the study site.

Having provided this background data, the past even record is examined statistically to discover the broad environmental conditions which lead to needle ice events and to produce a model for event prediction (Chapter V.).

Chapter VI. is a discussion of the principal results of field observations carried out during the needle ice season of 1967-1968. In this chapter some of the components of the needle ice growth system are examined in detail and a general model for needle ice growth is developed. The work in this chapter leads directly to the conclusion and recommendations which are the final items in the body of the thesis.

Review of Present Knowledge

Needle Ice Studies. As stated earlier, the main facts of needle ice growth were demonstrated by a group of Japanese school girls (Fujita et. al., 1937). These basic facts of needle ice growth are as follows: (1) the water source for the ice needles is the soil; (2) the major heat sink during soil freezing is the clear-cold night sky; (3) the rate of needle growth is controlled by the availability of water at the freezing plane; (4) steep soil temperature gradients increase growth rates; (5) the most susceptible soils are loosely packed low density members of the loam group.

The most recent and comprehensive treatment of the needle ice problem is that of Sayward (1966), who grew needle ice in the laboratory to test the heave susceptibility of various soils and the influence of additives on the ice segregation process. This work is of considerable interest because field observation and small scale freezing tests were demonstrated to be the most reliable methods of testing the needle ice susceptibility of soils.

These authors indicate that the following sequence is necessary for a needle ice event: (1) soil surface unfrozen; (2) the formation of an adequate heat sink to cool the soil surface; (3) under-cooling the soil surface to the nucleation temperature of the soil water; (4) the stabilization of the freezing plane near the soil surface as a result of ice segregation.

Atmospheric Processes. The first three items are essentially climatically controlled conditions which have been studied under such headings as "energy exchange during the night hours at..." or "nocturnal energy balance

at...etc. These studies of nocturnal energy budget, during periods of various intensities of radiation cooling, are reported by Geiger (1965) and Sutton (1953); however, none specify simultaneous needle ice growth or the absence of it. For this reason, the measurement of the energy transfer environment during needle ice growth as a means of locating and estimating the relative magnitude of heat sources and sinks was given a high priority in the author's field program.

Specific investigations of radiation fog, a feedback mechanism which limits the strength of radiation cooling, have been carried out experimentally and theoretically by Davis (1957) in the eastern United States and empirically by Belhouse (1961) at Vancouver International Airport. Sutton (1953) reported numerous physical and empirical models for the prediction of night minimum temperatures.

Soil Processes. The fourth item is essentially the formation and stabilization of an active plane of ice segregation near the soil surface. The mechanism of ice segregation has been studied by numerous investigators both in theory (Takagi, 1965) and experimentally (Williams, 1968). An evaluation of the effects of soil texture on ice structure was carried out by Byrnes (1951) and a study of the influence of the freezing rate on frost action reported by Penner (1960). Gradwell (1963) has recently completed a study of nocturnal heat losses from soils having varied bulk densities. An excellent review of current thinking and research on the problem was presented by Penner (1960). Williams (1966a) demonstrated that soil pore geometry and water tension at the freezing plane will determine if ice segregation, (stabilization of the freezing plane) or normal freezing, (continued descent of the freezing plane) shall occur at a given level in

the soil. For this reason the measurement of soil water tension was included in the author's field program.

Related Topics. Other topics such as the crystallography of needle ice (Steinemann, 1953) and the possible role of needle ice in the martian wave of darkening (Otterman and Browner, 1966) have been under study in recent years. Records of the geomorphic effects of needle ice growth in New Zealand have been compiled by Gradwell (1960,1954,1955) and Soons (1967). The effects of needle ice formation on agricultural lands in southwestern British Columbia has been treated by Brink et. al. (1967).

Forecasting. The only paper which considers the forecasting of needle ice events was that of Konko-Tatutaro et. al. (1967), which evaluated air and soil temperature patterns prior to needle ice formation in Japan. For this reason the author assigned a high priority to an attempt to develop and test a statistical model for event prediction using the unique needle ice event record which was available to him at the University of British Columbia.

The Choice of the Study Site

Because of the past history (Brink et. al., 1967) of needle ice investigations at the university agrometeorological site, a secondary weather station gathering data for agricultural users, a bare field (winter) adjacent to the meteorological lot was designated as the major study site for this investigation (see map, Fig. I-1.). The author's recorders and support equipment were stored in the Apiary and electrical lines run to the sensors at the study site. Regular agrometeorological data signals from the meteorological lot are recorded and sampled on the second floor of the Feed Building.

Summary of Field Procedures

The study of the past event record led the author to recognize the necessity for experimental work on needle ice growth. Initially small scale freezing tests were attempted in a large home freezing unit but numerous difficulties were encountered in attempts to faithfully duplicate natural boundary conditions. It was soon evident that additional data must come from the field measurement of soil and atmospheric conditions during natural needle ice events. Thus, the recording equipment, described in the appendix, was set in operation at the study site when either the weather office was predicting a sub-freezing night minimum or the author's statistical model indicated that interesting results might be obtained (near events etc...).

A considerable amount of the field instrumentation was of a prototype nature and thus, somewhat unreliable. Even the commercially manufactured equipment was delicate and subject to frequent malfunctions. For these reasons it was difficult to obtain complete data sets for any single event. However, using a knowledge of instrument response to natural processes it was possible to gain an adequate picture of an event even with malfunctions and limited recorders. Once the major details of the time dependent processes were known, the field experiments (reported in Chapter VI.) were designed to explore specific relationships. Thus, in the 1967-1968 season it was possible to concentrate on the measurement of the soil water tension-heave-soil temperature variable set and gain increasing insight into the conditions which determine the course of events, needle ice or normal freezing, on a frost night.

THE U.B.C. SITE

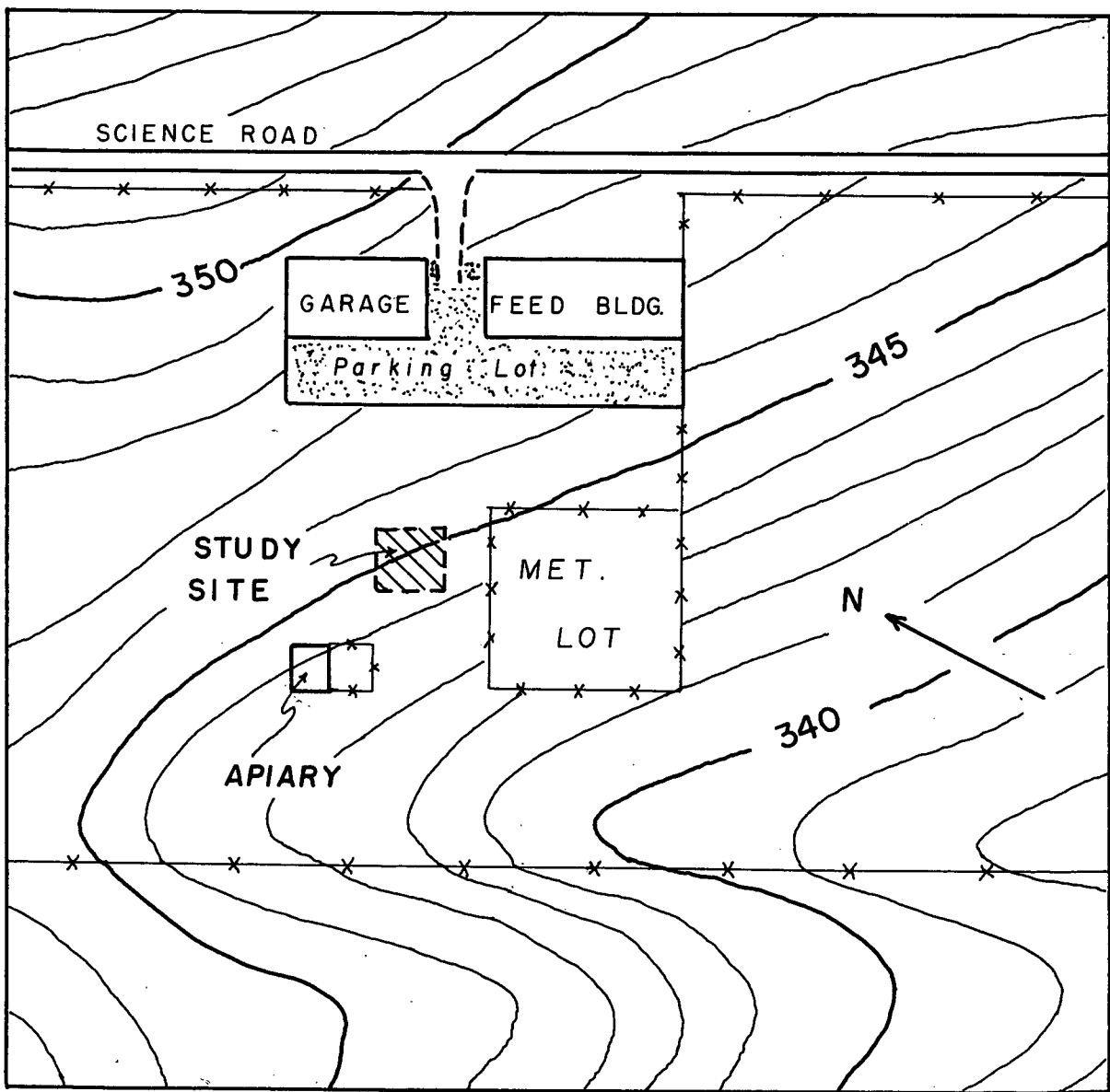

Ref: U.B.C. Dept. of Bldgs. & Grounds

1" = 100'

contour interval = 1ft.

Fig.I-1. Map of study site.

CHAPTER II.

THE GENERAL CLIMATOLOGY, NEEDLE ICE EVENT RECORD, AND SOIL TEMPERATURE DECLINE PATTERNS DURING THE NEEDLE ICE SEASON

The purpose of this chapter is to familiarize the reader with the general climatology, and the needle ice event record at the study site. In addition, nocturnal temperature decline patterns will be examined to set the stage for the further analysis of needle ice events.

The Temperature and Precipitation Regimes

Monthly means of air temperature and precipitation were calculated for the 1961-65 interval from the Agrometeorological Data Summaries. These data are presented below in tabular form.

TABLE II-1. MONTHLY MEAN AIR TEMPERATURE, SOIL TEMPERATURE AND PRECIPITATION

Month	Air Temp.(°C.)	Precip.(mm.)	Soil Temp. at 1 cm.(°C.)
January	3.3	167	3.2
February	5.7	160	5.6
March	5.8	94	7.2
April	8.7	69	11.6
May	10.9	57	15.6
June	15.0	35	20.5

TABLE II-1. (continued)

Month	Air Temp.(°C.)	Precip.(mm.)	Soil Temp. at 1 cm.(°C.)
July	17.0	45	21.9
August	17.1	63	20.9
September	14.2	59	16.9
October	10.9	145	12.3
November	6.7	176	7.0
December	3.9	195	4.1

It should be mentioned that the agrometeorological site was moved a quarter of a mile during the time interval. However, as the general trend is of interest here, no attempt was made to correct these data for the site change.

The main point is that the cold season is also the wet season at Vancouver. This is extremely important for needle ice growth since this condition indicates that, if winter season nocturnal cooling can bring the soil surface to the ice nucleation point, the soil may contain adequate water for the ice needle growth.

Soil Temperature and the Needle Ice Record

The soil layer within 2 centimeters of the surface is of special interest in investigations of needle ice. Three general conditions must be fulfilled, if one is to expect needle ice growth. The near surface layer must be unfrozen and near field capacity, and the soil surface temperature must be within the nocturnal cooling range of ice nucleation temperature (approximately -2°C.). At this time the soil temperature at the 1 centimeter depth will be considered (see Table II-1.). These measurements are not totally representative of conditions at the study site as

the probes in the meteorological lot are under grass cover. Note that during the winter months the mean temperature of soil near the surface is within 10°Celsius of the ice point.

The mean monthly soil temperatures are plotted as functions of depth and time in Fig.II-1. to illustrate two features of the soil thermal environment at the study site. The first being the greater relative intensity of the summer heat wave in comparison to the winter cold wave. This difference is due to the increased winter cloud cover which produces a "continental type" summer and a "maritime type" winter thermal regime at Vancouver.

The second feature illustrated in Fig.II-1. is the heat reservoir that is available to the soil surface during the infrequent winter cold-clear spells. Recall that the mean monthly soil thermal data are illustrated here and that the mean winter day is overcast and relatively warm in comparison with cold-clear spells. Thus, the cold-clear days during which needle ice events occur are days with unusually steep thermal gradients between the heat reservoir at depth and the surface, which is subjected to a large diurnal radiation flux range under these conditions.

The thermal diffusivity of the soil at the study site was estimated from the annual amplitude of soil temperature at depths of 1, 10, 20, 50, 100, and 150 centimeters. This was done using the following relationship (Sellers, 1965).

Eq.II-1.

$$a = \frac{\omega}{2}\left[\frac{Z_1 - Z_2}{\ln.(\delta_1 / \delta_2)}\right]^2$$

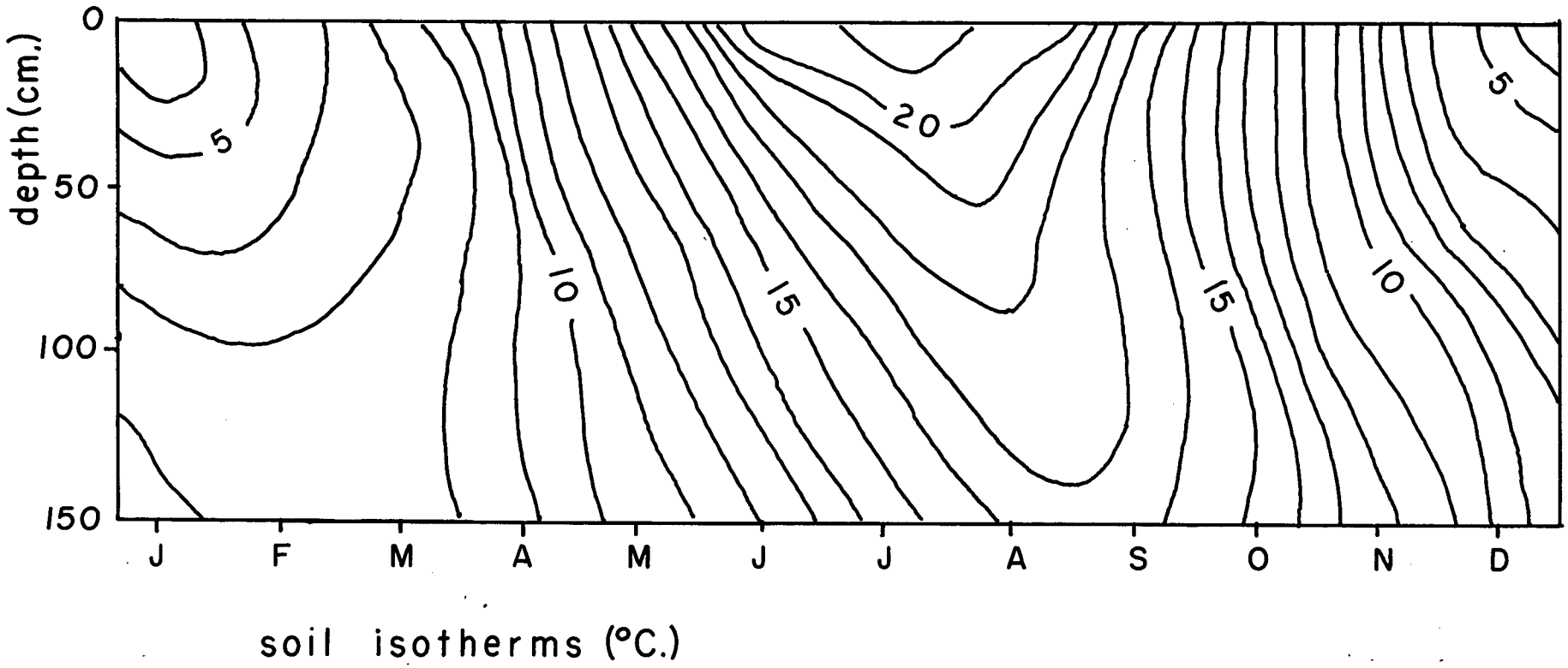

Fig.II-1. The soil thermal regime under grass cover at the agrometerological site.

These computations indicate a mean annual thermal diffusivity of approximately 45×10^{-4} $cm^2 . sec^{-1}$. The computed diffusivity is similar to the laboratory test values which were obtained by artificial heat pulse trials (see Chapter IV.). The thermal diffusivity of the soil can be employed using Equation II-2. to estimate the rate at which a thermal disturbance (e.g., the effects of a winter cold-clear spell) will advance through the soil. (Terzaghi, 1952).

Eq.II-2.

$$Z = \sqrt{12 \alpha t}$$

Using the earlier estimate of soil thermal diffusivity (45×10^{-4} $cm^2 . sec^{-1}$.) the results are as follows.

TABLE II-2. TERZAGHI THERMAL ADVANCE ESTIMATES

length of disturbance (hours)	penetration depth (cm.)
1/2	10
2	20
13	50
52	100
115 (5 days)	150

These data indicate that it would be approximately five days before a thermal disturbance could reach the 1.5 meter level. Thus, during the Vancouver winter, cold-clear weather spells of less than a week would be expected to create rather steep temperature gradients near the surface. This condition is known to favor needle ice formation (see Chapter I.) and may produce a thermally driven water flow directed toward the surface

(see Chapter VI.). The cloudy-rainy winter weather is a major factor in the growth of needle ice during the infrequent cold-clear spells. The normally cloudy-rainy weather keeps the soil unfrozen, by limiting nocturnal radiation cooling, and maintains the soil water content near field capacity, which by definition occurs after three days of infiltration following a soaking rain. Droughts of three consecutive days are infrequent during the Vancouver winter.

The record of needle ice events at the site is presented in Table II-3. These data were collected by the observer, Mr. Don Pearce, at the agrometeorological site during the morning (0815 Pacific Std. Time (P.S.T.)) observation series and include both needle ice and frozen ground events. The monthly mean number of events and the standard deviations from these means are also presented using integer values. It should be remembered that there is a tendency for such a record to underestimate the number of annual events due to the early morning ablation of short needles and night melting following increasing cloud cover. There are also cases on record (December 1967) when the normally frozen soil layer above polycyclic needle ice would support a man on foot giving no hint of the needles below.

TABLE II-3. THE NEEDLE ICE EVENT RECORD

	Oct.	Nov.	Dec.	Jan.	Feb.	Mar.	Total
1961-62	1	10	9	1	10	6	37
1962-63	0	1	6	19	0	8	34
1963-64	0	3	8	2	14	1	28
1964-65	0	4	6	0	5	7	22
1965-66	0	2	3	2	4	4	15
1966-67	0	2	2	2	7	6	19
Mo. Mean	0	4	6	4	7	5	
Std. Dev.	1	3	3	7	5	3	

The pattern is one of a general high event frequency in December and February with lower frequencies in October, November, March and January. The standard deviation of the monthly values peakes in January. This may result from the infrequent outbursts of Arctic air which freezes the ground to depth on some occasions and produces snow cover, preventing needle ice growth or discovery, at other times. The event season is limited by the soil temperature rising above the nocturnal cooling range to the nucleation point.

The Surface Nocturnal Cooling Curve

A necessary condition for needle ice formation is ice nucleation which occurs after the soil surface has been undercooled to approximately 2° Celsius below the freezing point. Thus, the time dependence of surface temperature during nocturnal radiation cooling is a major factor in determining the intensity of needle ice events. A test case will be employed to illustrate the general form of the cooling curve.

During the early evening hours of 4 March 1967 net radiation, surface temperature and soil heat flux at the 2 centimeter depth were recorded in the Apiary at the study site.

The portion of the temperature-time trace during the period before nucleation was of interest as the decline rate provided a test of Brunt's parabolic model for radiation cooling (Brunt, 1934). The formula is as follows.

Eq. II-3.

$$T = T_i + \frac{2}{\sqrt{\pi}} \frac{B_o^* \sqrt{t}}{C_s \sqrt{\alpha_s}}$$

*Note the heat flux sign convention: (+) toward the surface, (-) away from the surface.

The temperature time data gathered on this night are presented in Table II-4. and plotted as Figure II-2.

TABLE II-4. SURFACE TEMPERATURE DATA, 4 MARCH 1967

Time (Pacific Std.)	Surf. Temp (°C.)	$(T_i-T)_o$	t (10^3 sec.)	t (10^1 sec.)
1700	9.4	0.0	0.0	0.0
1800	4.9	4.5	3.6	6.0
1900	2.8	6.6	7.2	8.5
2000	2.0	7.5	10.8	10.4
2100	1.0	8.4	14.4	12.0
2200	0.0	9.4	18.0	13.4

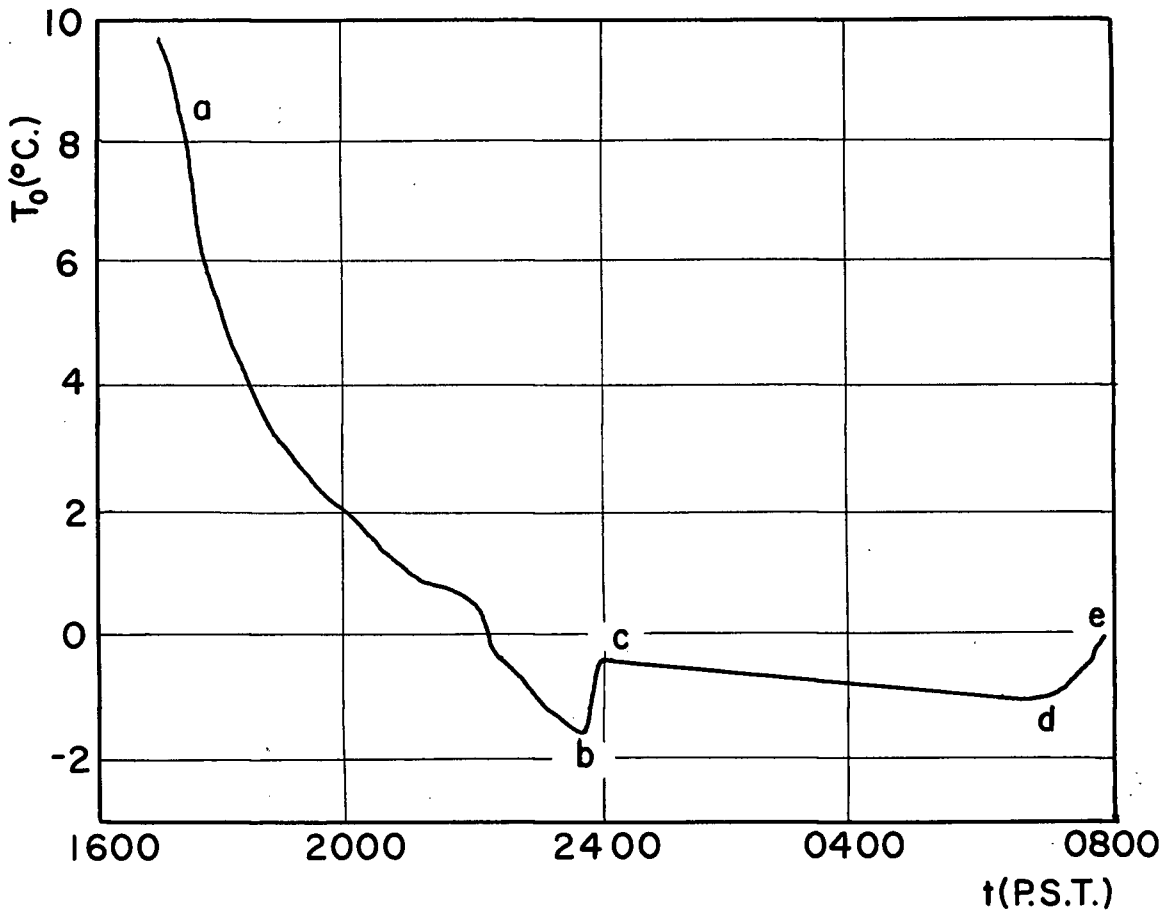

Fig.II-2. Soil surface cooling, 4-5 March 1967.

(a-b) Brunt cooling, (b) nucleation, (b-c) undercooling,
(c) soil water freezing pt., (c-d) needle ice growth,
(d-e) warming by beam radiation.

During the measurement series the mean net radiation flux was -.100 ly. $min.^{-1}$ and the mean value of the soil heat flux at the 2 centimeter depth was .037 ly. $min.^{-1}$. A plot of the relationship of the temperature decline to the square root of elapsed time is presented as Fig.II-3. The standard error of this graphical solution was approximately one-half of a degree Celsius or about the probable precision of the temperature determination. This result indicates that the Brunt model fits natural conditions on one occasion, but further verification is necessary.

The rule states that on relatively calm nights with stable cloud cover the surface cooling should be proportional to the square root of the elapsed time since the soil heat flux became directed toward the surface. A further test of the general validity of the rule, using data from a twelve night period (5-17 February 1968) when the sky was known to be clear, was carried out. Data taken at the study site indicated that the soil heat flux becomes directed toward the surface at approximately 1600 hours Pacific Standard Time (P.S.T.) during this observation period. Therefore, that time was selected as the initial time used in the calculations. Points (temperature in $^{o}C.$ and time in hours) along the decline curve were used to determine the degree to which the measured surface temperatures fitted Brunt's rule. The method of curve fitting was that of least squares in which a linear equation of best fit was calculated from the observed data. The equation, an empirical form of the rule, has the following form:

Eq.II-4.

$$(T_i - T) = a + m\sqrt{t}$$

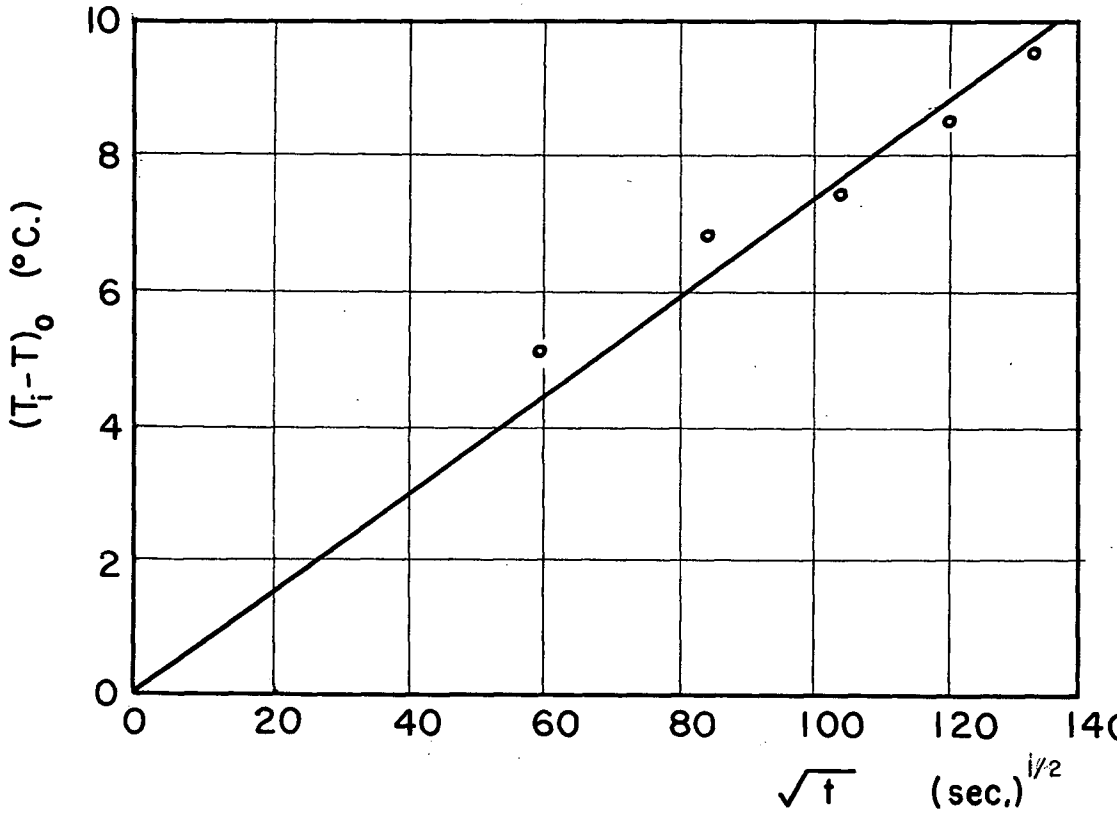

Fig. II-3. Accumulated temperature decline as a function of the square root of time, 4 March 1967. The linear equation is $(T_i-T)_o = .073\ t^{\frac{1}{2}}$.

The regression coefficient (a) is trivial as it will lie somewhere in the region of the 1600 hours temperature but the coefficient (m) indicates the "steepness" of the temperature decline and is thus an indication of the efficiency of the cooling environment. Points at one hour intervals between 1600 P.S.T. and the time of nucleation were used in the analysis.

The coefficients of determination were high in all cases indicating that between 97 and 100% of the variation in temperature could be treated as square root of time dependent. However, the standard error of the regression line yields a sensitive indication of the "goodness of fit" in each case and, thus, offers a test of the rule's validity. These results are presented in Table II-5.

TABLE II-5. LEAST SQUARES TESTING OF BRUNT'S RULE

Date, Feb. 1968	Slope (m) of Equation	Std. Dev.(^{o}C.)
5-6	-2.71	0.59
6-7	-2.57	0.36
7-8	-3.88	0.37
8-9	-3.86	0.38
9-10	-3.17	0.44
10-11	-3.11	0.63
11-12	-3.82	0.38
12-13	-4.51	0.52
13-14	-3.84	0.83
14-15	-4.54	0.61
15-16	-4.68	0.86
16-17	-5.00	0.14

Note that the mean value of the standard deviations was 0.54±0.17 °Celsius. This result indicates the general validity of Brunt's rule during clear weather. Some potential sources of variations in standard deviation and curve slope (m) are radiation fog formation, changing wind speed (level of turbulent exchange), dew formation, and soil water migration toward the surface (see Chapter VI.). These results also indicate a wide range of surface cooling rates even during relatively calm-clear nights.

Unfortunately the occurrence of weather conditions with the "stability" of the data reported above is infrequent as will be demonstrated by the examination of several temperature traces in the next section of this chapter.

Nocturnal Temperature Patterns

As noted earlier, the major environmental condition initiating a needle ice event is the cooling of an unfrozen soil surface to a temperature below the freezing point of the soil water to the ice nucleation temperature. After nucleation the growth of needle ice will depend upon soil water supply and the maintenance of heat sinks above the soil surface. A typical trace of surface temperature and soil water tension (see Chapters IV. and VI.) for the needle ice event of 1-2 January 1968 is presented in Figure II-4. Note that shortly after nucleation the increasing soil water tension, measured in the 4-6 cm. depth range, indicates that migration to the freezing plane (ice segregation, needle ice growth) has started. The question is then: In general, what weather conditions favor relatively

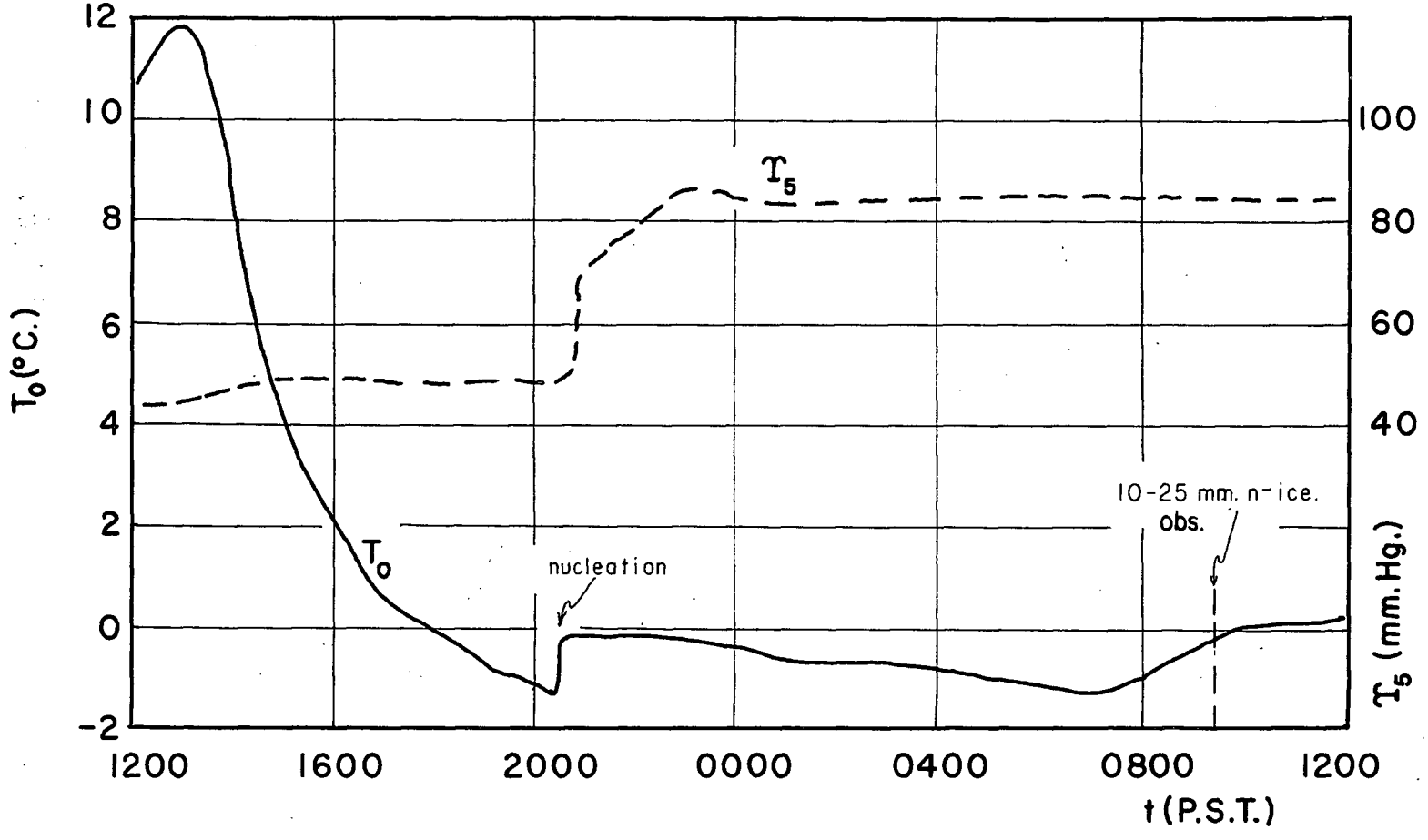

Fig.II-4. Surface temperature (T_0) and soil water tension (Υ_s), see chapter IV., 1-2 January 1968.

rapid nocturnal temperature declines to sub-freezing levels where first nucleation and later freezing and segregation (needle ice growth) are possible?

Some insight into the physics of the temperature decline can be gained through the examination of soil surface temperature traces on nights which produced needle ice in comparison with nights when events did not occur.

An instructive trace is that of the "New Years" event of 1968 shown in Figure II-5. It will be noted that on that evening the temperature decline during the early hours was slight and that the surface temperature oscillated between 3°4°Celsius until shortly after midnight when a steep decline began. The initiation of the temperature decline coincided with clearing skies and the decreasing level of thermal radiation from the sky hemisphere which would result from the decreasing cloud cover. The soil water tension trace shows a sudden jump at approximately 0730 P.S.T. which may indicate a brief period of ice segregation, although no needle ice was observed during a visit to the site just before noon.

Further evidence of the rapid response of the soil surface temperature and heat flux (disc at approximately 3mm., see appendix) to changes in the thermal radiation flux produced by clearing skies is illustrated on the trace of 2-3 February 1968 when no event occurred. The passage of a "clear spot" in the sky produced a rapid temperature drop just prior to 0400 P.S.T. (see Figure II-6.). Before this drop occurred the soil heat flux was near zero (actually a small flux directed toward the surface) indicating that the turbulent exchange was nearly balancing the thermal radiation loss at the surface. The protracted shallow decline of surface tempera-

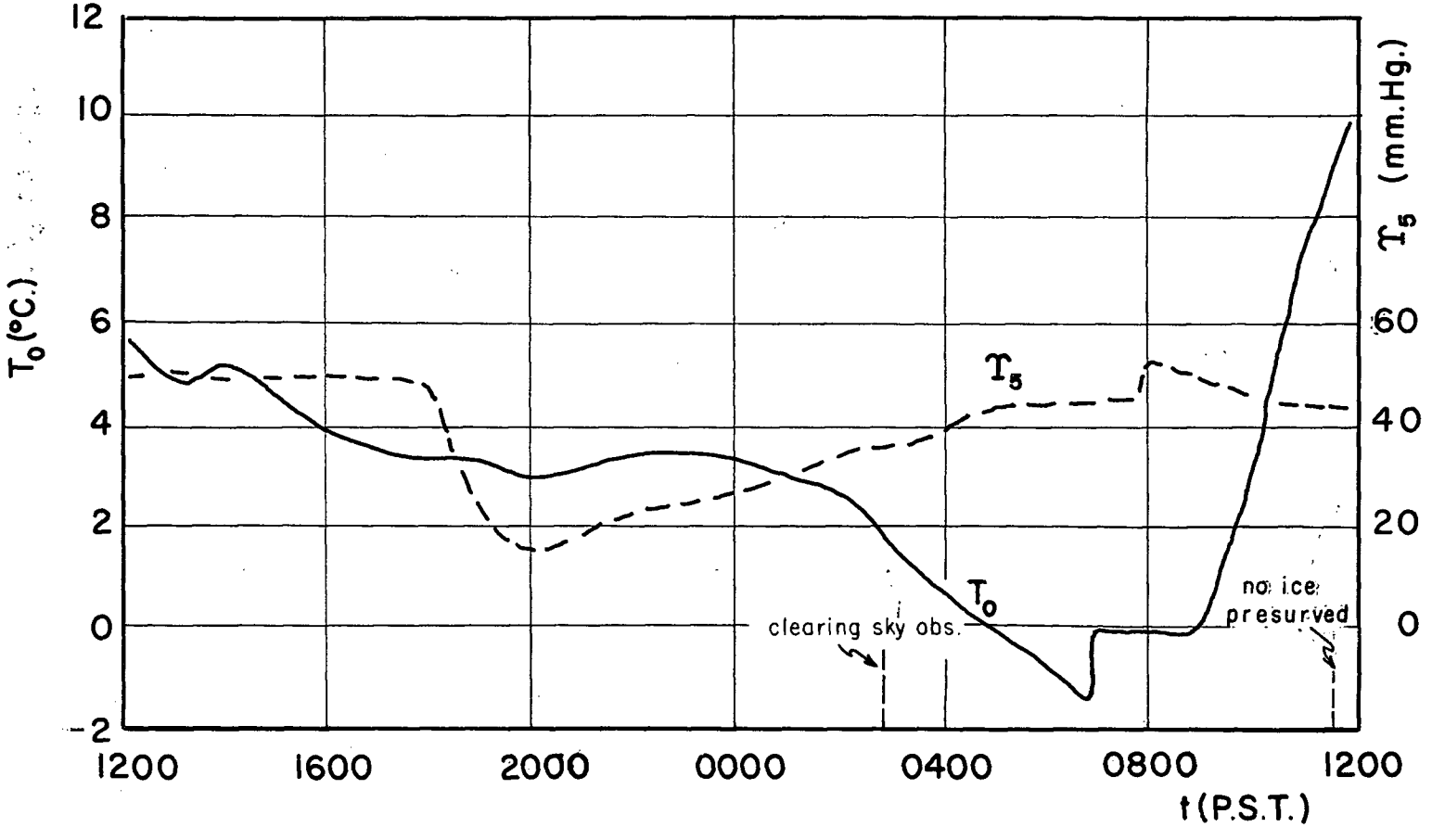

Fig.II-5. Surface temperature and soil water tension, 31 Dec.67- 1 Jan.68.

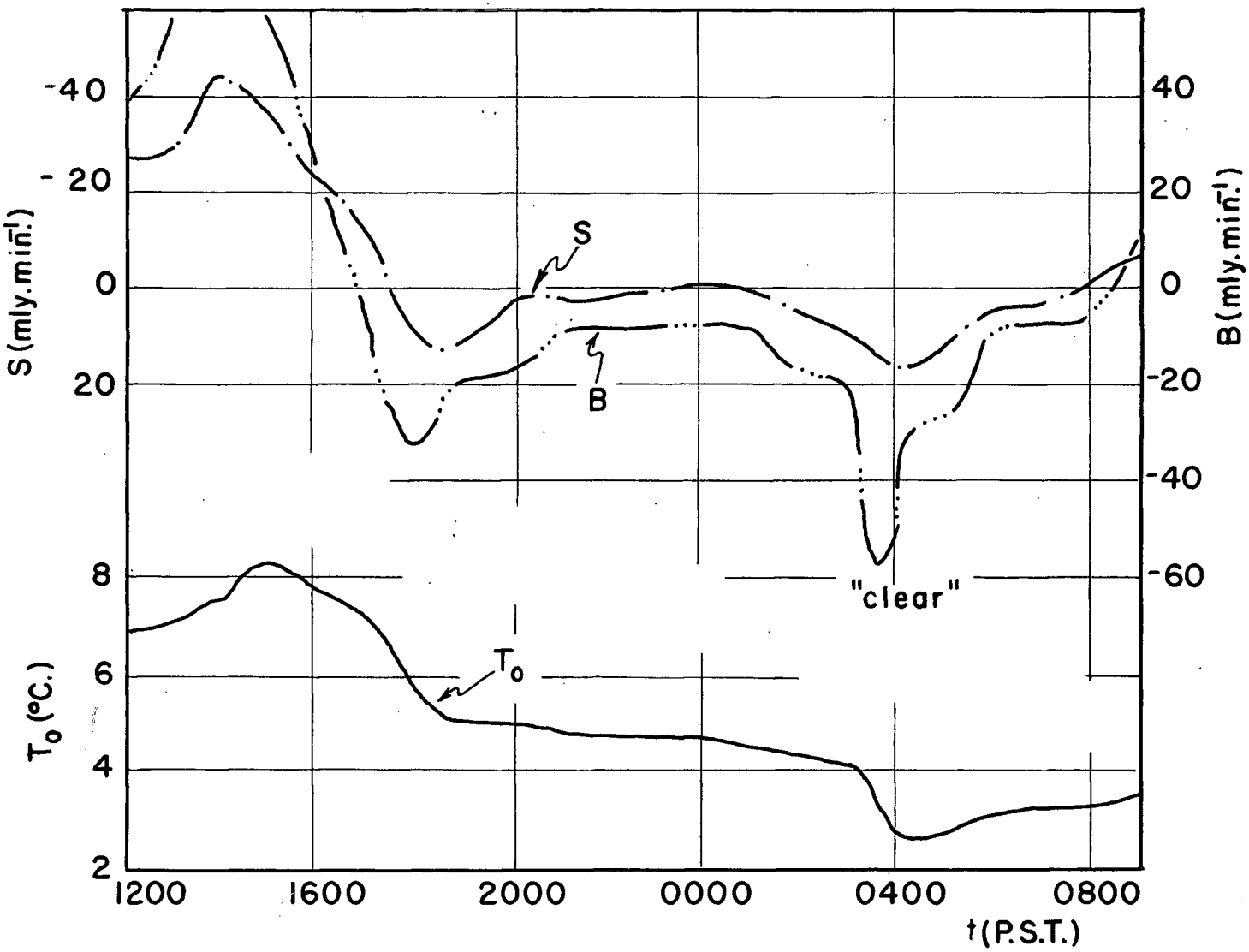

Fig.II-6. Conditions during a period of variable cloud cover, 2-3 Feb.1968.

The soil heat flux (S) and net radiation (B) are plotted with surface temperature.

ture in the period between 2000 and 0300 P.S.T. supports this interpretation.

Three surface temperature traces during needle ice events in February 1968 are presented in Fig.II-7. to demonstrate the persistence of the parabolic decline form during clear and partly cloudy periods and to illustrate the effect of variable cloud cover and/or turbulent exchange rates on the late evening portion of the 15-16 February 1968 trace.

The surface temperature conditions during the period from the 24th through the 25th of January 1968 are shown in Fig.II-8. to demonstrate conditions which nearly produced needle ice events. Three additional traces are presented in Fig.II-9. for periods when no events occurred. Of these traces, that of surface temperature on 30-31 December 1967 appears to have been the result of dense cloud cover conditions whereas the traces of 15-16 January 1968 and 16-17 January 1968 seem to reflect clear or partly cloudy conditions in the late afternoon followed by variable cloudiness and/or turbulent flux oscillation in the later portion of the night. (see Chapter III.).

The effect of variable turbulent flux, presumably due to wind velocity variation, is demonstrated by the soil surface temperature and heat flux record of 17-18 February 1968 (see Fig.II-10.). It should be noted that the net radiation balance during the 1430-0730 P.S.T. period was zero and thus, the general temperature rise in the interval must be due to increasing turbulent energy input, mainly a sensible heat flux from the air toward the ground surface. This effect would likely result from increasing wind velocities.

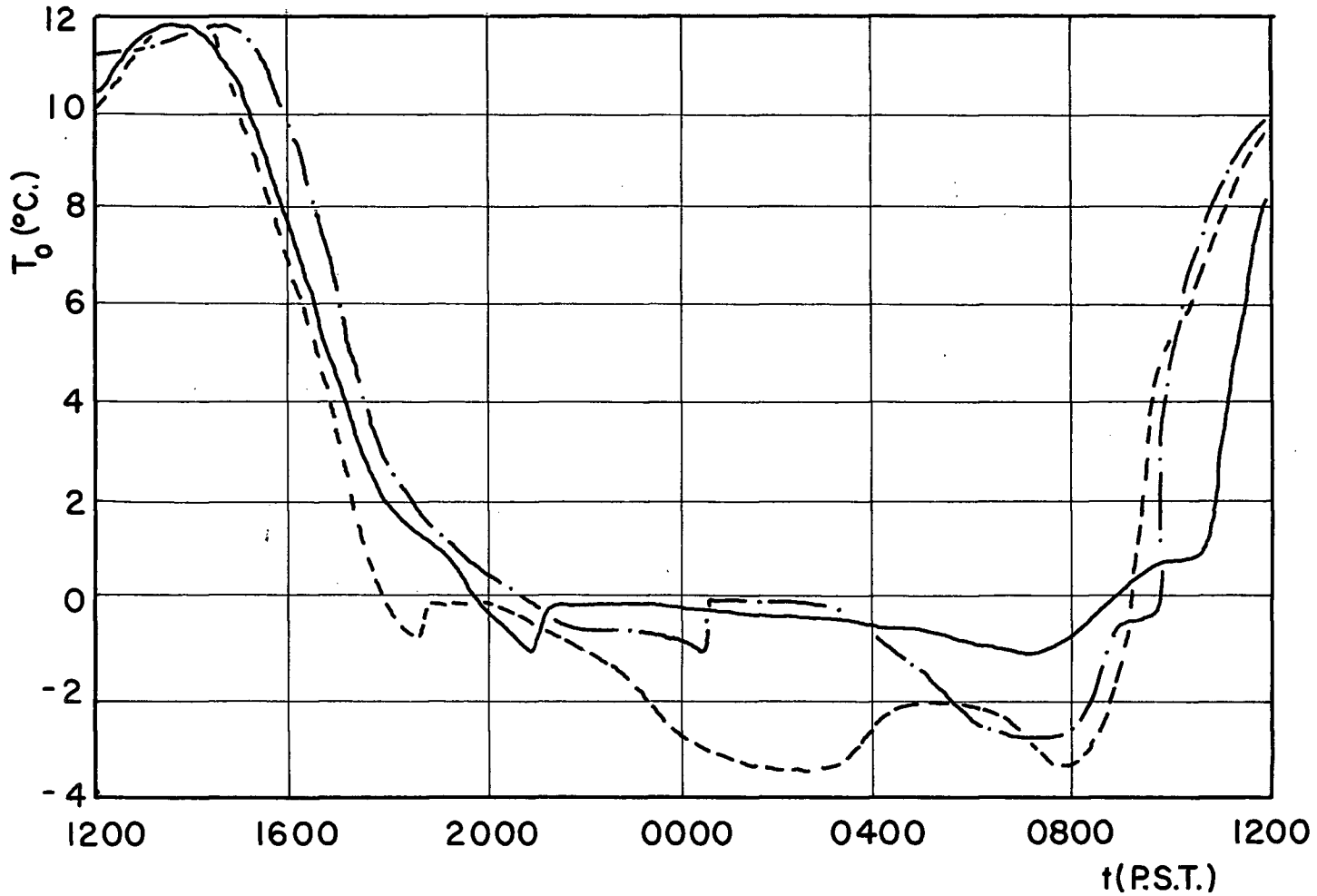

Fig.II-7. Surface temperature traces during needle ice events.

——— 7-8 Feb. 1968, ——·—— 13-14 Feb. 1968 (both clear)

— — — — 15-16 Feb. 1968 (partly cloudy)

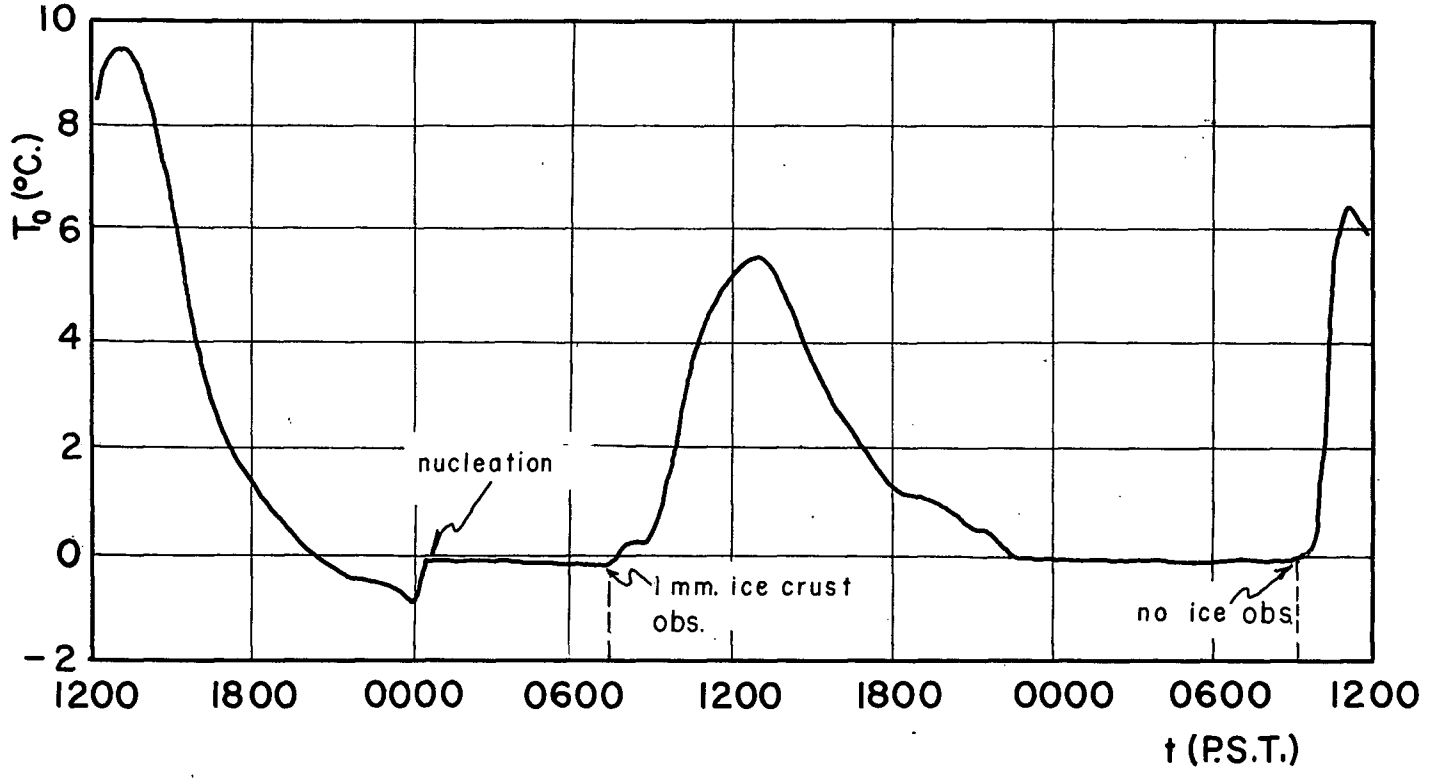

Fig. II-8. Surface temperature trace, 24-26 January 1968.

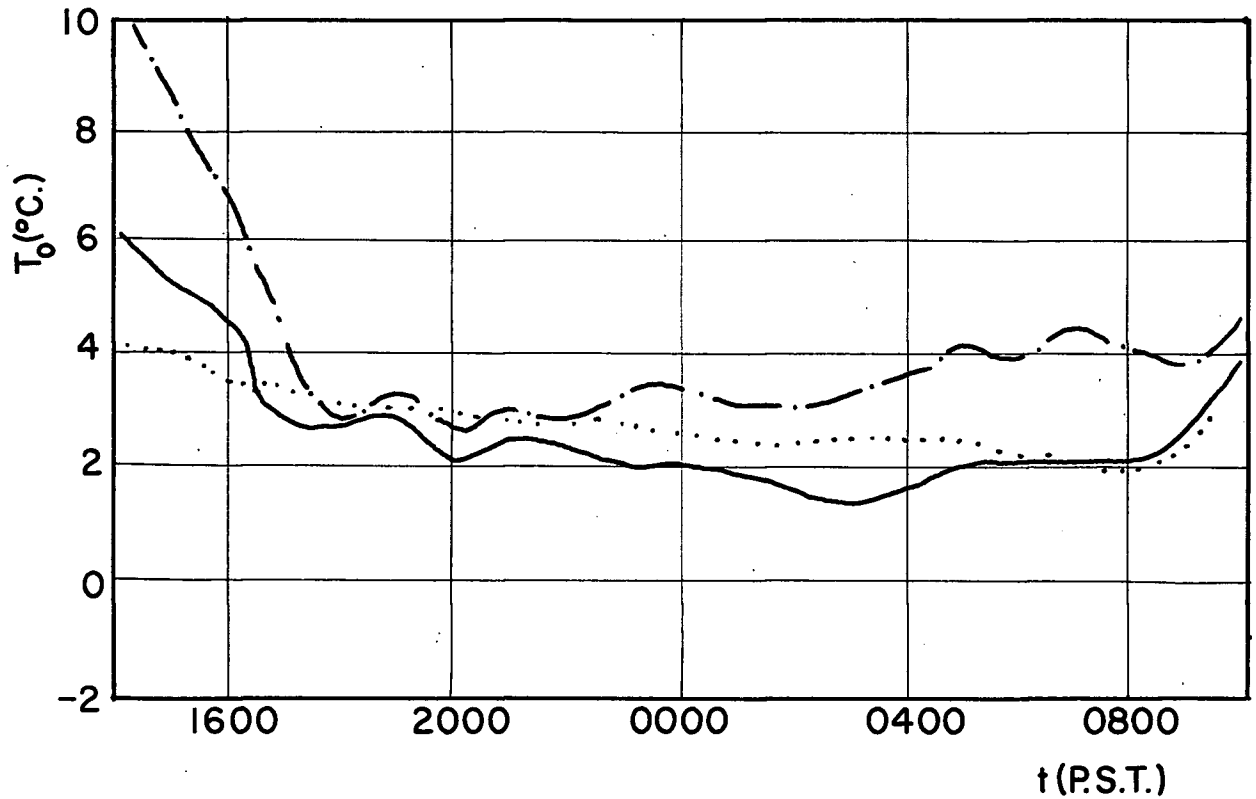

Fig.II-9. Surface temperature traces on nights without needle ice events.

····· 30-31 Dec.67, —·— 15-16 Jan.68, ——— 16-17 Jan.68.

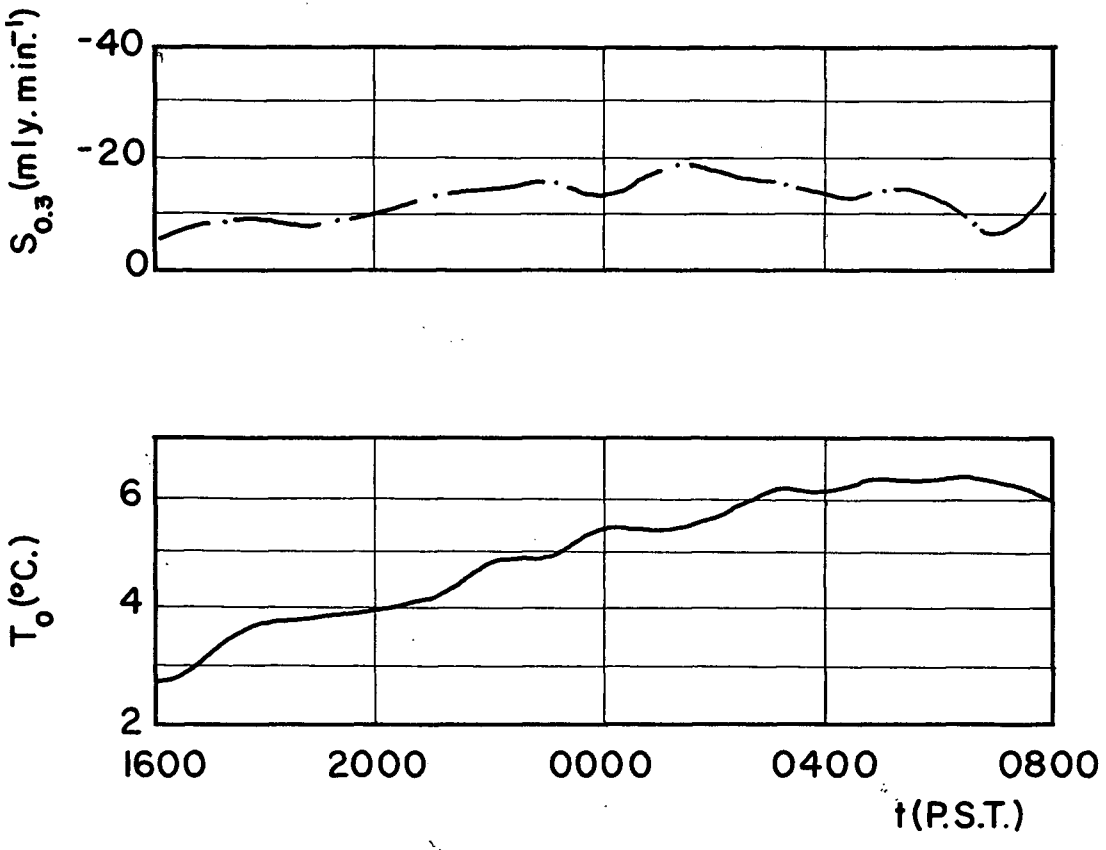

Fig. II-10. Surface temperature and soil heat flux at 0.3 cm. during a night with a nearly balanced thermal radiation flux, 17-18 Feb. 1968.

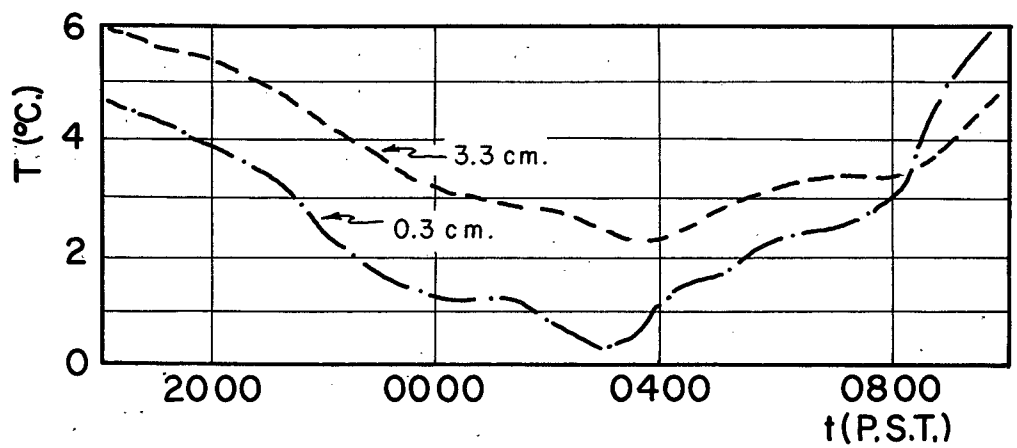

Fig.II-11. Soil temperatures at 0.3 and 3.3 cm. below the surface, 20-21 Nov.1967.

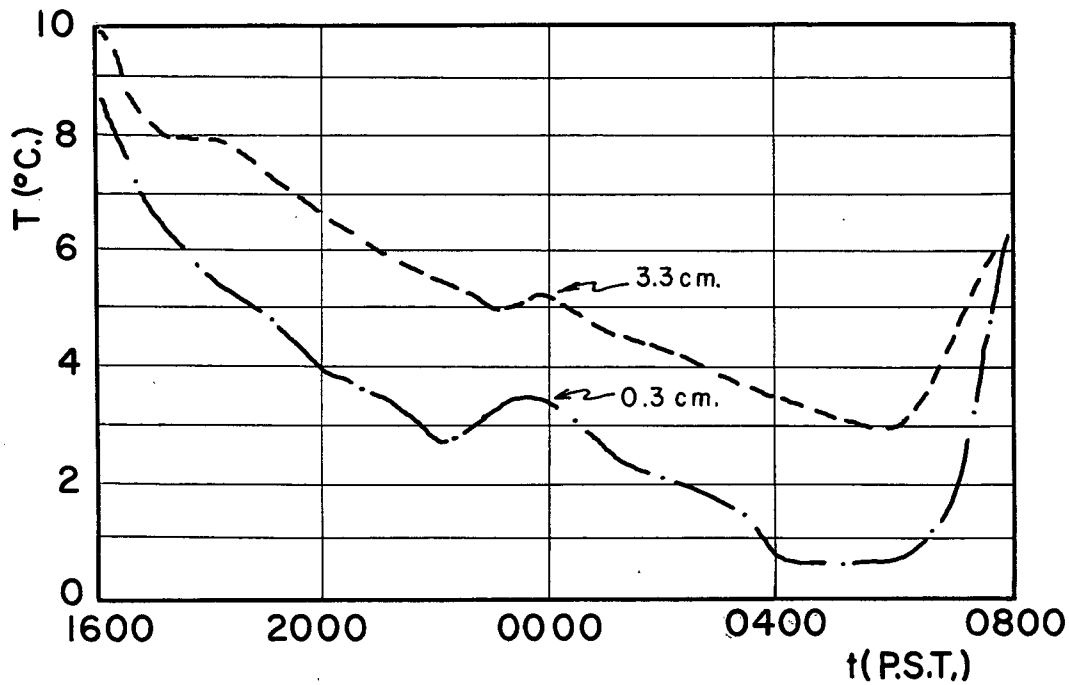

Fig.II-12. Soil temperatures on a clear night, 18-19 Nov.67.

The record of 20-21 November 1967 is presented in Fig.II-11. to demonstrate the termination of a temperature decline due to increasing cloud cover. At 0430 P.S.T. on November 21 cloud cover from the west was moving over a residential area six miles east of the study site at a time when frost had already formed on the local roof tops.

Finally, the record of soil temperature at two levels on 18-19 November 1967 is included as Fig.II-12. to illustrate the limiting effects of an initially high soil temperature under clear conditions and to show the curious bulge in the temperature decline curves which occurred at about 2300 P.S.T. This "blip" in the curves is a common occurrence in temperature decline curves and will be discussed in Chapter VI.

In summary, it would appear that the variation in cloud cover has a primary role in limiting the frequency of needle ice events at Vancouver, whereas turbulent exchange effects are secondary. The question of how the components of the surface energy exchange mechanism operate on needle ice nights will be explored in the next chapter. A second point of interest is the varification of the utility of the parabolic cooling curve predicted by the Brunt model. Lastly, Vancouver's winter cloudy-rainy weather pattern, broken by infrequent clear-cold-dry atmospheric conditions, was demonstrated as the major seasonal climatic factor leading to needle ice growth.

CHAPTER III.

HEAT SOURCES AND SINKS DURING NEEDLE ICE EVENTS

In Chapter II. the nature of the nocturnal temperature decline curve was discussed as a major element in the growth of needle ice. In this chapter the magnitude of the heat sources, including radiation fog, and sinks which control the rate of nocturnal surface cooling and needle ice growth will be examined.

Energy Exchange Conditions

During four nights in March 1967 net radiation and soil heat flux were recorded at the study site. In addition, soil surface temperature and air temperature 46 centimeters above the surface were also recorded (further information on instrumentation and measurement is included as an appendix).

Measurements of two of the energy exchange components, net radiation (B) and soil heat flux (S), were available from the recorder traces. The problem was then to estimate the values of the other two components of surface energy transfer, evaporation-condensation (V) and the sensible heat flux (L). The method used in the calculation of these values was the Bowen ratio (Geiger, 1965). This ratio is as follows:

Eq.III-1.

$$(L/V) = 0.65\ [(T_o - T_a) / (\ddot{e}_o - \ddot{e}_a)]$$

where: temperature (T, ^{o}C.) and vapor pressure (e, mb.).

The data required for computing the Bowen ratio were obtained from sling psychrometer profile measurements. The following data was taken

during clear-cold evenings.

TABLE III-1. TEMPERATURE AND HUMIDITY

1967	Time (P.S.T.)	Height (cm.)	Relative Humidity (%)	Vapor Pressure (mb.)	Dew Point (°C.)	Temp. (°C.)
2 March,	2300-2330	132	75	5.68	-1.3	3.1
		46	80	5.80	-0.6	2.4
		0	(100)	(5.91)	(-0.5)	-0.5
3 March,	1900-1930	132	79	6.98	1.7	5.2
		46	86	7.76	3.5	5.5
		0	(100)	(7.24)	(2.4)	2.4*
12 March,	1900-1930	132	78	6.10	-0.1	3.4
		46	82	6.26	0.3	3.3
		0	(100)	(6.67)	(1.2)	1.2
24 March,	2000-2130	150	88	6.67	2.1	3.0
		15	95	7.17	1.9	2.4
		0	(100)	(6.16)	(0.1)	(0.1)*

* The soil surface temperature is below the dew point of the middle measurement level.

( ) Saturation vapor pressure at surface temperature is assumed.

In all profiles, the relative humidity and vapor pressure increase as the soil surface is approached. There is also a temperature inversion between the top level and the soil surface in all the profiles. On the 3 March profile the inversion appears quite shallow as the inflection point is located between the soil surface and the upper measurement level. Field observations of soil water tension and trial water balance computations (Thornthwaite and Mather, 1957) indicate that the near surface layers of the study site soil are normally within the field capacity range of soil water tensions, 100-500 cm. of water, during the needle ice season. During

most of this period the soil surface may approximate a free water surface. Thus, saturation vapor pressure is assumed at the surface. The Bowen ratio was calculated using three measurement interval combinations; upper-surface, middle-surface and upper-middle. The results are as follows:

TABLE III-2. BOWEN RATIO ESTIMATES

Measurement Period 1967 (P.S.T.)	Computation Levels (cm.)	Estimate of Bowen Ratio
2 March/2300-2330	0,132	-10.2
	0, 46	-17.2
	46,132	- 3.8
3 March/1900-1930	0,132	-17.0
	0, 46	3.9
	46,132	- 0.3*
12 March/1900-1930	0,132	- 2.5
	0, 46	- 3.3
	46,132	- 0.4*
24 March/2000-2130	0,150	3.7
	0, 15	1.5
	15,150	- 0.8*

The method of the Bowen ratio is known to break down as the ratio approaches a value of minus one; from either direction (Sellers, 1965). For this reason all Bowen ratio estimates between minus two and zero are considered unfit for further use in computation. These are indicated by an asterisk (*) in the table above. Notice that those "unfit" values occur in three out of four cases when the upper-middle measurement levels are used in the computation. It was, therefore, decided to continue using only the upper-surface and middle-surface estimates of the Bowen ratio in computing the values of the sensible (L) and evaporation-condensation (V)

heat fluxes using the method described in Geiger (1965). From the law of energy conservation it is known that;

Eq.III-2.

$$S + B + L + V = 0$$

As (L/V) has been calculated and (S) and (B) are recorded, it is possible to estimate the magnitudes of (L) and (V).

Eq.III-3.

$$V = \frac{-(S+B)}{[1.+(L/V)]}$$

Eq.III-4.

$$L = \frac{-(L/V)\cdot(S+B)}{[1.+(L/V)]}$$

The results of these calculations are presented in Table III-3.

TABLE III-3. THE ENERGY EXCHANGE ENVIRONMENT (two level means)

	2 March 67 2300-2330	3 March 67 1900-1930	12 March 67 1900-1930	24 March 67 2000-2130
B (mly./min.)	-105	-105	-110	- 92
S (" ")	55	50	50	55
L (" ")	53	49	93	26
V (" ")	- 03	06	- 33	11
Wind Speed (meters/sec.)	0.6	1.3	2.9	0.7
Cloud Cover	0/10	0/10	0/10	3/10
Next Morning (0700-0730 P.S.T.):				
Cloud Cover	0/10	0/10	1/10	10/10
Needle Ice (cm.)	1	1/2	1	none

Note: The best needle ice growth occurred on nights without dew.

After calculating the sensible and latent heat flows by the Bowen ratio it was possible to compute the austausch exchange coefficient (the product of air density and eddy diffusivity, see Eq.III-10, III-11.) for the measurement intervals at two levels. The results are as follows:

TABLE III-4. AUSTAUSCH EXCHANGE COEFFICIENT ESTIMATES

Date	Time (P.S.T.)	Level (cm.)	Austausch Coeff. ($g.\ cm.^{-1}\ sec.^{-1}$)
2 March 67	2300-2330	23	.093
		66	.147
3 March 67	1900-1930	23	.040
		66	.208
12 March 67	1900-1930	23	.122
		66	.408
24 March 67	2000-2130	08	.016
		75	.104

During the four measurement periods it was possible to compute austausch coefficients at two levels. The coefficient value midway between the surface and instrument shelter level (1.2 meters) is valuable when using standard weather screen data. These values at a height of 60 cm. were determined graphically by plotting log height against log austausch as demonstrated by Geiger (1965). Mean wind velocities and austausch values are tabulated in Table III-5.

TABLE III-5. AUSTAUSCH COEFFICIENTS AND MEAN WIND SPEEDS

Test Period	$A_{60}(g.cm.^{-1}sec.^{-1})$	Mean Wind Speed (meters/sec.)
2 March 67/2300-2330	.140	0.58
3 March 67/1900-1930	.180	1.35
12 March 67/1900-1930	.385	2.91
24 March 67/2000-2130	.087	0.67

The A_{60} coefficients calculated from the Bowen ratio estimates were plotted in Figure III-1. The four values and the origin of the graph were used in a graphical fitting process. The line of best fit is tied to the origin as the **austausch coefficient** of still air is near 2×10^{-4} g.cm.$^{-1}$sec.$^{-1}$ (Geiger, 1965). Using only the origin and the three points which lie close to a straight line, a linear wind rule was developed to yield a rough estimate of the austausch coefficient at a height of 60 cm. above the surface (g.cm.$^{-1}$sec.$^{-1}$) from the mean wind velocity at an elevation of 120 cm. (meters sec.$^{-1}$).

Eq. III-5.

$$A_{60} = 134 \times 10^{-5} \cdot U_{120}$$

Considering the adiabatic profile assumption and other limiting assumptions, further refinement of this form is unwarranted at this time (see Light, 1943; Pasquill, 1949; Scott, 1964 and Sverdrup, 1936). Hubley (1957) developed a similar linear relationship between the exchange coefficient and a reference level wind velocity for the inversion conditions which are typical of a melting glacier surface and partially analogous to a wet soil surface during radiation cooling. In this approach the roughness parameter (Z_0) and the variations due to non-adiabatic flow are treated empirically, from an analysis of net radiation, soil heat flux, and temperature-humidity gradients above the surface. The relationships between this method of analysis and the exchange coefficient of Sverdrup (K_{SV}) and the von Karman constant (K_0) under adiabatic conditions, when measurements of reference level wind velocity, air temperature and humidity are carried out at a height (Z) above the surface and surface temperature and humidity are known, are illustrated in Equation III-6.

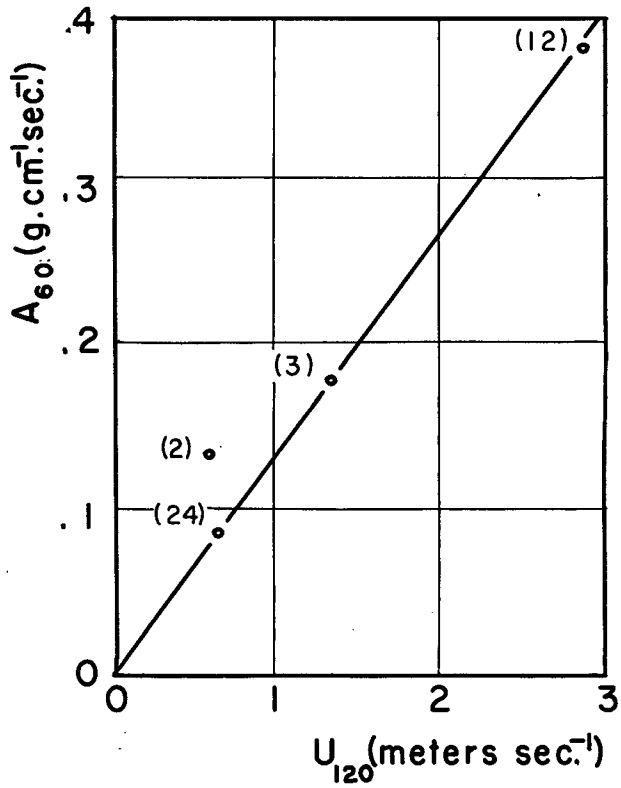

Fig.III-1. Austausch-wind speed plot.

( ) date March 1967.

Eq. III-6.

$$A_{z/2} = \frac{(B_o + S_o)\ Z}{\left[C\,(T_z - T_o) + r_v(q_z - q_o)\right]} = \frac{\rho\, K_o U_z}{\left[\text{ln. } Z/Z_o\right]} = K_{sv} U_z$$

The analysis of the March 1967 data yield the following computation forms:

Eq. III-7.

$$L_{60} = 16\ U_{120}\ (T_{120} - T_o)$$

Eq. III-8.

$$V_{60} = 25\ U_{120}\ (e_{120} - e_o)$$

where: wind speed (U, meters $sec.^{-1}$), temperature (T, $^{o}C.$), vapor pressure (e, mb.) and heat flux values (mly./min.).

These computation forms were checked with Bowen ratio estimates of turbulent transfer levels. This test indicated a standard error of estimate of approximately ± 8 mly. $min.^{-1}$ or about the same precision as the soil heat flux and net radiation recorders. It is therefore, probable, that even under ideal nocturnal conditions (e.g., wet surface and deep inversion) energy transfer estimates only approach a precision of 10-20% in estimating the relative magnitude of the heat flux components. The cases producing the largest variations were those of 2 March 67 when there appears to have been an increase in the roughness length due to air flow over the Apiary (see Fig.I-1.); and the latent heat flux of 3 March 67 when the vapor pressure profile was strongly bow shaped between the surface and 120 cm. This linear wind form will be employed in Chapter VI. as an aid in developing an equilibrium temperature model. Having constructed a rough model for estimating the magnitude of turbulent heat flux

at the study site it is now time to consider a major feedback mechanism which often terminates surface cooling and acts as an additional heat source.

Radiation Fog

During clear and near-clear nights when the air is relatively still and conditions are favorable for needle ice formation, the air near the screen level often reaches the dewpoint temperature and produces a deep radiation fog. The occurrence of nocturnal radiation fogs has been investigated at Vancouver International Airport and an empirical prediction model was developed (Belhouse, 1961). Field studies of radiation fog formation and thermal radiation flux divergence near the surface have been made by Davis (1957) and Funk (1960, 1962). An example of the effects of one of these events at Vancouver follows.

On the evening of 7 February 1967 a bead thermistor and an "economical net radiometer" were placed over a bare soil surface in a residential backyard. The radiometer was essentially the model described by Swan et. al. (1961) with only one layer of polyethene film shielding. The soil surface thermistor resistance was determined with a Wheatstone nulling bridge (see appendix) and the net radiation computed from the counters of a totalizer circuit similar to that described by Goodell (1962). During the measurement series there was some condensation on the shielding of the upper radiometer unit which was wiped dry at the end of each 30 minute measurement interval. After correcting for radiometer lag, approximately 15 minutes, it was possible to compute the radiation temperatures of the ground surface and the sky hemisphere. In these computations the emis-

sivity of both the ground surface and the sky hemisphere was assumed to be unity. It should be noted that at this site the sky hemisphere is composed partially of hot buildings and trees. The results of these measurements are presented as half-hour mean values centered on the indicated time in Table III-6.

TABLE III-6. NET RADIATION AND SURFACE TEMPERATURE DURING THE DEVELOPMENT OF RADIATION FOG ON 7 FEBRUARY 1967.

Time (P.S.T.)	Surface Temp. (°C.)	Net Radiation (ly./min.)	Sky Temp. (°C.)	Cloud Cover	Cloud Type
1815	1.7	-.042	-4.7	2/10	stratus
1845	1.3	-.049	-6.3	2/10	stratus
1915	1.1	-.047	-6.2	4/10	fog
1945	0.8	-.047	-6.5	4/10	fog
2015	0.6	-.040	-5.7	4/10	fog
2045	0.3	-.045	-6.8	4/10	fog
2115	0.1	-.038	-6.8	5/10	fog
2145	0.6	-.031	-4.2	5/10	fog
2215	1.3	-.034	-3.9	6/10	fog
2245	1.3	-.031	-3.4	6/10	fog

A graphical plot of the temporal variation of the ground surface temperature, with the radiation temperature of the sky hemisphere, is presented in Figure II-2. to illustrate the rapid response of surface temperature to the deepening radiation fog. It would appear that on clear-calm nights, when the air temperature reaches the dew point, radiation fog can build to great depths and, with the aid of the sensible heat flux, which

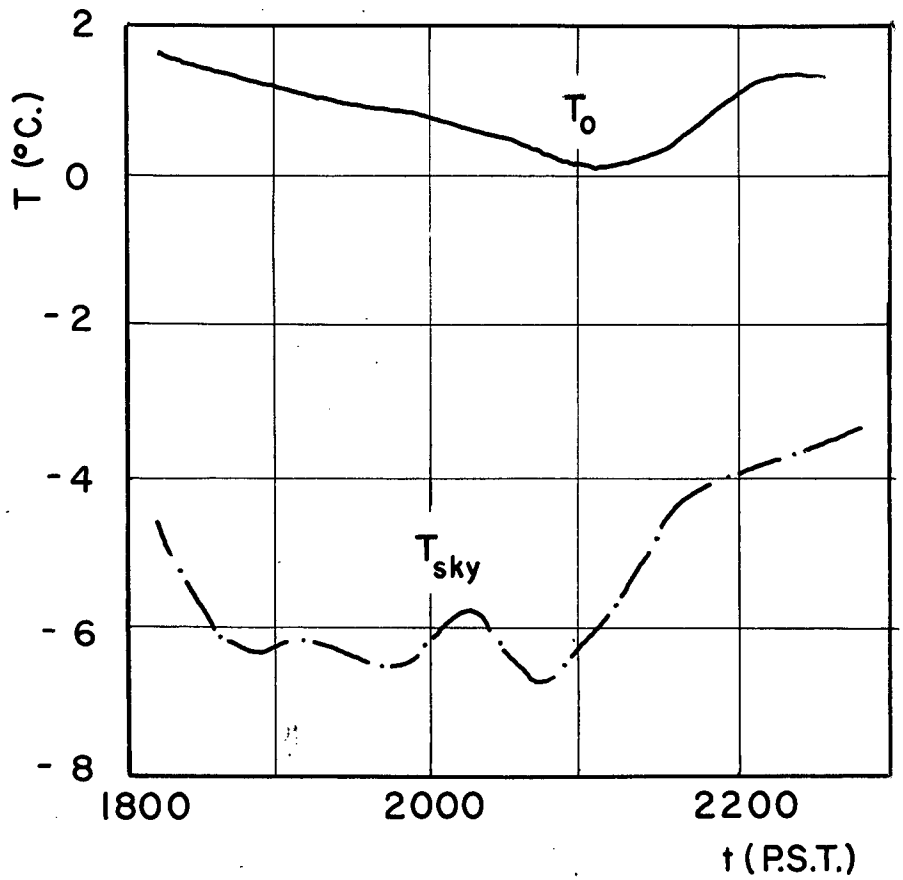

Fig. III-2. Conditions during the formation of radiation fog, 7 February 1967. The fog noticeably deepened just after 2100 P.S.T.

is always positive under inversion conditions, can terminate the cooling process and re-warm the soil surface. This re-warming is possible as the radiation fog blanket is occupying a warm portion of the atmosphere. The fog base, a radiating surface, may be several degrees warmer than the soil surface especially if the dew point at the screen level and higher is well above the ice point.

In summary, increased insight was gained in three areas from the material presented in this chapter. First, the relative magnitude of the components of surface energy exchange during needle ice growth were documented and the major heat sinks, evaporation and the night sky, available to the soil surface were located. Thus, from the energy exchange viewpoint an ideal needle ice night would be one on which both the thermal radiant and latent heat flows were directed away from the soil surface and were operating at optimum efficiency. These conditions can be produced in nature by a clear-dry-cold atmosphere above a warm-wet soil surface. The larger the contrast between atmospheric temperature and humidity, in comparison to soil surface temperature and humidity, the greater the efficiency of the radiation-evaporation cooling mechanism is and the more reduced the probability of re-warming due to either radiation fog or dew formation is. Second, the relationship between wind speed and turbulent exchange will permit rough estimates of the sensible and latent heat flux levels using wind velocity, temperature and humidity data. Third, the efficiency of radiation fog as a terminal feedback mechanism was demonstrated.

CHAPTER IV.

A PHYSICAL INVESTIGATION OF THE STUDY SITE SOIL

In the earlier chapters the discussion centered around the climatological conditions which lead to needle ice events. However, one major aspect of the environment was largely neglected; the soil. The geometry of the soil matrix and the particle size distribution have long been recognized as indices of the "frost heave susceptibility" of a soil sample. In addition, the hydraulic conductivity and water retention properties have a considerable influence upon the processes which result from soil cooling. In this chapter the particle size distribution, water retention and flow properties, and the thermal characteristics of the study site soil will be considered.

Particle Size Distribution and Classification.

Particle size distribution in a sample of the study site soil was investigated using a combination of the hydrometer and dry sieving techniques (Day, 1965). The results of this investigation are presented in Table IV-1.

TABLE IV-1. PARTICLE SIZE DISTRIBUTION (U.S.D.A.)

Classification	CLAY	SILT	SAND			
			Very Fine	Fine	Medium	Coarse
% of sample by weight	5	20	4	14	45	12
Effective diameter (microns)	2	50	100	200	500	2000

The classification of the soil is a sandy loam according to the United States Department of Agriculture (circa. 1950) classification of soils by texture. It is also of importance to note that the bulk of the sample (75%) is in the sand size range. The sample is extremely effervescent when hydrogen peroxide is added indicating the presence of organic matter. The presence of organic matter and, perhaps, some swelling clay minerals of the montmorillonite group (Yong and Warkentin, 1966) can also be inferred by the tendency of the air dried material to swell when water is added to the sample.

Soil Thermal Properties

Estimates of the soil thermal diffusivity were obtained from temperature measurements at depths of 0.2, 1.5 and 3.0 centimeters in the sample. A heat pulse was produced by two infrared lamps located 60 centimeters above the sample and controlled by a variable transformer. The data analysis was performed using the heat pulse method (Van Wijk and Derksen, 1966). These tests were carried out at several points in the low water tension range. The soil water tension was controlled by means of a hanging water column connected to the soil sample through a semi-permeable membrane (Richards, 1941, 1948) as illustrated in Figure IV-1. The duration of the heat pulse was limited between three and six hundred seconds restricting the magnitude of the surface temperature disburbance to approximately 10^{o}Celsius. Under these conditions of evaporation at the surface and temperature increasing toward the surface, the tension and thermal gradient components of soil water flow are opposed and tend

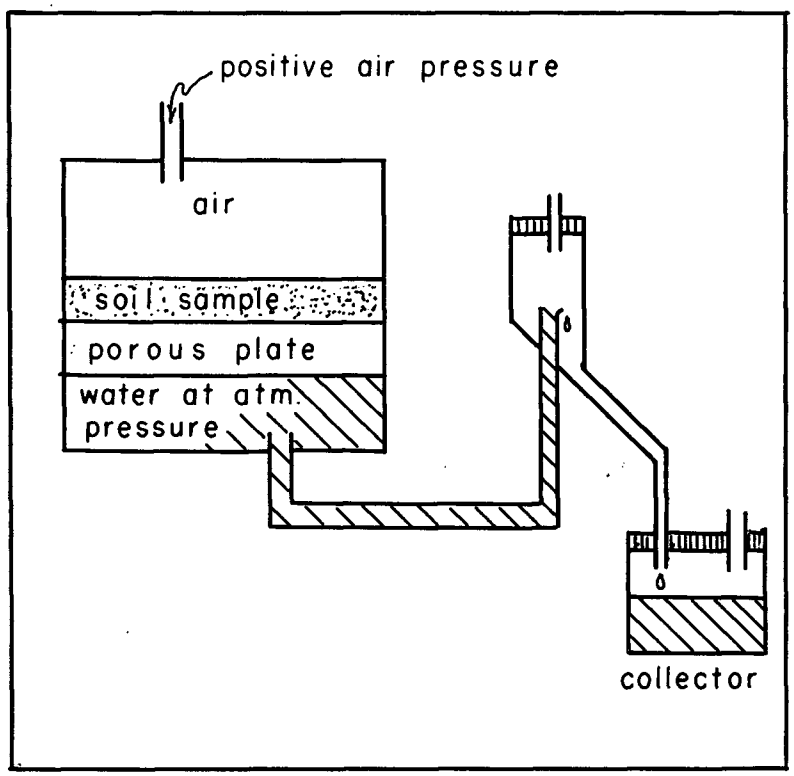

Fig.IV-1. Schematic diagram of the Porous Plate Extractor.

to cancel each other (Cary, 1965, 1966). Estimates of the volumetric heat capacity (computed from the low tension desorption curve with the aid of Equation IV-1.) and the results of the heat pulse diffusivity tests, at test tensions, are presented in Table IV-2.

TABLE IV-2. THE VARIATION OF SOIL THERMAL PROPERTIES WITH SOIL WATER TENSION AT 20°C.

Tension ($cm.H_2O$)	Heat Pulse Diffusivity ($cm.^2\ sec.^{-1} \times 10^4$)	Volumetric Heat Capacity ($cal.\ cm.^{-3}\ {}^{o}C.^{-1}$)
5	34	.50
40	56*	.47
73	52	.44
91	30	.43
151	32	.37

* structural change due to "cracking".

The variation of soil thermal properties as a function of soil water content is discussed by De Vries in Van Wijk (1966). There is a pronounced tendency for the volumetric heat capacity to decrease regularly with decreasing water content (increasing tension). De Vries (1966) gives the following method for estimating the volumetric heat capacity (C_s) of a soil from the volume fractions of water (X_w), organic matter (X_{or}) and mineral soil (X_m).

Eq. IV-1

$$C_s = X_w + 0.60\ X_{or} + 0.46\ X_m$$

This expression was used to estimate the volumetric heat capacities from the low tension desorption curve. In these estimates the organic fraction was lumped with the mineral fraction, as the independent organic content was not measured. Diffusivity (α) is related to volumetric heat capacity (C_v) and conductivity (K_v) in the following manner.

Eq. IV-2.

$$\alpha = K/C$$

It would be expected that decreasing the soil water content would produce a gradual decline in the thermal diffusivity if the conductivity remained constant. However, De Vries (in Van Wijk, 1966) indicates that conductivity is known to decline slowly with decreasing water content in a quartz sand. The net effect should then be a gradual decrease in thermal diffusivity, including the conductivity effects, with increasing soil water tension. The variation from this pattern, at a tension of 40 cm.H_2O in the experimental data, is quite probably due to structural changes in the soil sample. This condition makes estimates of volumetric heat capacity using Equation IV-1. only approximate, due to variations in bulk density. In any case, these values give reasonable computation estimates in general agreement with the estimate of the mean annual thermal diffusivity beneath the agrometeorological site which was a depth weighted mean of 45×10^{-4} $cm.^2$ $sec.^{-1}$ for the soil column between the surface and 150 centimeters.

The effect of soil water tension on the nocturnal cooling rate can be estimated by the substitution of the test values of the thermal properties listed in Table IV-1. into Brunt's cooling rule (Equation II-3.). The cooling rate, expressed as temperature divided by the square root of

time, is inversely proportional to the thermal property of the soil near the surface ($C_s \cdot \sqrt{\alpha_s}$). The thermal property varies directly with water content. Thus, in general, the drier a soil the more quickly it will cool. The maximum and minimum values of the thermal property derived from the experimental data occur at tensions of 40 and 151 cm. of water. Their ratio is approximately 1.7 which is similar to the ratio between the maximum and minimum empirical cooling slopes (m) in Table II-5. This value which was derived from field temperature decline data on similar clear-calm nights is approximately 1.8. This result suggests that with stable energy exchange conditions the entire variation in observed cooling rates could be produced by variations in near surface soil water tensions only slightly greater than the experimental range.

In this study the experimental values of the thermal properties of the soil, as a function of soil water tension, will be used as guides in selecting computation values of soil thermal properties at the study site. Where no conclusions can be drawn about the anticipated value of soil water tension the computation values are selected as 1×10^{-3} dy. sec.$^{-1}$ cm. $^{o}C^{-1}$ for conductivity and 50×10^{-3} g. cm.$^{-2}$ sec.$^{-1}$ for diffusivity.

The Theory of Ice Intrusion

It is known that some soils are more susceptible to "frost heaving" produced by ice segregation (i.e. the increased water content of the frozen soil due to water migration toward the freezing plane during soil freezing) than others. Extremely coarse soils in the sand range and dense clays are usually not "heave susceptible," whereas, medium textured soils (i.e. the

loams) are often highly susceptible. One notable attempt to relate the sensitivity of a soil to the ice segregation mechanism through the soil pore geometry was made by Williams (1966a). Following Williams, air will replace water in a capillary when:

Eq.IV-3.
$$Pa-Pw \geq (2\sigma_{aw})/r_c$$

In addition, the ratio of the interfacial energies between ice-water and air-water (σ_{aw}/σ_{iw}) is a dimensionless ratio equal to approximately .42 (Williams, 1966a). In the field problem, at the study site, the tensiometer (see appendix) measures the difference between atmospheric pressure and the pressure (here a tension) in the soil water. Thus, in the needle ice system, when the effect of overburden pressure is negligible, the air intrusion tension can be stated as:

Eq.IV-4.
$$\Upsilon_{awx} \geq \frac{2\sigma_{aw}}{r_c}$$

Still following Williams (1966a), ice intrusion near the soil surface should occur when the soil water tension at the freezing plane is greater than $.42\Upsilon_{awx}$. This statement of the ice segregation problem, which quite neatly specifies the conditions under which an ice front will advance forming a concrete ice-soil structure (i.e. soil water frozen in situ without segregation) or remain stationary at a fixed level producing an ice segregation (needle ice or ice lens), is the one result from a considerable theoretical and experimental programme (Byrnes, 1951; Everett, 1961; Penner, 1960, 1963); Sayward, 1966; Takagi, 1965; Tanuma, 1967 and Williams, 1963, 1966a-b). These workers have indicated that the freezing rate and

the soil water content exert a measurable influence upon the ice form and soil structure.

The needle ice problem is a test case for the application of this ice intrusion model. As a soil sample is moved along a desorption curve by applying a stepped pressure to it, preferably increasing the air pressure above the sample in an apparatus of the type described by Richards (1941, 1948) or used by Williams (1966a), water will be expelled from the sample. Keeping the water beneath the sample at atmospheric pressure prevents the gradual diffusion of air out of the water in the soil and into the reservoir in the base of the apparatus. This design consideration was employed by Dr. J. De Vries (Dept. of Soil Science, U.B.C.) in helping the author carry out desorption tests on the study site soil (see Fig.IV-1.). The water expelled at each pressure step is collected and weighed. An abrupt increase in the volume of expelled water should be noted when the air intrusion tension lies within the pressure step. The critical tension for ice intrusion ($\mathcal{T}_{iwx}$) is then known to be approximately 42% of this value.

The occurrence of a pronounced air intrusion value depends upon the frequency distribution of the effective pore diameters (i.e. the pore diameter that matches retention properties of the pore population in a finite volume of soil) in the sample under study. A soil sample with a uniform pore size distribution (i.e. all diameters having equal frequency over a tension range) may not be expected to show a pronounced air intrusion value on desorption. This does not indicate that the theory does not hold for this case, but rather, that it still operates at the scale of individual pores. This condition, however, does make the application of the theory untractable. This consideration may, in fact, be the theoretical varifica-

tion of the observed phenomena that soils, after slow freezing at temperatures just below the ice point, are more susceptible to ice segretation than before freezing. Freezing, especially with ice segregation, is known to loosen the soil structure (Baver, 1965). Therefore, a production of local inequalities in the pore size distribution near the surface is inferred.

The Low Tension Desorption Curve

An apparatus of the type described by Richards (1941, 1948) was used with a blotter paper-glass bead membrane, Air pressure was applied to the top of the sample to determine the low tension desorption properties of the study site soil (see Fig.IV-2.). The soil was weighed, mixed with deaired water, and puddled to a bulk density of .74 $g.cm.^{-3}$ before the pressure was applied. These manipulations permitted the volumetric water content to be recovered as the soil was initially air dried, with a known water content, and a running account of the sample water budget maintained during the test. Pressure increments of 10 $cm.H_2O$ were applied and a time period of at least six hours was allowed for the sample to attain equilibrium before the next step. This run was terminated by the failure of the blotting paper membrane at the 130 $cm.H_2O$ (96 mm. Hg.) step. These data are presented in Fig.IV-2. and illustrate two facts about the sample. (1) The pores emptied by tensions in the test range have an extremely uniform effective radius distribution and (2) if a pronounced air intrusion value does exist it is above 120 $cm.H_2O$ (88 mm.Hg.).

By deduction, if (2) is valid one should expect ice intrusion at some tension above 50 $cm.H_2O$. (37 mm.Hg.). This deduction is in good agree-

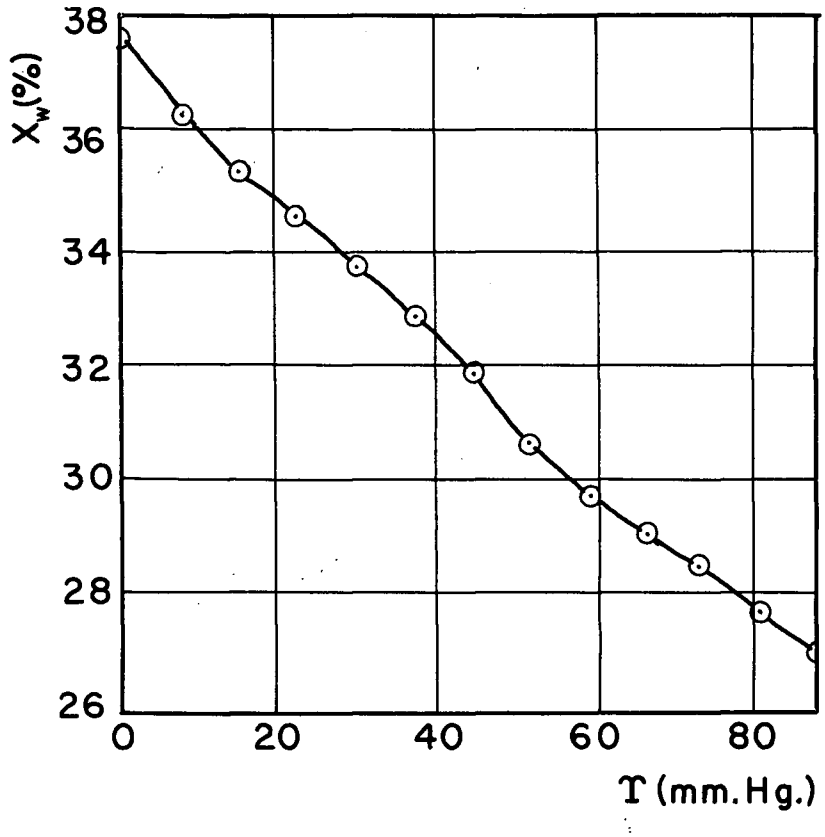

Fig.IV-2. The low tension desorption curve.
(⊙) test points.

ment with field observations as the field tensiometer (see appendix) buried at a depth of approximately 5 cm. recorded tensions of 100 to 120 mm.Hg. when needle ice was growing on the nights of 6-7 and 7-8 February 1968. The actual tension just below the freezing plane must have been even higher due to soil desiccation on freezing. It is, therefore, expected that if a pronounced air intrusion value exists in the laboratory sample it will be located in the tension region abovd 290 mm.Hg. (400 cm.H_2O.). It should be noted that the laboratory tests were carried out on disturbed samples and that the pore size distributions which determine the field conditions are in an extremely shallow layer within 2 cm. of the soil surface. Thus, laboratory studies can only be expected to produce an approximation of the natural conditions. Conversely, the study site is in a plot which is regularly disturbed by plowing and other agrarian activities and thus, the violent disturbances produced by laboratory manipulation may not greatly violate reality in the bulk sample.

The High Tension Desorption Curve

Due to the implications of the field measurements of soil water tension during needle ice growth, discussed in the previous section, it seemed advisable to run a desorption curve covering higher tensions in the realm of 300 mm.Hg.

The experimental arrangement was identical to that used for the low tension test except that a porous ceramic plate was used as the semi-permeable membrane. A 344 $cm.^3$ sample of the study site soil was saturated with de-aired water and allowed to reach an equilibrium water content

(27.2% by volume) at a tension of 100 mm.Hg. over a period of 24 hours. It was possible to compute water content by volume as the initial volume of water added to the sample was known and the volume of expelled water was measured at each step. The sample bulk density was approximately 0.95 $g.cm.^{-3}$. It will be noted that due to differences in geometry and methods of bringing the samples to an initial equilibrium, that in the region of overlap (projecting the low tension curve to 100 mm.Hg.), between the low and high tension desorption curves the volumetric water contents are slightly different. The high tension sample contains approximately 1% more water by volume at 100 mm.Hg. This value has a sign which indicates that an air intrusion point was not missed in the region between the two curves (88-100 mm.Hg.).

Pressure increments of 20 mm.Hg. were applied over one day periods. This equilibrium time was necessary because of the relatively high impedence of the ceramic plate. The results of this test are illustrated in Figure IV-3. The resulting curve indicated, as in the low tension test, a relatively uniform pore size distribution and no pronounced air intrusion value. This outcome further strengthens the author's opinion that in the needle ice system the operational air intrusion value is not a bulk property of the soil sample and cannot be treated as it is in the deeper ice lens system (Williams, 1966a). Instead, it is a property of the upper 0-2 cm. near surface of the soils (sandy-loans, loamy-sands) which are susceptible to needle ice formation. The pore-particle geometry of this near surface zone is in a constant structural flux during the needle ice season not only due to frost phenomena, but also due to the effects of rain splash and sheet wash, etc.

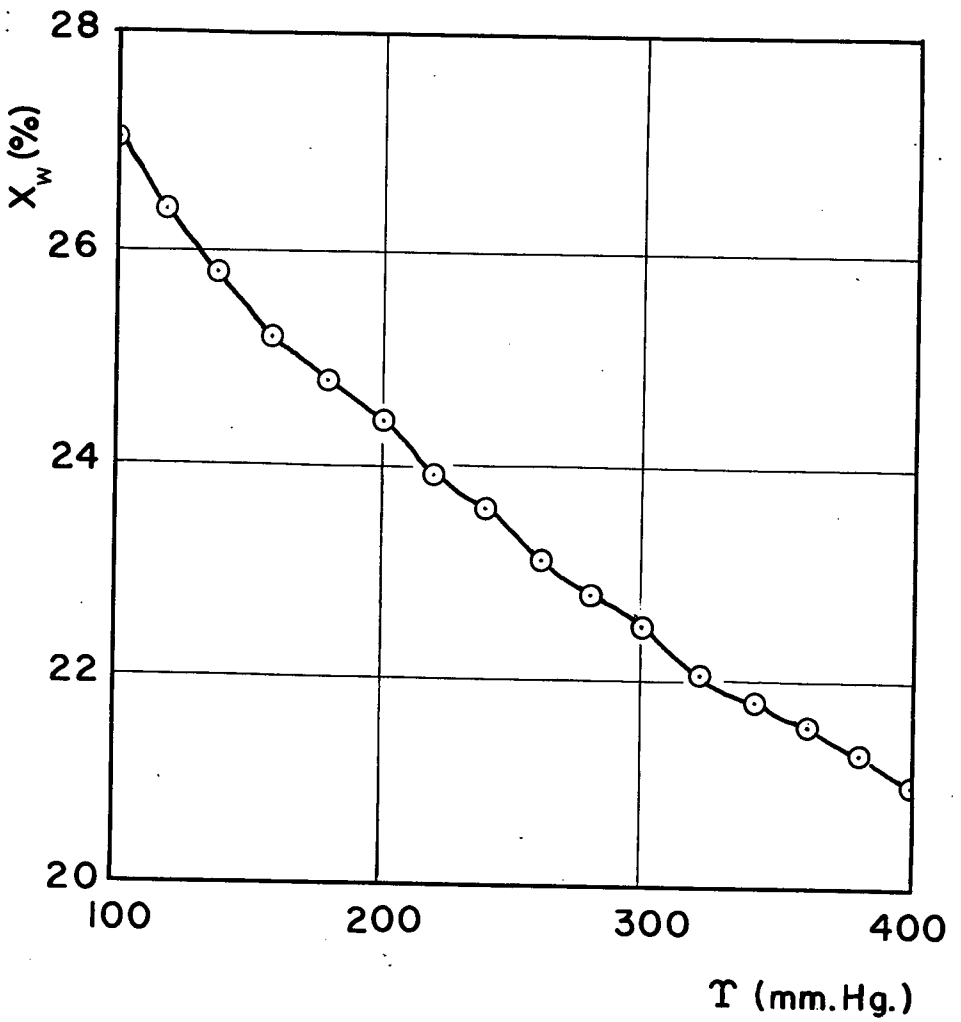

Fig.IV-3. The high tension desorption curve.

These conditions limit the range of experimental methods available for specifying the critical ice intrusion tension in the needle ice system. Two possible methods of attack are (1) the application of air intrusion tests to thin (1-2 cm.) slices of surface soil samples expelling the water in situ and (2) continued observations of soil water tension during natural freezing events. Both of these approaches require the development of new or modified instrumentation. The first would require a device similar to that used by Williams (1966a), but modified to permit the introduction of undisturbed field samples. The second would utilize an extremely small recording tensiometer which could be placed within 1 cm. of the soil surface.

The Big Step Water Expulsion Curve

A test of the water expulsion-tension properties of the study site soil was run using the same apparatus and soil sample used in the high tension desorption test. The sample was allowed to take up water for a 72 hour period at a tension of 0 mm.Hg. The sample was then subjected to a 100 mm.Hg. tension increase at 24 hour intervals. Before each increased tension step the accumulated amount of water expelled from the sample was determined. The results are listed in Table IV-3.

TABLE IV-3. TENSION-WATER EXPULSION

Tension (mm.Hg.)	Accumulated Expelled Water ($cm.^3$)
0	0.0
100	68.4
200	80.4
300	86.6
400	91.0

These results were plotted on linear graph paper transforming both tension and expelled water volume to their natural logarithms. The relationship between these variables is listed in Equation IV-5.

Eq.IV-5

$$\ln E = .21 \ln T + \ln 3.3$$

The expelled water volumes estimated from this graphical fit were within the realm of possible experimental error (1 $cm.^3$) indicating that the tension-expulsion relationship is well represented by an exponential function which produces a curve without an "S" type inflection exhibited by soils having pronounced air intrusion values (Williams, 1967). These data further substantiate the interpretation of the preceding sections and, in addition, indicate the absence of an "S" type expulsion curve. Inflections of the "S" type are quite probably uncommon in well packed disturbed samples with approximately 75% of their particles in the sand textural range.

Rapid Expulsion Testing

Williams(1966a) tested the study site soil in his air intrusion apparatus at the Soil Mechanics Section of the Division of Building Research, National Research Council, Ottawa. His unit uses a much shorter interval between tension steps (0.5 - 1.0 min.) and does not establish the desorption curve of the soil. The results indicated a larger variation in air intrusion values of .15, .21, .25 and .05 $Kg.cm.^{-2}$. The last result of the series was considered "anomalous" and the remaining values were considered to have "larger divergence in the three results than normally found". This divergence was attributed by Williams to the wide grain size distribution and the problem of obtaining uniform samples. This author would add that in addition these results indicate differences in pore size distribution resulting from variations in bulk density and geometry within ("uniform") samples during laboratory manipulation. Ice intrusion, according to Williams' reports, is to be expected in the tension region of 46-86 mm.Hg. The Williams method of testing is more practical than the long equilibrium desorption methods used by the author for obtaining air intrusion values as the method is much faster. However, the divergence of results and the proximity of Williams' values to tension measurements at a depth of 5 cm. during field needle ice growth (100-120 mm.Hg.) indicate the realm of the critical ice intrusion value for the study site soil is highly variable and in the realm of 100 mm.Hg.

The Unsaturated Hydraulic Conductivity

The unsaturated hydraulic conductivity of the soil was determined by applying air pressure to the sample and varying the head across the sample, which was 2.5 cm. thick. The cross section area of the porous membranes, between which the sample was placed, was 136 $cm.^2$. The results of this test are presented in Table IV-4.

TABLE IV-4. UNSATURATED HYDRAULIC CONDUCTIVITY

Soil Water Tension (mm.Hg.)	Conductivity (10^{-7} cm. $sec.^{-1}$)
0	990
22	740
49	82
88	16
141* shrinking	4

It should be remembered that this test does not duplicate the field situation as the experiment was run under isothermal conditions at a temperature of 20°C. When hydraulic conductivity is plotted as a function of tension on semi-log paper (see Fig.IV-4.) the steepest portion of the curve is in the region of 50 mm.Hg. and no sharp changes in slope are evident at higher tensions where the effects of air intrusion might be expected.

It is interesting that three orders of magnitude were covered in the 0-141 mm.Hg. tension range. This suggests that at some point the inability of a desorbing soil to transmit water at the fusion rate to the freezing

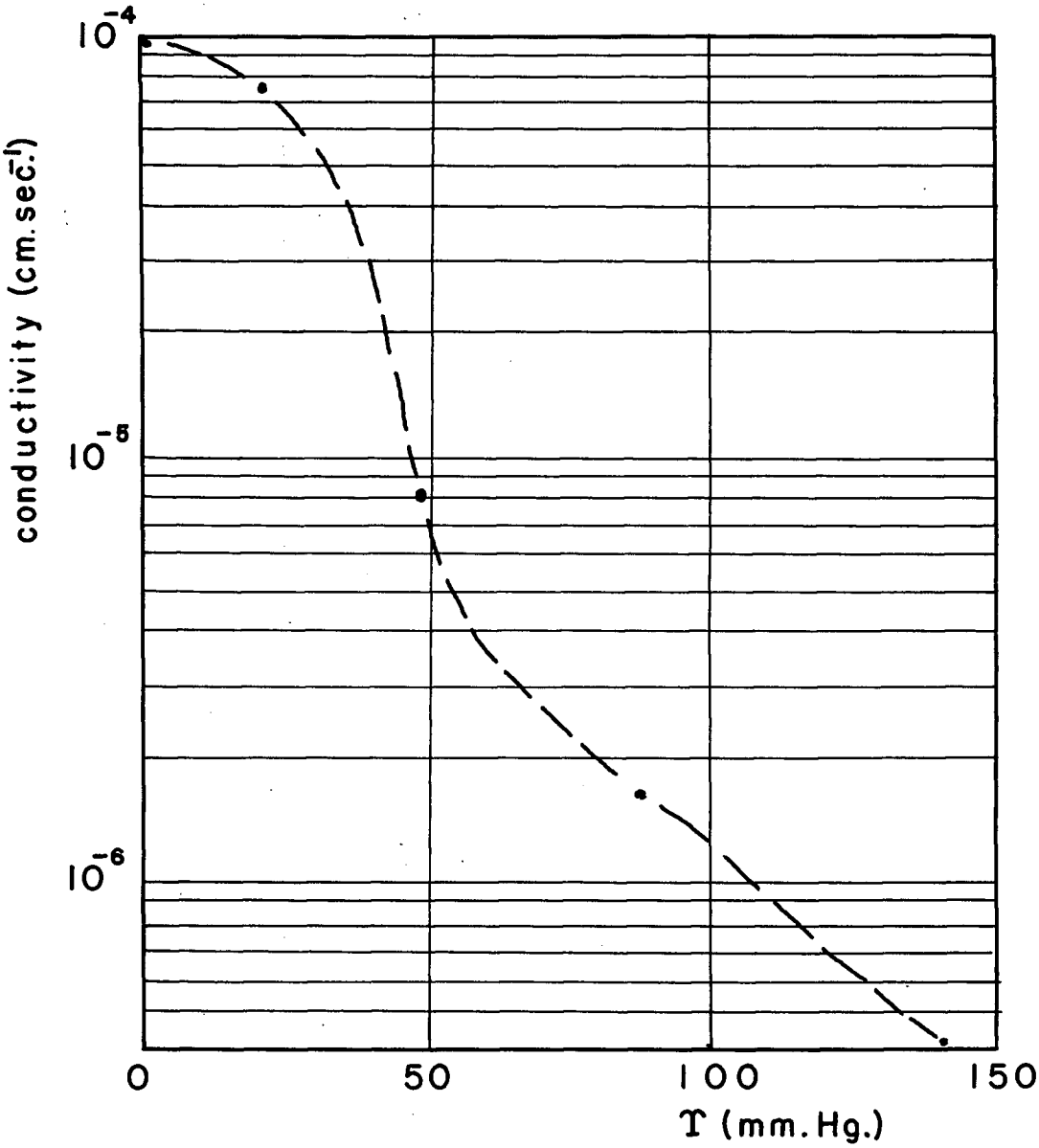

Fig.IV-4. The hydraulic conductivity-tension curve under isothermal conditions at 20°C. (•) sample points.

plane should produce dessication and ice intrusion. It was impossible to follow this line of investigation due to the absence of field data on water table depths and tension gradients during needle ice formation.

In summary, the material in this chapter reports some of the physical characteristics of the study site soil and examines the ice intrusion model as a method for estimating the effects of variable soil water content (tension) on needle ice growth. It is found that this approach in practice is complicated by the fact that ice intrusion in the near surface soil (0-2 cm.), where segregation occurs during needle ice growth, is dependent on both soil water tension and soil structure (effective pore radius). As structure and tension near the surface are time dependent in nature, laboratory tests which destroy near surface structure were found to be of limited value in the analysis of needle ice growth. The results, reported in Chapter VI., of soil tension measurements at the study site which were made in conjunction with post-freezing observations of soil conditions provide a more efficient means of examining tension effects on the needle ice system.

As the highest measured values of soil water tension occurred during needle ice growth; it is reasonable to believe that tension is only a limiting factor at the study site during unusually dry periods within the needle ice season and at better drained sites in the Vancouver area. However, at the study site soil water tension gradients appear to have a pronounced effect upon the depth of the normally frozen soil layer or cap which rides atop needle ice growth (see Chapter IV.) and the nocturnal cooling rate.

CHAPTER V.

THE ANALYSIS OF THE PAST EVENT RECORD

At the agrometeorological site adjoining the study site a unique record of needle ice events has been compiled covering the period from 1964 onward (the record actually begins in 1961 at another site on the University of British Columbia Campus). It is the purpose of this chapter to analyse this record to discover if additional information about the nature of needle ice events is forthcoming from a statistical analysis of routine meteorological data.

The Statistical Model

In an attempt to produce a model that could be used at the study site to estimate the probability of a needle ice event, it was decided to develop a statistical model based upon an examination of the 1615 P.S.T. air temperature, relative humidity, dewpoint temperature and the nocturnal wind velocity and cloud cover. The data used was the record of all months when needle ice events occurred during the period from 1964 through 1967.

These data were divided into two groups, the data collected during 1964-65 and that collected during 1966-67. These data were tested using the Kolmogorov-Smirnov test to examine the probability that the data belong to a known distribution (Siegel, 1956). The results are as follows:

TABLE V-1. THE RESULTS OF K-S TESTING

Hypothesis	Result of Hypothesis Testing
The 64-65 variables in the non-event group are normally distributed.	Reject at the .05 level for cloud cover. Accept at the .05 level all other variables.
The 64-65 variables in the event group are normally distributed.	Accept at the .05 level all variables.
The 64-65 event variables are a sample from the distribution of non-events.	Accept at the .05 level all variables.

These test show that all the variables appear to have reasonably normal distributions about their means, with the exception of cloud cover which is skewed to the high value side of the mean in the non-event group.

The variables in the 64-65 event and non-event groups were also tested for homogeneity of variance using the F-distribution (Alder and Rossler, 1962) with the following results.

TABLE V-2. RESULTS OF F-TESTING FOR HOMOGENEITY OF VARIANCE

Variable	Results at 5% Level
air temperature	not homogenous
relative humidity	not homogenous
dew point	homogenous
wind speed	homogenous
cloud cover	homogenous

Because of these results, it was necessary to set up the following hypothesis to test the variable means for significant differences between the event and non-event groups. The assumption was made that the population parameters were defined by the 64-65 non-event group and then the hypothesis was tested that the event group variables were random samples from this population. The results of a T-test for significant differences in the variable means of the two groups are as follows (Alder and Rossler, 1961):

TABLE V-3. THE RESULTS OF THE T-TEST FOR SIGNIFICANT DIFFERENCES BETWEEN GROUP VARIABLE MEANS

Variable	64-65 non-event Means (Variance)	64-65 event Means (Variance)	T-test Results at the .001 level
air temp.* (^{o}F.)	41.9 (52.7)	39.7 (21.1)	Reject
relative humidity* (%)	84.8 (148)	72.0 (345)	Reject
dew point (^{o}F)	37.4 (59)	30.6 (59)	Reject
wind speed (m.p.h.)	3.33 (2.9)	2.54 (2.9)	Reject
Cloud cover (tenths)	6.7 (10.1)	3.1 (10.1)	Reject

*variance non-homogenous

Thus, there are statistically significant differences in the mean values of variables measured on event and non-event nights. As one would expect, the air temperatures are cooler on event evenings at 1615 indicating more rapid surface cooling under clear skies. In addition to the reduced cloud cover on event nights, the atmosphere is also drier as

shown by the lower relative humidity and depressed dewpoint. It should be noted that these are precisely the variables used in empirical estimates of the thermal radiation balance (Sutton, 1953) and that a relatively dry, cloudless atmosphere, with reduced wind, presents excellent conditions for the rapid cooling of the soil surface (Veitch, 1960). The variance of air temperature is somewhat less and the variance of relative humidity is greater on event nights, whereas the variances of the other variables appear similar. Thus, by showing a near normal distributions and significant differences among variable means in the event and non-event groups the stage has been set for an attempt to produce a statistical model for event prediction.

All pairs of variables were examined using discriminant analysis to determine which of these variable pairs gave the best indication (discrimination) of needle ice events in the 64-65 data. The variable symbols are listed below:

TABLE V-4. VARIABLE LISTING

Symbol	Meaning	Units
T	1615 air temperature	°F.
RH	1615 relative humidity	%
DP	1615 dew point temperature	°F.
W	nocturnal wind speed	m.p.h.
N	nocturnal cloud cover	tenths

The application of the BMD 04M discriminant analysis programme, which was developed by the Health Sciences Computing Facility at the University of California, to these data yielded two matrices which are of interest in

evaluating the sensitivity of the variable pairs for discrimination. These are the Mahalanobis D^2 statistic, which is an estimate of the probability of misclassification, and the F-statistic, which indicates if there is a significant difference between the mean values of the discriminant function between groups (Freese, 1964). Due to the characteristics of these statistics, their maximum values should indicate the best variable combination for discrimination.

TABLE V-5. MAHALANOBIS D^2 MATRIX, 64-65 DATA

	T	RH	DP	W	N
T	--	1.02	1.13	.32	1.80
RH		--	1.07	.97	1.60
DP			--	.93	2.13
W				--	1.38
N					--

TABLE V-6. F- MATRIX, 64-65 DATA

	T	RH	DP	W	N
T	--	10.8	11.9	3.4	19.1
RH		--	11.3	10.3	16.9
DP			--	9.9	22.5
W				--	14.7
N					--

It will be noted that the most sensitive variable pair is the dew point - cloud cover combination, which indicates the overriding influence of thermal back radiation in needle ice and frost forecasting (Vietch,

1960). In this case, the F-statistic is significant at the .001 level. The probability misclassification estimated from the Mahalanobis D^2 statistic is approximately 23%. These results are consistent with the program output which yields the following results.

TABLE V-7. CLASSIFICATION OF THE 64-65 DATA BY DISCRIMINANT ANALYSIS

	Events	Non-Events	Sum
Correct Group	19	109	128
Incorrect group	6	35	41
sum	25	144	169

The actual misclassification was 41/169 or approximately 24%, which indicates that the assumption that D/2 can be treated as a standard normal deviate appears justified in this case, even though it will be recalled that the cloud cover variable failed the K-S test for normality at the 5% level. This most sensitive two variable equation is as follows:

Eq.V-1. Discriminant Function derived from the 64-65 data.

$$L = -.00068\ DP - .00228\ N + .03438$$

event region when $L > 0$

Eq.V-2. Plotting form of the Discriminant Function (see Fig.V-1.)

$$DP = -3.35\ N + 50.6$$

The 1966-67 data were run using the event region defined by the analysis of the 1964-65 data with the following result:

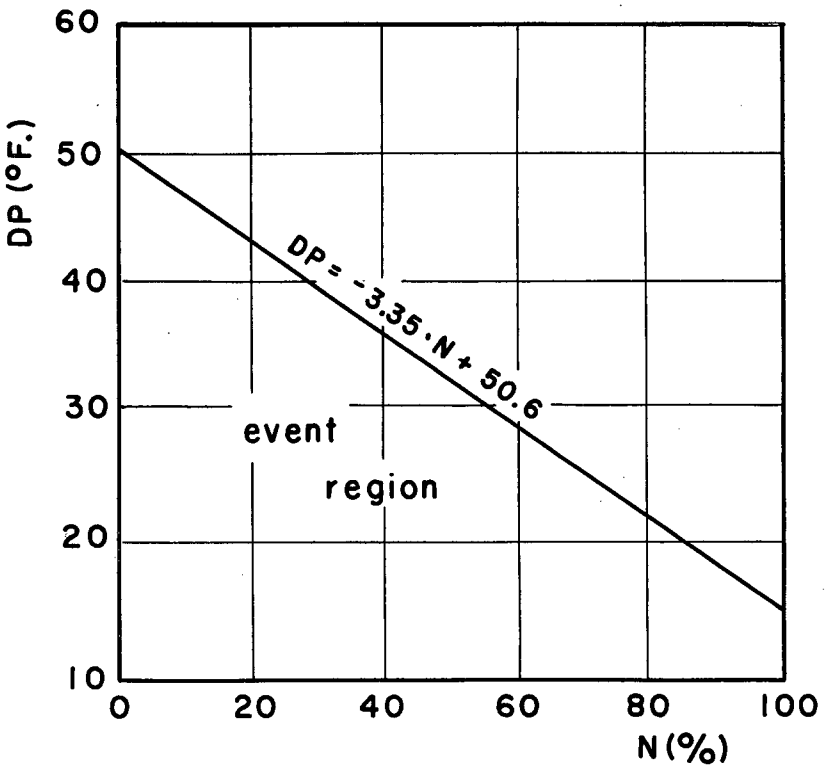

Fig. V-1. Regions defined by the discriminant analysis of dew point (DP) and cloud cover (N) from the 1964-65 data.

TABLE V-8. CLASSIFICATION OF THE 66-67 DATA.

	Events	Non-Events	Sum
Correct Group	23	180	203
Incorrect Group	8	30	38
Sum	31	210	241

The total misclassification of items was 38/241 or approximately 16% which was better than the classification for the original data. In addition, the misclassification of events was 8/31 or approximately 26% in the anticipated realm, whereas, the misclassification of non-events was 30/210 or approximately 14%, which, though not anticipated, must be put down to good luck at this stage.

Radiosonde Data

The statistical model indicated that thermal radiation from the sky hemisphere was a major factor in limiting the frequency of needle ice events. Because of this situation the amount of precipitable water in the atmosphere is a critical factor which must exert an overriding influence on the timing of needle ice events due to the effects of atmospheric back radiation.

A short analysis of precipitable water depth at Quillayute, Washington, and Port Hardy, British Columbia, was carried out over a four month period (November 1966 - February 1967) using punch card data from the United States Weather Bureau and the Canadian Meteorological Branch. A computer program was written to yield the depth of the precipitable water column between the surface and the 400 mb. levels. Canadian Department

TABLE V-9. PRECIPITABLE WATER (CM.) OVER QUILLAYUTE, WASH., AND PORT HARDY, B.C., AT 0400 P.S.T.

	Nov. 66		Dec. 66	
	Quillayute	Port Hardy	Quillayute	Port Hardy
1	1.02	2.37	(1.53)	1.18
2	0.97	1.08	1.24	1.13
3	1.61	1.87	1.28	0.89
4	1.26	1.52	1.07	1.07
5	1.82	(0.96)	0.93	0.77
6	0.65	0.67	1.11	(0.44)
7	0.90	0.97	0.85	0.48
8	(0.76)	(1.01)	0.64	0.55
9	1.73		0.95	0.95
10	0.57	0.59	1.57	1.28
11		0.75	1.82	1.54
12	0.84	1.00	1.44	1.01
13	1.21	0.79	1.65	1.20
14	1.24	1.15	1.04	1.08
15	1.05	1.07	1.76	1.63
16	1.10	0.79	1.69	1.09
17	1.16	0.95	1.65	1.42
18	1.52		(1.77)	(1.22)
19	(1.67)	1.59	(1.73)	(1.74)
20	1.22	1.26	0.90	
21	1.20		0.93	1.08
22	0.96	1.09	0.65	0.88
23		0.85	1.17	0.91
24	(1.41)	1.57	1.24	1.12
25	(1.70)		0.78	0.61
26	0.76	0.88	0.74	(0.64)
27	1.37	1.22	0.78	
28	(1.24)	0.65	1.30	1.40
29	1.55	0.77	1.63	
30	1.35	0.89	1.63	
31			0.99	1.35

_____ needle ice event. ( ) neglect in analysis.

TABLE V-9 (Cont.) PRECIPITABLE WATER (CM.) OVER QUILLAYUTE, WASH., AND PORT HARDY, B.C., AT 0400 P.S.T.

	Jan. 67		Dec. 66	
	Quillayute	Port Hardy	Quillayute	Port Hardy
1	0.84	0.92	(1.15)	(1.08)
2	1.42	1.41	(1.45)	(1.56)
3	0.92	0.91	1.64	0.88
4	1.11	0.67	1.81	0.72
5	0.56	0.51	0.80	0.88
6	0.90*	0.94	1.15	1.16
7	1.31*	1.30	0.93	0.99
8	(1.72)	0.75	0.84	1.30
9	1.09	1.58	1.33	
10	1.01	1.61	0.94	0.97
11	0.92	0.97	1.43	(1.29)
12	0.98	1.00	1.27	(1.13)
13	1.17	0.91	0.87	0.79
14	1.50	1.51	0.69	0.70
15	(1.54)	(0.85)	(0.88)	(0.79)
16	0.85		(0.99)	(0.95)
17	0.82	0.91	1.63	1.56
18	1.20	1.22	0.93	0.90
19	1.34	1.25	0.62	0.81
20	1.14	1.01	0.67	1.11
21	0.80	0.80	0.81	0.89
22	0.82	0.75	0.79	
23	0.86	0.77	1.11	1.37
24	0.70	0.58	0.90	0.83
25	0.92	0.54	0.87	1.06
26	1.20	0.91	1.05	1.17
27	1.62	1.19	0.89	
28	1.45	1.26	1.30	(0.89)
29	1.53	1.10		
30	0.78	1.54		
31	0.69	0.53		

_____ needle ice event.
( ) neglect in analysis.
* snow on surface at Vancouver.

of Transport synoptic charts prepared for the same observation time as the radiosonde launch (0400 P.S.T.) were examined to determine if air mass conditions at the radiosonde sites were obviously different from Vancouver. The results of these computations are presented in Table V-9.

It will be noted that there is a general tendency for needle ice events to occur when the depth of the precipitable water column declines. It is also interesting to note that needle ice events quite frequently occur toward the end of a low precipitable water spell after there has presumably been sufficient time for the soil surface to cool to a temperature near the ice point.

Synoptic conditions during the eight needle ice event groups in this period were examined on United States Weather Bureau daily charts to determine if recurring patterns leading to needle ice events could be recognized. The results of this investigation are shown in Table V-10.

TABLE V-10. AIR MASS DATA 1966-67

Event Date	Air Mass Type*	Circulation over Vancouver
10-11 Nov.	cA Front near/ Pacific High	SW quad. High
26 Nov.	Pacific High	NE, NW quad. High
8-9 Dec.	cA Front near	SE quad. Low
24-25 Jan.	cA Front near	NE quad. High
31 Jan.	Pacific High	center High
7 Feb.	Pacific High	NE, NW quad. High
13-14 Feb.	Pacific High	NE quad. High
18-21 Feb.	cP over Vancouver	NE, NW quad. High

*cP,cA (continental polar and arctic air masses)

Although this record is brief it was possible to recognize two distinct patterns which lead to needle ice events. (1) Those events during which Vancouver was located in the northeast to northwest quadrants of a Pacific High as it crossed the coast moving eastward and (2) the invasion of Arctic or Polar air into the Fraser Lowland. In addition, there appear to be frequent combinations of these types. This occurs when the lower Fraser Valley is either located in a limb or northern sector of a Pacific High and a front of Arctic/Polar continental air is located within 50-100 air miles northeast of Vancouver. Under this latter condition it is impossible to determine the distribution of cold continental air in the rugged topography of southwestern British Columbia without a more detailed study.

An examination of the computer output for the statistical model during this test period indicated that this model was quite sensitive to precipitable water depth variations and that the failure in event prediction, when events were predicted but did not occur, resulted from real reductions in precipitable water depths over Vancouver. This indicates that prediction failure is largely the result of near surface and soil conditions and not a model failure in estimating gross thermal radiation conditions, excluding radiation fog, from limited cloud cover data.

In summary, a two variable discriminant function was developed from the standard weather data. This model was correct in placing a night in the event or non-event group better than 75% of the time. In addition the model was demonstrated to be quite sensitive to real variations in precipitable water depth over Vancouver. This analysis illustrates the overriding influence of the gross thermal radiation environment on empirical models and real event frequency. Model failure must largely result from variations in the near surface micrometeorological environment, which is the topic of the next chapter.

CHAPTER VI.

TIME DEPENDENT PROCESSES

The earlier chapters have described the nature of some processes active on event nights and the environmental conditions which accompanied needle ice growth. These observations in conjunction with the examination of the past event record demonstrated the necessity for an exploration of the nature and interaction of the time dependent processes of water and energy transfer near the soil surface. This chapter will explore some of these processes with an increased emphasis upon the dynamic nature and interaction of the phenomena under investigation.

Polycyclic and Monocyclic Needle Ice Events

Two distinct types of needle ice growth were recognized, during the 1967-68 observations, those produced by a single cycle of growth and those which continued to grow for several days. The conditions which determines whether a growth will be monocyclic or polycyclic is a complex function of terrain and climate. The observed cases of polycyclic growth were on a north facing water saturated road bank next to a forest margin and in a flower bed on the northern side of a four foot wooden fence. These two sites had one major feature in common. Both were located where they were shaded from direct beam radiation during most of the daylight hours.

The effect of this shading is easily demonstrated by shading the net radiometer at the study site. This net radiometer was shaded from beam radiation between 1345 and 1350 P.S.T. on the afternoon of 10 March 1968. The result was a change in the net radiation flux from 290 mly./min.

directed toward the surface to a value of 97 mly./min. directed away from the surface toward the cloudless sky. The radiation balance at shaded sites is determined by the thermal radiation budget and the absorption of diffuse hemispherical short wave radiation, which is usually assumed to have a value in the neighborhood of 10% of the absorbed beam radiation. As a further illustration, it was noticed that while the needle ice at the back fence flower bed was often polycyclic, a similar flower bed next to the south wall of the house, exposed to beam radiation, was producing a sequence of monocyclic growths which completely melted during the daylight hours. It would seem that an ideal site for the development of large polycyclic deposits would be one with a plentiful water supply in a position shielded from beam radiation during the cold season, namely those conditions which exist at north facing wet bank sites.

Photographs of monocyclic and polycyclic growths are presented in Figure VI-1. The new (youngest) layers of the compound growths are at the base, in contact with the soil which is the source of water for growth (Fujita et. al., 1937). There may be an exception to this rule when impermeable frozen ground thaws at the surface during the day and ice needles form during the following evening.

The diurnal layers of a polycyclic deposit are usually separated by a thin layer of ice which runs horizontally between the vertically oriented needles of different ages and is sub-parallel to the soil surface. This layer is believed to form during the daylight hours when energy sources at the surface diminish the heat flux through the needle ice and the thermal gradient in the needle ice is not sufficient to transport all of the heat arriving from the warm soil layers at depth. As a result melting occurs

Fig.VI-1. Monocyclic (above) and polycyclic (below) needle ice.

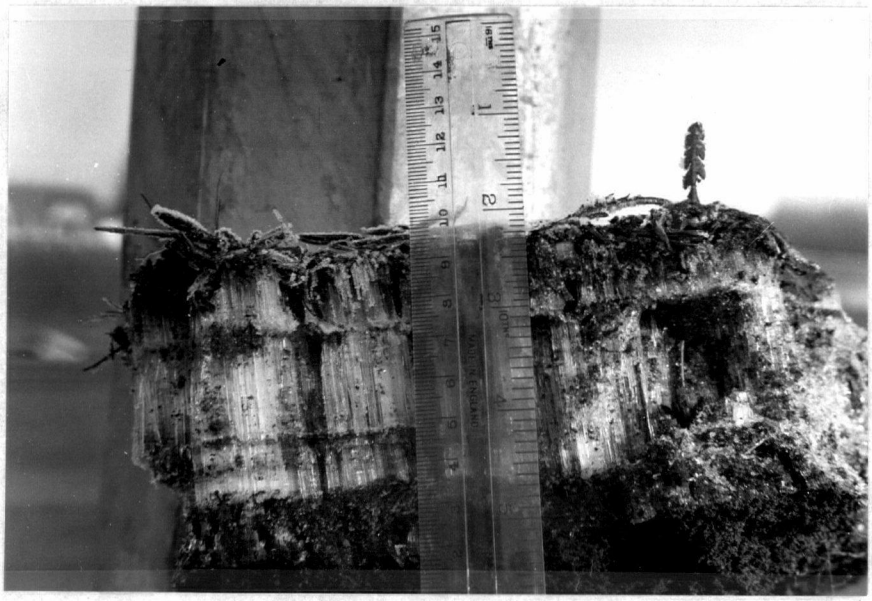

at the base of the needles. This hypothesis is substantiated by soil heat flux measurements made during the extended period of needle ice growth which ran from 10 December 1967 through 21 December 1967, when polycyclic growth was occurring beneath a concrete soil-ice crust at the study site. During the daylight hours the upper soil heat flux disc (pre-heave position at a depth of 0.3 cm.) was showing no heat flux, indicating that it had become entrapped in isothermal melting needle ice; the lower disc (pre-heave depth 3.3 cm.) was recording a heat flow directed toward the surface and the base of the needles. Values recorded during a typical period of this type are presented in Table VI-1.

TABLE VI-1. SOIL HEAT FLUX TOWARD THE SURFACE, 13 DECEMBER 1967.

Time (P.S.T.)	Upper Heat Flux (mly./min.)	Lower Heat Flux (mly./min.)
0800	15	11
1000	00	11
1200	00	11
1400	00	11
1600	00	11
1800	27	11

Other measurements in the 1967-68 series showed that even during extended polycyclic events the surface temperature frequently climbed above the ice point, indicating that the needle ice was melting from both above, due to heat imput from the atmosphere and solar radiation, and below, by conduction of heat from the warmer soil layers at depth. Typical temperature data of this type are shown in Table VI-2. using the original probe

depths as position indicators. Only the surface probe position and the 3 cm. spacing between the buried probes, which are attached to the ends of copper tubes set in a perspex slab, are reliable due to heave.

TABLE VI-2. SOIL TEMPERATURES, 16 DECEMBER 1967.

Time (P.S.T.)	Soil Temperatures (°C.) 0.0 cm.	0.3 cm.	3.3 cm.
0800	-0.8	0.0	0.5
1000	2.8	0.3	0.4
1200	5.1	1.7	0.4
1400	1.6	1.6	0.5
1600	0.0	0.0	0.5
1800	-0.6	0.1	0.5
2000	-0.7	0.1	0.5
2200	-1.3	-0.2	0.5

These data demonstrate the ablation of needle ice from both above and below. Further, these data indicate that at the time of measurement the probe originally buried at a depth of 0.3 cm. was near the base of the needle ice when the surface began to thaw at midday. The lower probe is well below the needles in a soil layer which is well insulated from surface thermal disturbances by the diurnal growth and ablation of the ice needles above.

The downslope movement of material overlaying needle ice growths and the distinctive ground surface patterns resulting from needle ice ablation may be produced largely by the structural failure of the needles at the base due to basal melting and not a gradual melting commencing from the

top. It should be noted that, although the destructive effects of needle ice growth on plant materials have been a topic of extended discussion, these same materials below the needle ice layer are protected from both sub freezing temperatures and large diurnal temperature extremes by the growth and ablation of the ice needles above them.

Clear Sky Non-Events

There are occasions when, on a clear or near clear night during the needle ice season, nucleation fails to occur and the soil surface temperature becomes quasi-stable a few degrees above the realm of the nucleation temperature (-2°C.). This occurred during the night of 26-27 February 1968. A photograph of the study site on that evening is presented as Figure VI-2. The cloud cover varied between 10% and 30%, but the surface temperature never undercooled to the nucleation point. Cloud cover conditions were quite similar to the event nights of 16-17 February 1968 and 15-16 February 1968.

This problem may be attacked using the equilibrium temperature model described in Kreith (1967), which in effect states that the heat load across a surface will be balanced at some equilibrium temperature ($T_{\ddot{o}}$). In the needle ice problem there are two thermal conductivities ($K_{\ddot{a}}, K_s$) and two distances from the surface (Z_a, Z_s). It is known that the thermal conductivity of the air increases with wind velocity and that the thermal conductivity of the soil is a complex function of soil structure and water content. The air (T_a) and soil (T_s) temperatures at some distance from the surface are additional components of the problem. The thermal radia-

Fig.VI-2. The study site on 26 February 1968.

tion balance ($\sigma[T_{sky}^4 - T_o^4]$) is the remaining major component of the nocturnal energy transfer system, neglecting latent heat to simplify the problem. The simplified nocturnal energy conservation equation may be expressed in the form of Equation VI-1.

Eq. VI-1.

$$\sigma T_{sky}^4 - \sigma T_o^4 + \frac{K_s}{Z_s} (T_s - T_o) + \frac{K_a}{Z_a} (T_a - T_o) = 0$$

The third term, in Equation VI-1., is known from measurements in March of 1967 to have values in the realm of 52 mly./min. on clear nights with the fourth term ranging between 26 and 96 mly./min. under the same conditions. It is also known that as a prerequisite for needle ice growth, the ground surface temperature must descend to the region of -2°C. It is thus possible to use this value (-2°C.) in computing the second term. Therefore, needle ice events can be expected when the sky hemisphere has a radiant temperature between -15 and -20°C. (or below). This hypothesis is in agreement with Stoll-Hardy radiometer (see appendix) measurements on the three nights in question (see Table VI-3.).

TABLE VI-3. SKY RADIANT TEMPERATURES

Date	Radiant Temperature of Sky Hemisphere (°C.)	Outcome
15-16 February 1968	-23	needle ice
16-17 February 1968	-21	needle ice
26-27 February 1968	- 9	no event

The Sequence of Time Dependent Phenomena

It was discovered that certain important sequences during needle ice events could be easily recognized from the environmental conditions recorded at the study site. These sequences are illustrated by data taken during the needle ice event of 5-6 February 1968 (see Figure VI-3.). The same time sequence occurred on each of the following eleven nights producing a twelve event series. The events occurred during a period of clear weather, Monocyclic needle ice formed and was completely melted during each diurnal cycle. Total melting is indicated by the return of the heave meter (see appendix) to the original starting position and varified by a sudden increase in the heat flow across the upper disc. Further evidence of the complete melting of all ice nuclei, which indicates monocyclic events, is the diurnal registration of an ice nucleation thermal "snap back" (see Jumikis, 1966) on both the surface temperature trace and the soil heat flux record. The twelve event record is presented in Table VI-4.

It will be noted that several features of these events are regular during this twelve day clear weather spell, namely the net radiation balance times are close. Further, there is considerable regularity in the times when the soil heat flux turned toward the surface in the late afternoon, although this event is a function of turbulent exchange magnitudes and directions, in addition to the net radiation balance. The events which follow the soil heat flux balance show a wide scatter in their times of occurrence as the energy transfer environment is determined on clear nights by variations in the thermal properties of both the soil (e.g. heat capacity varies with water content) and the atmosphere (e.g. eddy dif-

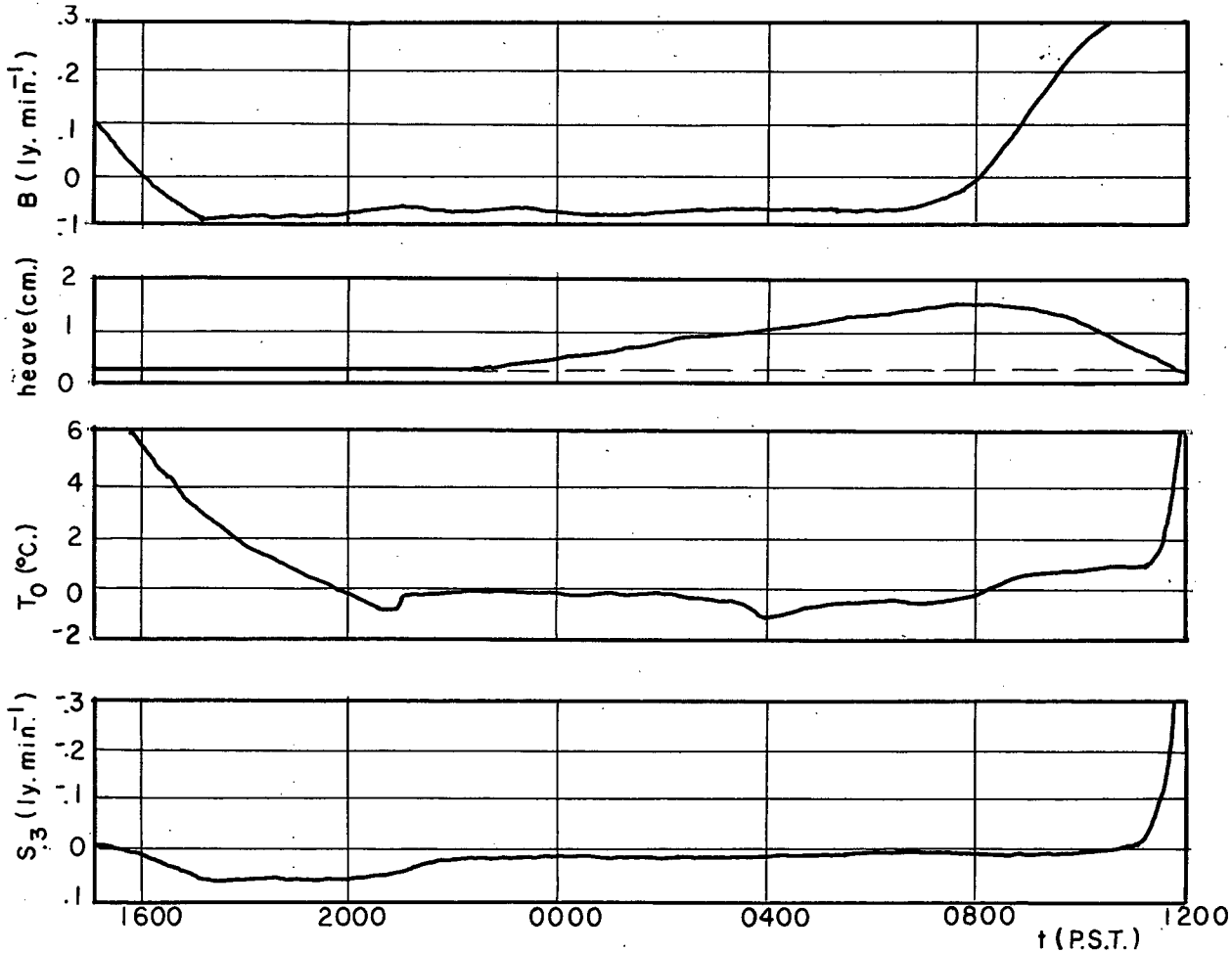

Fig. VI-3. Net radiation (B), soil heave, surface temperature (T_0), and soil heat flux (S) at 0.3 cm. during the needle ice event of 5-6 February 1968.

TABLE VI-4. SEQUENCES IN MONOCYCLIC EVENTS, 5-17 FEBRUARY 1968 (P.S.T.)

	5-6	6-7	7-8	8-9	9-10	10-11	11-12	12-13	13-14	14-15	15-16	16-17
Net Rad. Neg.	1615	1615	1600	1610	1610	1600	1615	1610	1610	1610	1615	1615
SHF Pos.	1605	1550	1615	1620	1620	1615	1630	1645	1630	1615	1620	1625
Soil Surf. cools to 0°C.	2015	2145	1955	2050	2145	2220	2040	2210	2110	1835	1805	1815
Ice Nucleation (temp.)	2100	2315	2105	2240	2340	2355	2155	2255	0040	2040	1855	1940
Ice Nucleation (SHF)	2100	2305	2050	2240	2330	0000	2150	2250	0045	2045	1855	1940
Soil Heave Begins	2215	0000	2330	0045	0230	0315	0020	0310	0400	2315	2230	2350
Net Rad. Pos.	0835	0835	0840	0835	0835	0845	0830	0840	0845	0840	0845	0800
Surface warms to 0°C.	0830	0915	0900	0915	0925	1000	0915	0915	0920	0930	0925	0825
Soil Heave Max.	0845	0940	0915	0920	0850	0915	0945	0935	0940	0945	1010	0940
SHF starts steep climb	1130	1110	1040	1015	0900	0930	0930	0920	0945	1015	1030	1115
Surf. temp.starts steep climb	1130	1105	1050	1015	0950	1000	0940	0930	0940	0930	0925	----
SHF Neg.	1140	1120	1120	1040	0950	1010	0945	0940	0950	1020	1040	1145
Heave decline stops	1120	1110	1110	1110	1010	1020	1115	1030	1035	1130	1150	1515

fusivity varies with wind velocity). Between nucleation and the time at which noticeable heave begins; the soil-ice cap, which will ride atop the growing needles, forms. The depth of this cap is dependent upon the surface soil heat flux and soil water conditions just below the surface. During this period heave is limited to a maximum value of 10% of the product of the depth of the freezing plane, and the soil water content.

The most surprising item is the temporal regularity of the completion of needle ice ablation during this measurement series. It has been noted by Mackay (1966) that the lineations on bare soil surfaces that appear during the midday, on days following needle ice events, have approximately the same orientation as the shadows from the sun at 1000 P.S.T. However, Troll (1944) believed these features to be the products of wind action. This measurement series indicates that this time is precisely centered on the period of needle ice ablation. Thus, the process which results in the lineations would be due to needle ice ablation although the precise process mechanics are obscure.

Temporal Patterns of Soil Water Tension

During the 1967-68 observations; of soil water tension was measured at a depth of 5 cm. using the tensiometer described in the appendix. Two rather persistent time dependent patterns appeared in these data which are of importance in the needle ice problem. These are the reduction of soil water tension during the late afternoon hours and the tension increase associated with ice segregation. Both phenomena occur during clear weather in the needle ice season.

On the clear sunny afternoons which characterize needle ice days during the cold season the soil water tension rises in the early afternoon and then declines rapidly shortly after the soil heat flux turns toward the surface. Records taken during the clear period of 28-29 February 1968 will demonstrate this pattern which has been given considerable attention by Cary (1965, 1966).

TABLE VI-5. SOIL WATER TENSION

Date	Time (P.S.T.)	Soil Water Tension (mm.Hg.)
28 February 68	0900	50
28 February 68	1400	82
28 February 68	1600	79
28 February 68	1715	77
29 February 68	0830	52

The pattern appears to be produced by evaporation early in the afternoon. At this time, the thermal and water content gradient components of soil water flow are opposed and the evaporation rate is so great that there is a progressive decrease in the soil water content as the surface is approached. This produces a tension increase at the measurement level, due to an advancing drying front. Later in the afternoon the thermal gradient near the soil surface becomes negative and soil temperature increases with depth, causing both the thermal and water content flow components to be directed toward the surface. A soil water tension decline is frequently recorded shortly after this event. This tension decline would appear to represent the effect of the thermal component of the soil water flow overriding evaporation losses in the presence of continued flow

down the water content gradient, as the evaporation rate decreases with surface cooling.

A further characteristic of this pattern is illustrated in Fig.VI-4., which is derived from data taken on the clear non-event night of 26-27 February 1968. It will be noted that the tension decrease was at first rapid, stabilizing at about 2000 hours, and slowly declining thereafter. This pattern is believed to result from the increase in measurement level enthalpy produced by the vertical flow of warm water from lower soil layers to the measurement level. The thermal gradient which initiated the flow is weakened by the arrival of warm water from the lower soil zones which are under the influence of the diurnal heat wave. It would appear that the slope break in the tension-time curve at 2000 hours resulted from both a reduction in the thermal gradient and the response of the soil water flux rate to the reduced nocturnal evaporation rate, once the effective conduit diameter has been increased by the decline in soil water tension (see Fig.IV-4.). The effect of water flow in reducing the rate of cooling in the soil layers beneath growing needle ice was noted by Kinosita et. al. (1967) who calculated the vertical velocity of soil water flow to the freezing plane from the notable reduction in subsurface cooling rates.

The major importance of the thermal gradient component of vertical soil water flow in the needle ice problem is that this process, <u>in effect</u>, wets and prepares the near surface soil for a needle ice event because freezing point depression and, perhaps, ice nucleation, (Palmer, 1967), are dependent upon soil water tension. Of prime importance, needle ice growth velocity is strongly dependent on soil water tension and a low water

tension environment is necessary for the initiation of needle growth (ice segregation, a more complete discussion in Chapter IV.). Further, at low tensions the hydraulic conductivity of the soil is increased; facilitating water flow to the freezing plane. To maintain needle growth sufficient water must reach the freezing plane to match the fusion rate. If this condition is not satisfied, the soil below the freezing plane dries, tension increases and ice intrusion follows.

The second phenomena, a tension increase during ice segregation, is well documented, but infrequently measured in the field (Williams, 1966a). As ice segregation begins there is a reduction in the soil water content of the unfrozen region beneath the freezing plane producing a tension gradient which drives water vertically toward the freezing plane. The plot of soil heave and water tension on two growth-ablation cycles, 6-8 February 1968, (see Fig.VI-5.) demonstrates the range of diurnal soil water tension variations during a twelve day sequence of monocyclic needle ice events. This diurnal sequence produced low water tensions after ablation. It should be noted from this record that soil heave begins just after the tension increase which indicates dessication due to ice segregation above the water tension measurement level at a depth of 5 cm. During the time period between nucleation and soil heave, the freezing plane is assumed to be advancing downward, forming the concrete soil-ice cap structure without segregation.

A major fact is that the highest tensions recorded at the 5 cm. depth were recorded during needle ice growth. This indicates that the water content (soil water tension) gradient does prohibit ice segregation when there is sufficient time for the freezing plane to descend below the uppermost soil layers into the region 2 cm. below the surface. However, above

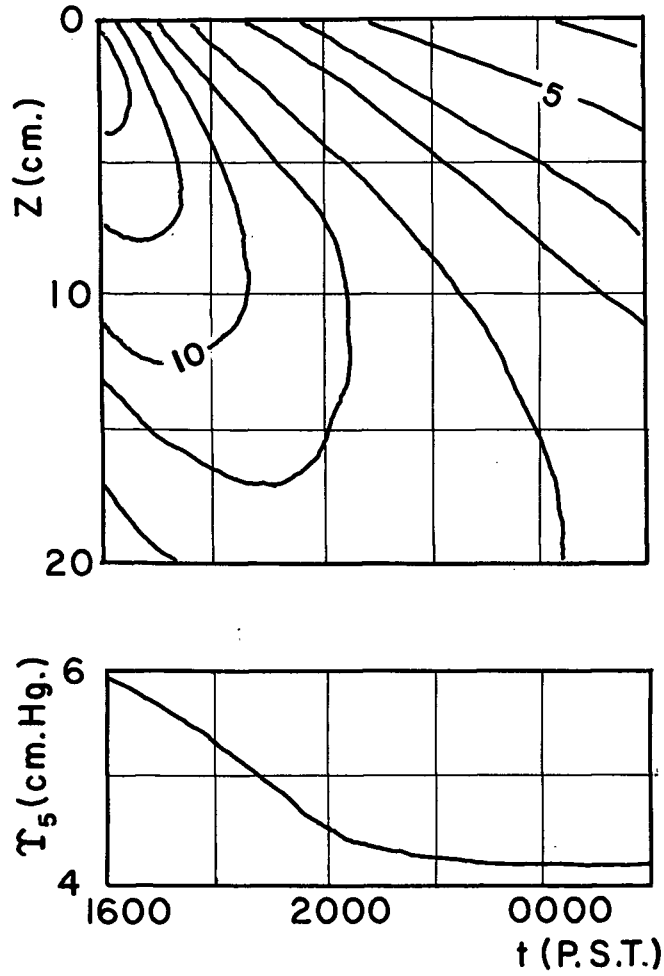

Fig.VI-4. The time dependent variation of soil temperature isotherms (°C.) and water tension, 26-27 Feb. 1968.

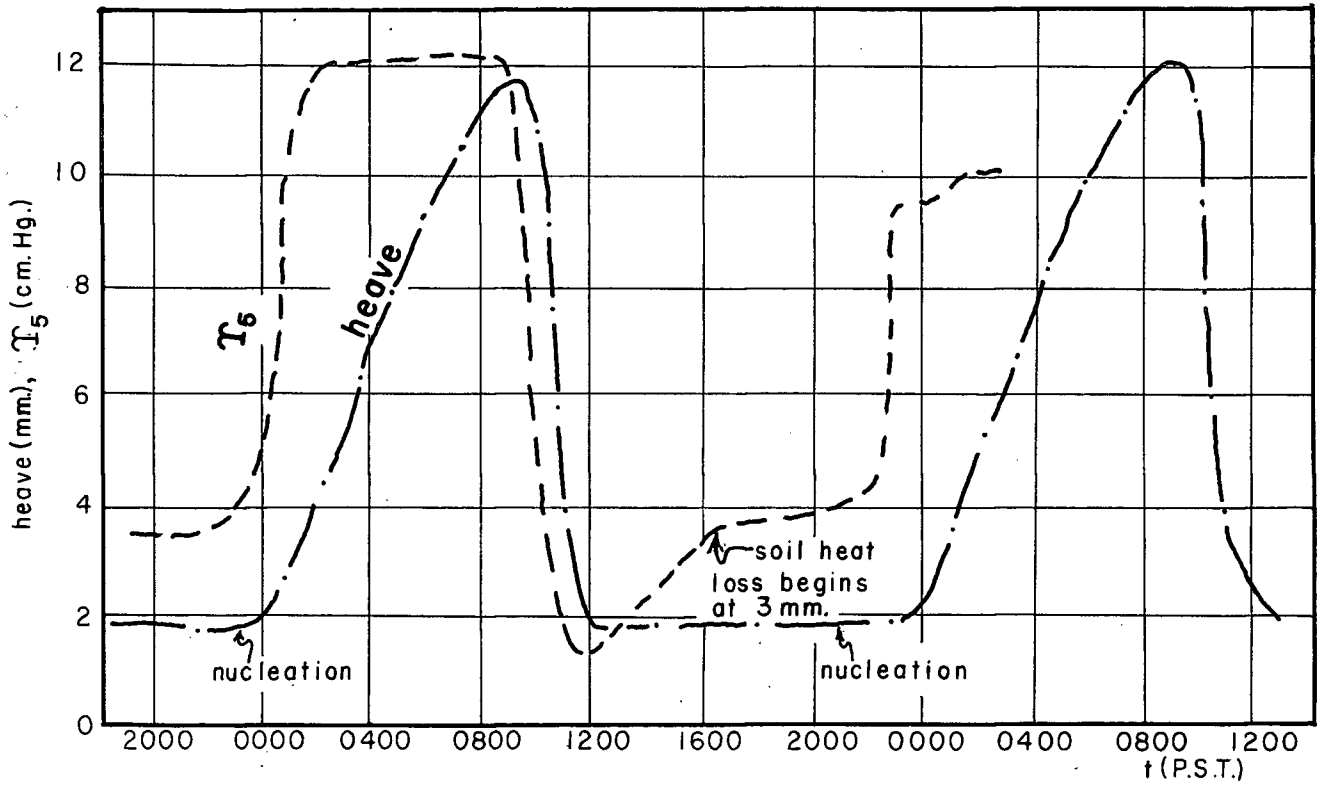

Fig.VI-5. Heave and soil water tension, 6-8 Feb.1968.

the measurement level there must frequently be steep tension gradients produced by evaporation especially during periods when the soil thermal gradient is weak and there is no prolonged pre-soaking flow of soil water toward the surface prior to nucleation. On several occasions when the field surface at the study site was "hard frozen" to a depth of approximately 1 cm. nearly 2 cm. of needle growth was observed at nearby wet roadbank sites. However, if the freezing plane had descended to slightly greater depths (2-5 cm.) lower water tensions would be encountered with increased proximity to the water table and segregation should begin. Evidence of a similar phenomenon was recorded during the extended polycyclic needle ice event of 10-21 December 1967 and noted on both the 13th and 15th of that month. On these occasions a solid mass of concrete frozen soil 5-10 mm. in depth was overlying polycyclic needle ice. The surface was of sufficient strength to support a man on foot. At these observations the needles at the base of polycyclic growth were "hard frozen" to the underlying soil increasing the bearing strength of the overlying materials. This structure resulted from the inability of the soil water flux to the freezing plane to match the fusion rate followed by dessication below the needles and ice intrusion. Note that in a polycyclic growth diurnal ablation is incomplete and as a result the total amount of soil water "tied up" in needle ice is much greater than in diurnal monocyclic growth series in which the same water is essentially cycled through a phase changes.

The Soil Cap Depth

The frozen soil cap which rides atop growing needle ice has now been introduced. It is of interest to estimate the depth of this cap given the following assumptions:

(1) Assume the unfrozen and frozen soils have roughly equivalent thermal conductivities (1×10^{-3} cly. sec.$^{-1}$ cm. $^{o}C.^{-1}$).

(2) Assume a mean surface temperature of $-2^{o}C$. during the formation of the cap, from an examination of field data.

(3) Assume the range of time for cap formation to be 1-4 hours in agreement with the data taken during 5-17 February 1968.

(4) From laboratory testing it is known that ice intrusion should not occur at soil water tensions less than 100 mm.Hg. The desorption curves (see Chapter IV.) indicate that a reasonable computation value for volume fraction of soil water under these conditions would be .25.

(5) The final assumption is that the Stefan solution for soil freezing depth is valid in this case (Jumikis, 1966). This solution specifies that there must be no ice segregation at the freezing plane and that the heat used in cooling the soil in the frozen zone is negligible compared to the heat expended in fusion. The development of the problem is presented by Jumikis (1966) and using the thesis notation is as follows:

Eq.VI-2

$$Z = \sqrt{\frac{2K_f}{r_f X_w} (T_o - T_f)\, t}$$

The cap could be expected to be between 8-17 mm. in depth after 1-4 hours of growth. This figure is in general agreement with the heights of the caps (1-2 cm.) on samples collected during the December 1967 polycyclic event and indicates the general utility of the Stefan solution in the period of ice intrusion between nucleation and segregation. It should also be noted that the cap depth varies inversely with the square root of the soil water content once the ice intrusion tension is exceeded. This

indicates that a study of cap depths, and the climatological conditions which preceded their formation, may be a rewarding object for future investigation.

In summary, the soil cap indicates that water tensions in that zone were above the critical value for ice segregation. The base of the cap is precisely the level at which the vertically descending freezing plane first encountered soil water tensions low enough for segregation to begin, under the condition that soil water content decreases from the water table to the soil surface. Further the evidence, so interpreted, indicates the presence of a strong water tension gradient just below the soil surface and, by inference, evaporation in the near surface soil layers during and prior to needle ice growth. This hypothesis is in agreement with both macro and micro scale studies of the climatological environment of needle ice events. Finally, the temporal variation between nucleation and noticeable heave in the records of the monocyclic event sequence (see Table VI-4.) must represent intervals of normal freezing (ice intrusion) which produce the soil-ice cap and indicate the range of influence exerted by water tension gradients near the soil surface under late winter conditions.

The Equilibrium Temperature Model

A further analysis of the three clear nights during February 1968, when cloud cover conditions and wind speeds were quite similar, was attempted using an equilibrium temperature model which employed estimates of the values of the sensible and latent heat flux using the linear wind model (see Chapter III.). The resulting computation form of this equation is presented as Equation VI-3. (reference Eq.VI-1.).

Eq. VI-3.

$$\sigma(T_{sky} + 273.15)^4 - \sigma(T_o + 273.15)^4 + .0005\ (T_{s2} - T_o)$$
$$+ .022\ (T_{a55} - T_o) \cdot U_{90} + .036\ (e_{a55} - e_o) \cdot U_{90} = 0$$

where: U(meters/sec.), T(^oC.), e(mb.)

It was also possible to treat the surface vapor pressure as a function of surface temperature only, if the assumption is made that the surface water is held at a low tension. This assumption is in agreement with field observations of soil water tension prior to needle ice growth. Thus, if the surface vapor pressure is assumed to be at the saturation vapor pressure at the surface temperature, it is possible to approximate this relationship over the -10 to 10^oC. temperature range by a simple logarithmic expression.

Eq.VI-4.

$$\log_{10} e_o = 9.361 - [2341 / (T_o + 273.15)]$$

The sky hemisphere temperatures used in the calculations were taken using the Stoll-Hardy radiometer in the manner described in the appendix. The expression in Equation VI-4., may be rearranged grouping all the terms which are functions of the surface temperature on the left side.

Eq.VI-4

$$\sigma(T_o + 273.15)^4 + .0005\ T_o + [.022\ T_o + .036\ e_o] \cdot U_{90}$$
$$= \sigma(T_{sky} + 273.15)^4 + .0005\ T_{s2} + [.022\ T_{a55} + .036\ e_{a55}] \cdot U_{90}$$

It is apparent that the left side of the expression is a function of surface temperature and wind speed only, and thus, can be computed for incremented steps of wind speed and surface temperature. Tables of these

left side values (ly./min.) were produced for wind velocities ranging from 0-5 meters per second using 0.1 meter per second steps. Each table for a fixed wind velocity contained left side values for -10 to 10 °C. temperature range. These tables were prepared using the facilities of the University's Computing Centre. It is then possible to estimate the equilibrium surface temperature by substituting the measured values in the right side of the expression and then to consult the table prepared for matching wind velocity conditions. The results for the three nights are as follows: using data taken at 2200 hours.

TABLE VI-6. EQUILIBRIUM SURFACE TEMPERATURES, 2200 P.S.T.

Date	Temperature (°C.)	Outcome
15 February 68	-3.3	needle ice
16 February 68	-3.2	needle ice
26 February 68	2.8	no event

The measured surface temperatures during these same nights are reported in Table VI-7.

TABLE VI-7. MEASURED SURFACE TEMPERATURES, 2200 P.S.T.

Date	Temperature (°C.)	Ground Condition
15 February 68	-1.0	concrete ice
16 February 68	-1.4	concrete ice
26 February 68	4.1	unfrozen

It should be restated that the computation values used in the right side of the expression were in no way derived from the measured surface temperature (e.g. the radiation temperature of the sky was determined by methods independent of surface temperature and net radiation). The equilibrium temperature values appear to be in reasonable agreement with the measured surface temperatures. This can be demonstrated further by examining the time dependent values of equilibrium surface temperature in comparison to Stoll-Hardy radiometer and thermistor probe measurements of the surface temperature on the two nights of 16 and 26 February 1968.

TABLE VI-8. EQUILIBRIUM AND MEASURED SURFACE TEMPERATURES, FEB. 68

Date	Time (P.S.T.)	Equilibrium* Temperature (°C.)	Thermistor Temperature (°C.)	Radiation Temperature (°C.)
16	1800	-1.6	0.4	-2.3
16	2000	-3.5	-0.4	-0.3
16	2200	-3.1	-1.4	-1.0
16	2400	-3.4	-1.1	-1.1
26	1800	6.5	7.5	5.2
26	2000	5.4	5.9	4.4
26	2200	2.8	4.0	5.4

*T-testing showed no significant departure from measured values at the 5% level.

In conclusion, the equilibrium temperature model appears to be a powerful tool for linking frost events to the climatic environment (e.g. during the two event nights reported in Table VI-6. the estimated equilibrium temperature was below the ice nucleation temperature of approxi-

mately -2°C.). However, more data is necessary to evaluate the time dependent behavior of the model.

The Environment of a Late Winter Needle Ice Event

During the night of 16-17 February 1968 manual measurements of soil and air temperatures were carried out at the study site. These data, when combined with the recorded data, gave a detailed picture of the needle ice event. Temperatures at 120 cm., 55 cm., and the surface, as well as the air dew point, wind speed, and cloud cover during the observation period are illustrated in Fig.VI-6. Note that the dew point is normally above the surface temperature indicating that evaporation predominates during this event, which is consistant with the pattern of earlier measurements (see Chapter III.). Only for a short time interval from 0045 to 0330 P.S.T. is there any indication of condensation at the surface. Another interesting item is the stability of the air temperature gradient and the wind velocity during the period of needle growth. Using the equilibrium temperature model, it is possible to use wind velocity, temperature and humidity data, with net radiation records to estimate the temporal variation of the soil surface heat flux, treated as a residual. These data are reported in Table VI-9. where positive values indicate heat flux toward the surface from either above or below.

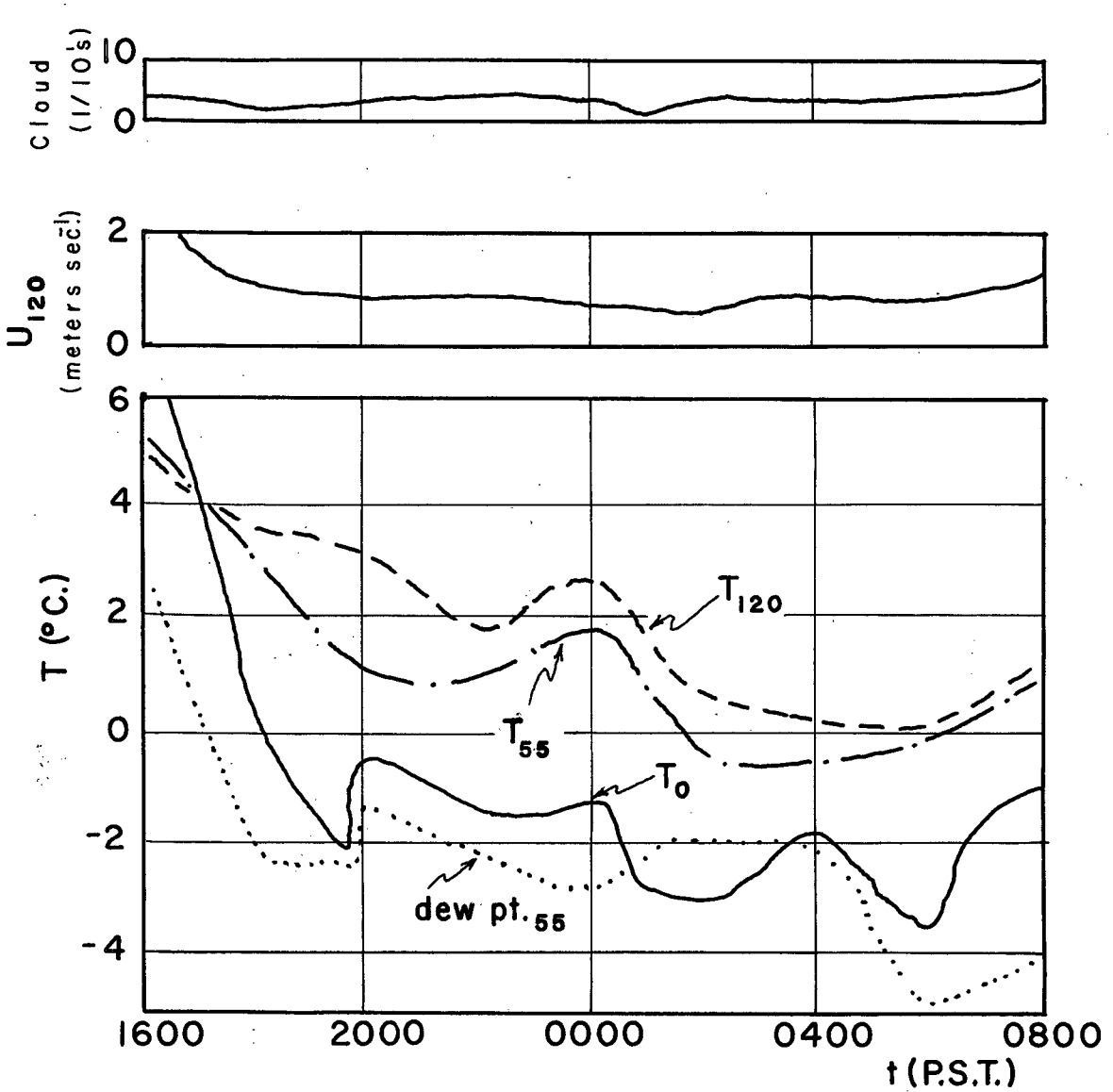

Fig. VI-6. Conditions over bare soil at the study site, February 16-17, 1968. Subscripts refer to distance (cm.) above surface.

TABLE VI-9. ENERGY EXCHANGE COMPONENTS, 16-17 FEBRUARY 1968

Time (P.S.T.)	Net Radiation (mly./min.)	Sensible Heat Flux (mly./min.)	Latent Heat Flux (mly./min.)	Soil Surface Heat Flux (mly./min.)
1600	53	- 53	-131	131
1800	-106	80	- 54	80
2000	- 88	26	- 12	74
2200	- 88	45	- 5	48
0000	- 88	51	- 17	54
0200	- 79	43	12	24
0400	- 62	24	- 2	40
0600	- 72	68	- 22	26
0800	00	36	- 8	28

It is known that these values present only a "rough sketch" of the actual energy transfer environment due to the use of an unventilated net radiometer, the linear wind model, and changing soil thermal properties, etc. However, the estimated pattern of the directions and relative magnitudes of the components of energy transfer is temporally consistent with observations of dew formation and subsurface temperature. The pattern is one of a diminishing rate of heat flow toward the soil surface. The subsurface isotherms for this period are presented in Fig.VI-7. These data illustrate the descent of the diurnal heat pulse as it produces a strong temperature gradient near the surface during the early evening hours and also illustrate the effects of soil water flow toward the surface in the upper 10 cm. of the soil. The weakening of the soil thermal gradient through time, which is consistent with both the predicted heat

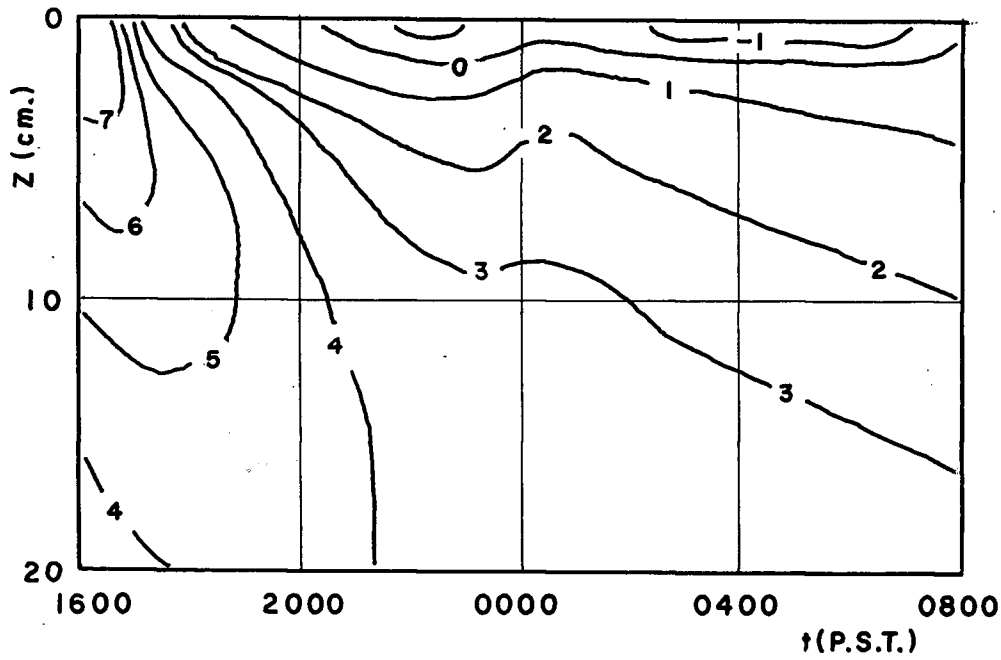

Fig.VI-7. Soil temperature isotherms (°C.), 16-17 Feb.68.

flux and needle ice growth below the former surface, is worthy of further consideration.

The presence of both a thermal and a tension induced water flow to the freezing plane during needle growth was discussed earlier. With the aid of the data now under examination it will be possible to explore the effects of these water flows upon the time derivative of soil temperature at the 5 cm. level. A general equation for the variation of temperature at a point with time, in which the calculation value of thermal diffusivity is assumed to have been measured under conditions where the effects of soil water flow were either minimal or canceled due to periodicity, can be written following Kinosita et. al. (1967):

Eq.VI-6.

$$\partial T/\partial t = \alpha(\partial^2 T/\partial Z^2)+U_w(C_w/C_s)(\partial T/\partial z)$$

The laboratory and mean annual soil diffusivity were examaned and a computation value of $5x10^{-3}$ cm.^{2}/sec. discussed earlier, was used in the computations of the finite difference form of Eq.VI.6. discussed by Kreith (1967). An estimate of the volumetric heat capacity of the soil at a tension of 120 cm.H_2O (see Chapter IV.) of .38 cal.cm.$^{-3}$$^oC.^{-1}$ was used in these calculations.

Eq.VI-7.

$$\Delta T_5/\Delta t=\alpha[(T_o - 2T_5 + T_{10}) / (\Delta Z)^2]$$

In the computations the initial surface temperature was assumed to be 0^{o}C. after nucleation at 1940 P.S.T. The results are presented in Table VI-10.

TABLE VI-10. ESTIMATED TEMPERATURES AT 5 CM., 16-17 FEBRUARY 1968.

Time Interval (P.S.T.)	Temperature Change Predicted (°C.)	Temperature Change Obs.* (°C.)	Prediction Corrections* (°C.)
1600-1800	-1.3	-1.2	0.1
1800-2000	-6.2	-2.1	4.1
2000-2200	-3.3	-1.3	2.0
2200-0000	-1.3	0.2	1.5
0000-0200	-1.9	-0.4	1.5
0200-0400	-1.2	-0.1	1.1
0400-0600	-1.2	-0.3	0.9
0600-0800	-0.7	-0.2	0.5

*T-testing showed significant differences at the .5% level.

The correction which must be applied to the predicted temperatures to obtain the observed values must represent the thermal effects of vertical soil water flow which can be expressed in a finite difference form as follows (ref. Eqs. VI-6., VI-7.):

Eq.VI-8.

$$\Delta T_5/\Delta t = (C_w/C_s)\ [(T_{10}-T_o)/\Delta Z]\ U_w$$

When this equation is solved for flow velocity in units of millimeters per hour the results are compared to soil heave rates as follows:

TABLE VI-11. WATER FLOW AND SOIL HEAVE, 16-17 FEBRUARY 1968.

Time (P.S.T.)	Estimated Water Flow Velocity at 5 cm. (mm./hr.)	Soil Heave Velocity (mm./hr.)
1600-1800	1	0.0
1800-2000	20	0.0
2000-2200	9	0.0
2200-0000	9	0.0
0000-0200	9	1.4
0200-0400	7	1.3
0400-0600	7	1.4
0600-0800	4	1.0

Recognizing noise sources resulting from water flux divergence, soil geometry, evaporation etc., the order of magnitude and time dependent response of water flow and heave velocity appear to be significant although experimentally primitive. If the relative magnitude of the velocity estimates is accepted, and the assumption is made that the water flow conduit area is constant through time, the early evening water flux down the temperature gradient has twice the magnitude of the flow maintained by desiccation at the freezing plane under the relatively high tension gradients during needle ice growth. The flux of warm water to the soil surface may be the mechanism which produces a positive bump just prior to undercooling in soil surface temperature traces (see Figs.II-2., II-12.) and breaks the smooth parabolic noctural temperature decline produced by radiation cooling. It is interesting to

note that this same bump appears in Funk's data (1962, Fig.3.) and may be a universal phenomena associated with the radiation cooling of moist soil surfaces.

These data also indicate the importance of water content conditions in the near surface soil layers. The highest water flow velocity observed during growth was in the realm of 1 cm./hr. It follows that if growth continued for 10 hours water from the 10 cm. layer would be arriving at the freezing plane when growth stopped. It can, therefore, be assumed that the growth environment for needle ice is dependent upon soil water tension and the pore geometry of the upper 10 cm. of the soil and that even within this layer dependence rapidly decreases with depth.

Initial estimates of the energy used in needle growth (fusion rate) were calculated using the nucleartion "snap back" of the upper heat flux disc as an indicator of the rate at which energy was withdrawn for fusion. The diurnal heave recorded (see appendix) during the twelve event sequence, 5-17 February 1968, was also used in the problem.

The soil heat flux snap back (ly./min.) was multiplied by the time (min.) between nucleation and the time of the inflection point in the soil heave record when ablation begins (i.e. maximum soil heave, see Fig.VI-3.). Estimates of the total fusion heat were between 5 and 13 ly. during these twelve nights. These values divided by 72 ly. estimate the height of pure ice ($cm./cm.^2$). It follows that this figure divided by the peak heave height is an estimate of the bulk density of needle ice. The result of these calculations for the twelve night period was an estimated needle ice bulk density of $0.15 \pm .01$ $g.cm.^{-3}$. Two independent checks on this value were furnished by the determination of bulk density by evaporating melt

water from a 225 $cm.^3$ monocyclic needle ice-soil sample collected on 26 November 1967 which yielded a value of 0.17 $g.cm.^{-3}$ and four published measurements (Brink et. al., 1967) which showed a mean bulk density of 0.19 $g.cm.^{-3}$ and a range of 0.27 to 0.12 $g.cm.^{-3}$ for the loosely packed sandy loam at the study site. Here 0.17 $g.cm.^{-3}$ is selected as a computation value for needle ice bulk density at the study site. If bulk density is known or estimated, it is then possible to estimate the mean fusion rate from the heave rate when ice segregation is taking place. The following computation method was used:

Eq.VI-9.

$$F = 72\ X_i\ h\ t^{-1}$$

The fusion rate computed by the method outlined above is plotted with the estimated heat flux through the soil surface (from Table VI-9.) in Figure VI-8. In these computations it was assumed that the freezing rate prior to soil heave was equal to the post heaving rate. This pattern of heat flux variation is in good agreement with soil temperature data on this night (compare Figs. VI-7. and VI-8.). During the early evening there is a rather large heat flux toward the surface which decelerates in a roughly parabolic manner as the evening progresses.

At the time of nucleation, 1940 P.S.T., the temperature gradient in near surface zone is still rather steep (see Fig.VI-7.) and cooling in the near surface zone continues until shortly after the time when soil heaving begins, 2350 P.S.T.. At this time there is a noticeable warming in the upper 10 cm. of the soil due to the flow of water from deeper (warmer) layers toward the freezing plane. From the beginning of ice segregation (needle growth) nearly all of the heat lost at the surface represents

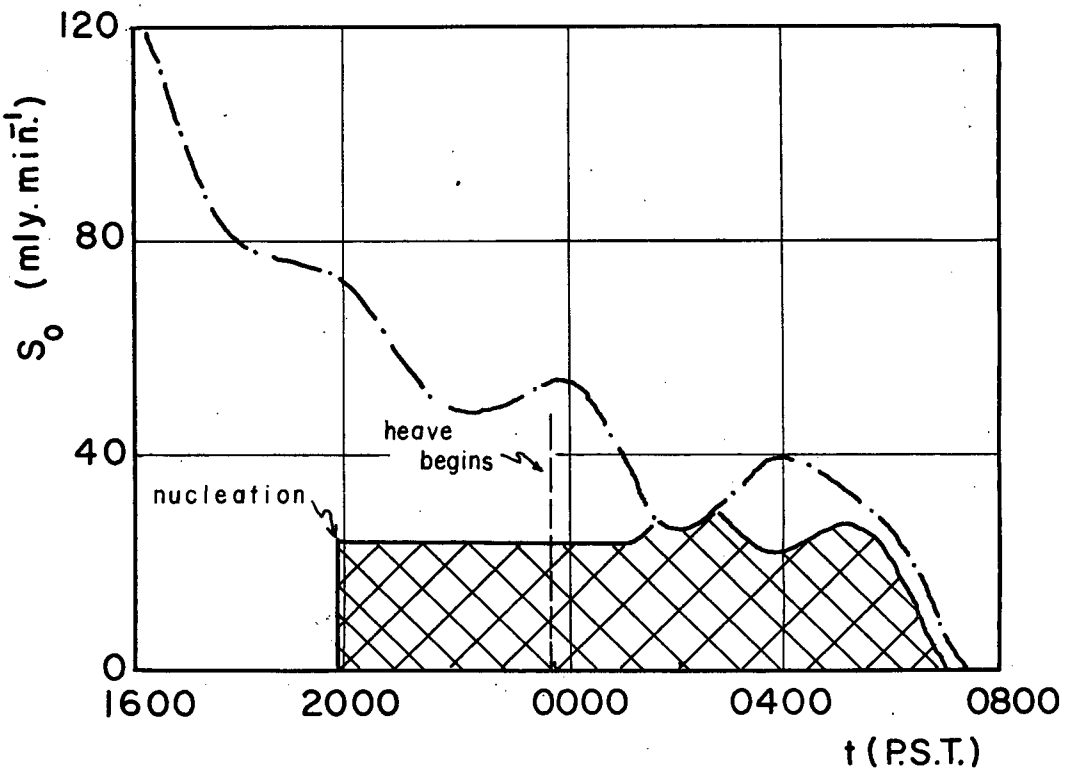

Fig.VI-8. Soil heat flux toward the surface on 16-17 Feb.68.
Note: the crossed area indicates the heat expended in fusion.

fusion at the base of the growing needles. The remaining heat loss maintains a slight decrease in the surface temperature which tends to preserve a quasi-stable heat flux across the growing needles as their height increases.

In summary, the purpose of the observations reported in this chapter is the demonstration of some driving and feedback mechanisms active in the needle ice growth system. The two major mechanisms in the system can be combined into a general equilibrium temperature-ice intrusion model for needle ice growth. These mechanisms and feedback, to and from the surrounding environment, constitute a general model for needle growth in unfrozen heave susceptible soils. This model, which is presented as Figure VI-9., also demonstrates the sequence of events which produce some of the distinctive forms of needle ice morphology (e.g. cyclic deposits and caps).

The model is developed by asking three questions about the needle ice environment. Sustained needle growth, at an instant, is indicated by three sequential yes answers. Steps in the evolution of a needle ice event are completed by escaping from no loops as time passes. However, needle growth may be terminated by a negative (no) condition at any step. The model is valid for one instant at a point on the soil surface (step #1.) and the freezing plane (steps #2.&3.). It should be remembered that after needle growth begins a sudden increase in the heat flux from the freezing plane to the surface can increase soil water tension. Thus, there is an additional feedback loop from the energy exchange environment at the soil surface (equilibrium temperature) to the final question. In its present form the model cannot be used as a predicting device but does accurately specify the state of the needle ice growth environment.

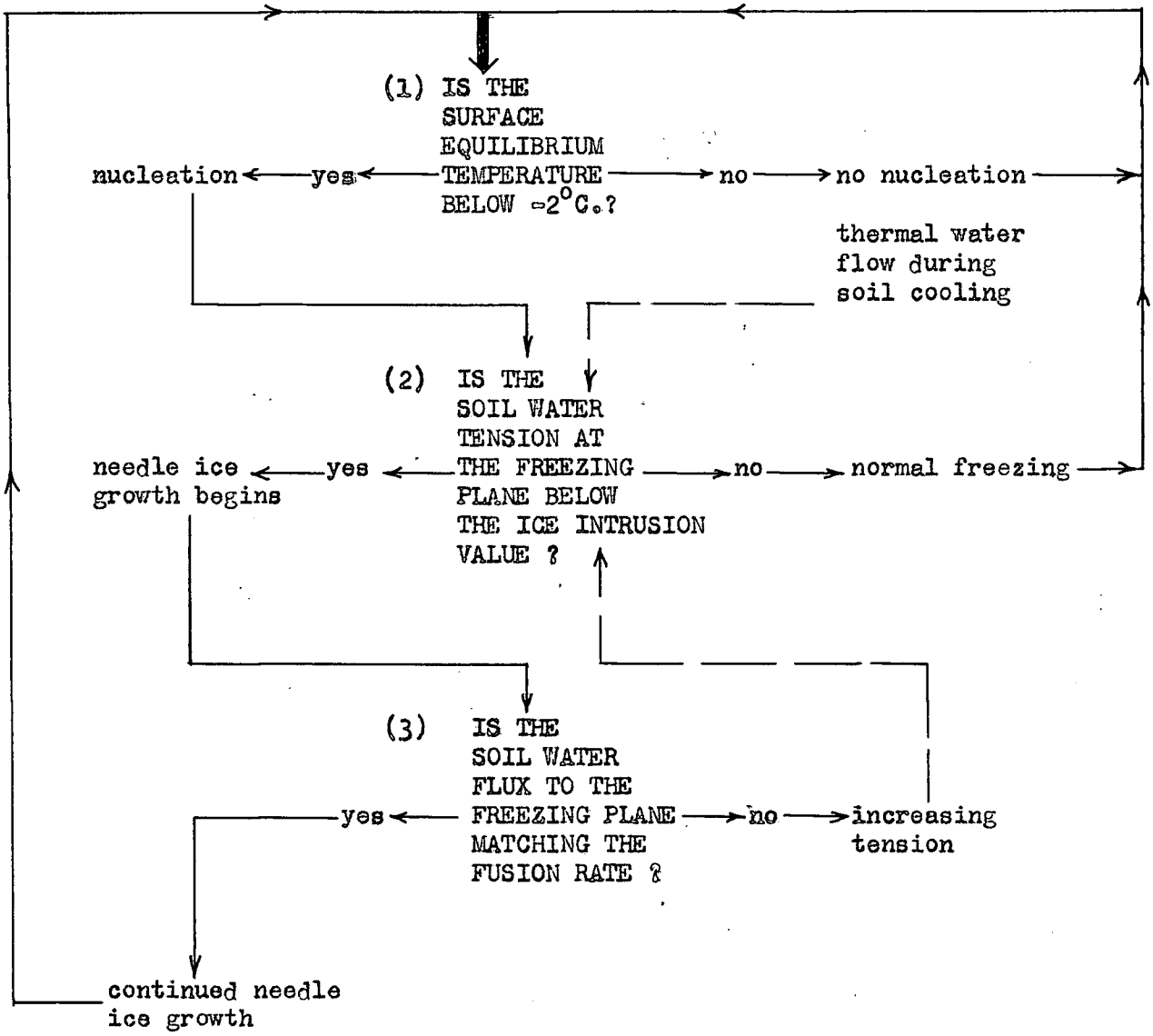

Fig.VI-9. The equilibrium temperature- ice intrusion model.

CHAPTER VII.

CONCLUSION

General Description

The principal contribution of this thesis is the analysis of needle ice growth under natural conditions and the development of an equilibrium temperature-soil water tension model to explain and pin-point combinations of environmental factors which produce needle ice. In addition, the tabulation in statistical form of the unique six year record of needle ice events collected by Mr. Don Pearce at the university's agrometeorological station and analysed by the author is (to the author's knowledge) the longest record of diurnal ground surface conditions to be compiled and analysed in North America. Specifically it is shown above, in the equilibrium temperature model, that when micrometeorological conditions (e.g. sky radiant temperature, wind speed, temperature and humidity gradients, etc.) combine in such a manner as to yield a surface temperature less than $-2^{o}C.$ (approx.) ice nucleation will occur. After nucleation there is a rise in temperature, due to fusion effects, to the freezing temperature of the soil water which is just below $0^{o}C.$ Then, the course of soil freezing is determined by the soil pore size distribution and soil water tension at the freezing plane. If the soil water tension is below a critical value, determined by the pore geometry, at the freezing plane, the descent of the freezing plane will stop and ice segregation will begin. If the soil water tension is above the critical value (estimated between 80-150 mm.Hg. at the study site) the freezing plane will continue to descend and

soil water will be frozen in situ (i.e. normal freezing). Once the freezing plane has been stabilized vertically and segregation (i.e. needle growth) started, the maintenance of the process is controlled by the ability of the unfrozen soil to transport water upwards to the freezing plane commensurate with the fusion rate (i.e. the soil heat flux through the ice needles and soil cap), which is determined primarily by the energy transfer environment at the soil surface. The mechanisms which draw water to the freezing plane are water flow along both a tension and a thermal gradient. The tension gradient is produced by desiccation due to ice formation at the freezing plane. The thermal gradient flux is upwards from the warm unfrozen subsurface zone to the cold freezing plane. If either the fusion rate increases because of cooling conditions above the surface or the soil permeability decreases due to a decreasing supply of soil water and increasing soil water tension, water will not arrive at the freezing plane in sufficient quantity to keep pace with the fusion rate. Therefore, a further desiccation on the unfrozen side of the plane will occur. If this process is continued the soil water tension both at and below the freezing plane will increase and eventually exceed the critical ice intrusion value. When this occurs, the freezing plane will descend, thus, terminating needle ice and leaving the needles frozen to the soil at their bases.

The bump which frequently is observed as the surface temperature briefly increases or stabilizes during clear sky radiation cooling, is probably the result of a thermally driven soil water flow upwards from the warmer soil at depth. This addition of water to the near surface zone lowers the soil water tension and also favors early needle ice growth by minimizing the depth to which normal freezing will occur.

The soil cap which rides atop the needles indicates that during normal needle ice weather conditions the soil water tension in the upper 0-2 centimeters of the soil is above the ice intrusion value. Under these conditions, both statistical studies of past events and energy exchange measurements indicate that evaporation normally occurs at the soil surface just prior to nucleation, the freezing plane then descends through increasingly wetter (i.e. lower tension) soil layers until the depth of the critical ice intrusion tension is reached and segregation begins. In short, the presence of the normally frozen soil cap is further evidence that the major difference between needle ice night energy exchange and conditions on non-event nights is that, in addition to higher values of the net thermal radiation flux from the surface to the sky, evaporation on event nights is the rule. This additional heat sink may speed nucleation but leaves the soil cap as evidence of increased soil water tension due to evaporation prior to nucleation.

The variety of micrometeorological influences exerted by slope and exposure at a site are illustrated by the concurrent examination of polycyclic and monocyclic growth of needle ice. At sites with shaded north facing exposures polycyclic growths are common because needle ice ablation was incomplete during the daylight hours due to the absence of beam radiation as a heat source. It was demonstrated that the net radiation balance was already negative at shaded sites during the early afternoon hours on clear mid winter days. Observations at wetter road-bank sites within 100 meters of the study site demonstrated that on some nights (especially when nucleation occurred after midnight) when the study site soil was normally frozen, the road-banks where the water table intersected the surface were producing up to 2 centimeters of needle ice.

Further, the formation of radiation fog was demonstrated to have a major role in altering the equivalent sky temperature. On nights when radiation fog formed, the increased sky temperature was shown to actually re-warm the surface.

Finally, it is possible to briefly summarize the experience gained by the statistical analysis of the past event record and field observations during both event and non-event nights by listing favorable and unfavorable conditions for needle ice growth at Vancouver with some guideline values. This listing appears as Table VII-1.

TABLE VII-1. FAVORABLE AND UNFAVORABLE CONDITIONS FOR NEEDLE GROWTH

Weather at 1630 P.S.T.:	Favorable	Unfavorable
Radiant Sky Temperature:	less than -20°C.	greater than -15°C.
Wind Speed:	less than 1.2 meters/sec.	greater than 1.5 m./sec.
Cloud Cover:	less than 3/10.	greater than 7/10.
Dew Point:	less than -2°C.	greater than 3°C.
Air Temperature:	less than 4°C.	greater than 6°C.
Soil:		
Texture:	intermediate	pure clay or sand
Water:	near saturation	below field capacity
Structure:	loose at surface	compact at surface
Site:		
Horizon:	unobstructed	obstructed
Vegetation:	none (bare)	trees and turf
Slope and Exposure:	shadowed, north	unshadowed, south

Specific Results and Recommendations

In summary, the thesis results have indicated that there are certain lines which should be followed by future investigators to further advance the understanding of the needle ice problem to a state of increased predictability and process knowledge.

The Equilibrium Temperature Model: As the equilibrium temperature model is entirely physically based, it should be possible to improve upon it and make it an extremely valuable model for both general frost and needle ice damage forecasting. It is suggested that detailed radiation thermometer measurements of sky and soil surface temperatures with parallel determinations of wind velocity at a reference height, soil-air temperature and humidity be used to establish the relationship between the turbulent exchange coefficient and reference level wind velocity to produce a "site model" for regular frost forecasting from late afternoon and early evening data.

Soil Water Tension at Nucleation: The research indicated that the soil-ice cap depth was largely determined by the soil water tension-depth gradient at nucleation and that at some critically high tension needle ice would not form, but rather soil water would be frozen in pore spaces in situ (i.e. normal freezing). Therefore, the production of an extended measurement series yielding information about soil water tension at nucleation and the soil structure after freezing would provide a means of correlating structure with tension. By this means, the realm of critical tension beyond which normal soil freezing occurs could be specified at a site.

Soil Water-Temperature Effects: It was noted in near saturated soils, that water flow down thermal gradients during surface cooling and toward the freezing plane during needle ice growth produced a recognizable effect upon sub-surface temperature patterns through time. A detailed field study of these effects could furnish yet another method of investigating the magnitude of water flux in wet soils. Extreme refinement of this approach might lead to a method of evaporation estimation from below the surface and should furnish increased precision in estimating the probability of ice segregation at a site.

Time Dependence of the Air Intrusion Value: An analysis of the variation of the critical air intrusion value through time as the surface soil structure (i.e. frequency distribution of pore diameters) is modified by changing weather (e.g. swelling and cracking during wet and dry periods) would define the range of surface structural states which affect the outcome (i.e. frozen structure) of frost events. This knowledge would increase the precision of needle ice forecasting as the air intrusion value is known to be an index of soil susceptibility to ice segregation.

Time Dependence of Nocturnal Energy Exchange Components: Net radiation, air temperature and humidity, and wind velocity are traditionally treated as independent variables which in concert determine the heat loss at the soil surface and, thus, the rate of surface temperature declines. These investigations, however, indicate a strong interdependence among these variables which results in a continuous spectrum of environmental states which at some point favor needle ice formation. The feedback mechanisms

which lead to radiation fog and soil water flow down thermal gradients were demonstrated in the thesis.

As the investigation of the needle ice process becomes more sophisticated, it will become necessary to treat these feedback mechanisms in models which predict their time dependent behavior or indicate their probability. In a continued investigation the characteristics of the time dependence and feedback between environmental variables should be explored in greater detail. This approach could provide a means for limiting the input data necessary in the equilibrium temperature model to a degree which will make it tractable as a normal forecasting tool.

Energy Budgets and Process Geomorphology

During the past decade energy budget climatology has become an increasingly prominant research area for workers in many fields. Lacking a specific object of application, these efforts are either channeled into instrument development technology or into a rather demanding sophisticated book-keeping, which often appears to have as its object the verification, ad infinitum, of the energy conservation law.

Examples of applied studies in agriculture are the current investigations of evapotranspiration and frost damage which both employ energy exchange climatology as a major tool. In geomorphic research the application of energy budget methods is less frequent. The author believes that the major value of this thesis lies in the demonstration of the use of energy budget climatology, be it incomplete, to yield process information in geomorphology.

BIBLIOGRAPHY

Alder, H. L. (1962), Roessler, E. B., Introduction to Probability and Statistics; W. H. Freeman, San Francisco.

Baver, L. D. (1965), Soil Physics; John Wiley & Sons, New York.

Belhouse, H. C. (1961), 'An empirical method of forecasting radiation fog and clear sky minimum temperatures at Vancouver, B.C.' Bulletin Amer. Meterological Society, Vol. 42, No. 5, May 1961, pp. 349-358.

Brink, V. C., et. al. (1967), Mackay, J. R., Freyman, S., Pearce, D. G., 'Needle Ice and Seedling establishment in Southwestern British Columbia': Can. Jour. of Plant Science, Vol. 47 (1967), pp. 135-139.

Brunt, D. (1934), Physical and Dynamical Meteorology: Cambridge University Press, 1934.

Byrnes, W. R. (1951), The Effect of Soil Texture on the Occurrence and Type of Freezing: Unpublished Master of Forestry Thesis, Penn. State College.

Cary, J. W. (1965), Water Flux in Moist Soil: Thermal Versus Suction Gradients: Soil Science, Vol. 100, No. 3, pp. 168-175.

Cary, J. W. (1966), Soil Moisture Transport Due to Thermal Gradients: Practical Aspects: Soil Sci. Soc. Amer. Proc., Vol. 30, 1966, pp. 428-433.

Conner, A. J. (1949), The Frost Free Season in British Columbia: Dept. of Transport, Meteorological Division, Toronto, 1949.

Davis, F. K., Jr. (1957), Study of the time-height variations of micrometeorological factors during radiation fog: Thornthwaite Laboratories (then Drexel Inst. of Climatology Centerton, N. J., 1957.

Day, P. R. (1965), Particle fractionation and particle size analysis: In Black (ad.) Methods of Soil Analysis: Agronomy (9), Amer. Soc. Agron. Inc., Madison, Wisc., U.S.A.

De Boer, H. J. (1965), Comparison of Water Vapor, Water Drops of Various Sizes as Means of Preventing Night Frost: Agricultural Meteorology, 2 (1965), pp. 247-258.

Dixon, W. J. (ed.) (1964), BMD - Biomedical Computer Programs: Health Sciences Computer Laboratory, University of California, Los Angeles.

Everett, D. H. (1961), The thermodynamics of frost damage to porous soils: Transactions of the Faraday Society, Vol. 57, No. 9, 1961, pp. 1541-1551.

Freese, F. (1964), Linear Regression Methods for Forest Research: Forest Products Laboratory, U. S. F. S. ? U. S. D. A., Madison, Wisconsin, Dec. 1964, p. 136.

Fujita, M. et. al., (1937), (Research on Frost Needles) Shimobashira no Kenkyn: Jiyugakuew: Series in Arts and Sciences, Tokyo, Japan: Summary in Takagi (1964) Unpublished, will appear as Crrel Report 140, Translation for CRREL - Aztec School of Languages.

Funk, J. P., (1960), Measured Radiative Flux Divergence near the Ground at Night: Quart. Jour. Roy. Met. Soc., 86, pp. 382-389.

Funk, J. P., (1962), Radiative Flux Divergence on Radiation Fog: Quart. Jour. Roy. Met. Soc., 88, pp. 233-249.

Geiger, R. (1965), The Climate Near the Ground: Harvard University Press, Cambridge, Mass., 1965.

Goodell, B. C. (1962), An inexpensive totalizer of solar and thermal radiation: Journal of Geophysical Research, 67 (4): pp. 1383-1387, April 1962.

Goss, J. R. and F. A. Brooks, (1956), Constants for Empirical Expressions for Downcoming Atmospheric radiation under Cloudless Sky: Jour. Met., 13, pp. 482-488.

Gradwell, M. W. (1954), Soil Frost Studies at a High Country Station I: New Zealand Jour. of Sci. and Tech., Sec. B., Vol. 36, No. 3, Nov. 1954.

Gradwell, M. W. (1955), Soil Frost Studies at a High Country Station: New Zealand Jour. of Sci. and Tech., Vol. 37, No. 3, Nov. 1955.

Gradwell, M. W. (1960), Soil Frost Action in Snow - Tussock Grassland: New Zealand Jour. of Sci., Vol. 3, No. 4, Dec. 1960, pp. 580-590.

Gradwell, M. W. (1962), Physical Properties and Instability in South Island High Country Soils, New Zealand Soc. of Soil Sci. Proc., Vol. 5, 1962.

Gradwell, M. W. (1963), Overnight Heat Losses from the Soil in Relation to its Density: New Zealand Jour. of Sci., Vol. 6, No. 4, Dec. 1963, pp. 463-473.

Hamelin, L. and F. A. Cook (1967), Illustrated Glossary of Periglacial Phenomena: Les Presses d'l Universite Laval, Quebec, 237 pp.

Hubley, R. C. (1957), An Analysis of Surface Energy During the Ablation Season on Lemon Creek Glacier, Alaska: Trans. Amer. Geophysical Union, Vol. 38, No. 1, pp. 68-85.

Jumikis, A. R. (1966), Thermal Soil Mechanics: Rutgers University Press, New Brunswick, New Jersey, 1966.

Kendrew, W. G. and D. Kerr (1956), The Climate of British Columbia and the Yukon Territory: The Queen's Printer, Ottawa, 1956.

Kinosita, S. et. al. (1967), Wakahama, G., Horiguchi, K., Formation of Ice Columns on Electrically Heated Ground, Low Temperature Science, Ser. A. 25, p. 184-195.

Konko - Tatutaro (1957), On the foresite for the Appearance of Ice-Columns by Meteorological Conditions of Air and Soil: Sci. Report: Faculty of Agriculture, Fbraki University, No. 5, 1957, pp. 97-108, Source: Takagi, Sayward CRREL.

Kreith, F. (1967), Principles of Heat Transfer, International Textbook Co., Scranton, Penna.

Krumbein, W. C. (1965), Graybill, F. A., An Introduction to Statistical Models in Geology: McGraw-Hill Book Co., pp. 454, New York, 1965.

Lettau, H. (eds.) (1957), Davidson, B., Exploring the Atmosphere's First Mile (Project Great Plains), Vols. I and II, Pergamon Press, London.

Light, P. (1943), Boundary - Layer Problems Involved in Snow Melt: Annals: New York Academy of Science, Vol. 44, 1943, pp. 55-67.

Mackay, J. R. (1966), Personal communication.

Otterman, Jr. (1966), Browner, F. E., Martian Wave of Darkening a Frost Phenomena? Sciénce, Vol. 153, 1 July 1966, pp. 56-60.

Palmer, A. C. (1967), Ice Lensing, Thermal Diffusion and Water Migration in Freezing Soil: Journal of Glaciology, Vol. 6, No. 47, pp. 681-694.

Panofsky, H. A. (1963), Brier, G. W., Some Applications of Statistics to Meteorology: Penn State University Press, p. 224.

Pasquill, F. (1949), Some Estimates of the Amount and Diurnal Variation of Evaporation from a Clayland Pasture in Fair Spring Weather: Journal Royal Meteorological Society, Vol. 75, 1949, pp. 249-256.

Penner, E. (1960), The Importance of Freezing Rate in Frost Action in Soils: Proc. of the Amer. Soc. for Testing Materials, Vol. 60, 1960, pp. 1151-1165. (also: Res. Paper No. 126, Div. Bldg. Research, Ottawa, July 1961/NRC. 6152.)

Penner, E. (1963), Frost Heaving in Soils; Proc: Permafrost International Conference, Nov. 1963, pp. 197-202. (also: Res. Paper No. 295, Div. of Building Research, Ottawa, 1966, NRC 9271).

Portman, D. J. (1958), Conductivity and Length Relationships in Heat-Flow Transducer Performance: Transactions, Amer. Geophysical Union, Vol. 39, No. 6, Dec. 1958.

Reifsnyder, W. E., and H. W. Lull (1965), Radiant Energy in Relation to Forests: Tech. Bull. No. 1344, U. S. D.A., Forest Service, Dec. 1965, U. S. Gov't. Printing Office, Washington, D. C.

Richards, L. A. (1948), Porous Plate Apparatus for Measuring Moisture Retention and Transmission by Soil: Soil Science, 66: 105-110.

Richards, L. A. (1941), A Pressure-Membrane Extraction Apparatus for Soil Solution: Soil Science, 51: pp. 377-386.

Sayward, J. M. (1966), Miniature Tests: Re: Frost Heaving and Needle Ice: Simple Means of Comparing Soils and Testing Additives: U.S. Army, Cold Regions Research and Engineering Laboratory (CRREL), Hanover, N. H., U. S.A., Internal. Report 19.

Scott, R. F. (1964), Heat Exchange at the Ground Surface: II-A1 Cold Regions Sci. & Eng.; Cold Regions Research and Engineering Laboratory, Hanover, N. H., U. S. A.

Sellers, W. (1965), Physical Climatology: The University of Chicago Press, Chicago and London, 1965, p. 272.

Siegel, S. (1956), Non-Parametric Statistics for the Behavioral Sciences: McGraw Hill, New York.

Soons, J. M. (1967), In Arctic and Alpine Environments (H. E. Wright, Jr., and W. H. Osburn, eds.), pp. 217-227. Indiana University Press.

Steinemann, S. (1953), Mushfrost, an anomalous growth form of the ice crystal: Z. Agnew, Math. U. Phys. (Zamp) 4: 500-506, 1953. Tech. Translation: National Research Council of Canada. TT-528, Ottawa, 1955.

Sutton, O. G. (1953), Micrometeorology, McGraw-Hill Book Co., Inc., 1953, London, Toronto and New York.

Sverdrup, H. U. (1936), The Eddy Conductivity of the Air Over a Smooth Snow Field: Geogysiske Publikasjoner, 11 (7).

Swan, J. B., C. A. Pederer and C. B. Tanner (1961), Economical Net Radiometer Performance, Construction and Theory: Soils Bul. 4, University of Wisconsin, Madison.

Takagi, S. (1965), Principles of Frost Heaving (CRREL) Research Report No. 140. Cold Regions Research and Engineering Laboratory, U. S. Armys Hanover, N. H., U. S. A.

Tanuma, K. (1967), The Relation Between the Heave Amount and Water Content During Unidirectional Freezing I.: Low Temperature Science, Ser. A, 25, pp. 179-184.

Terzaghi, K. (1952), Permafrost: J. Boston Soc. Civil Eng., Vol. 39, No. 1, 1952, pp. 319-368.

Thornthwaite, C. W. and Mather, J. (1957), Instructions and Tables for the Computation of Potential Evapotranspiration and Water Balance: C. W. Thornthwaite Associates, Laboratory of Climatology, Publications in Climatology, Vol. X, No. 3, 1957, Centerton, New Jersey, 1957.

Troll, C. (1944), "Strukturboden, solifluktion und frost klimate der Erde," Geol. Rundschau 34: 1944, 545-694 (Translation SIPRE, 1958, 121 pp.)

Van Wijk, W. R. (1966) (editor): Physics of Plant Environment: North-Holland Publishing Co., Amsterdam, 1966.

Van Wijk, W. R. (1966) and Derksen, W. J., Thermal Properties of a Soil Near the Surface: Agr. Meteorology, 3, (1966), pp. 333-342.

Veitch, L. G. (1960), Further work on Minimum Temperature Prediction in the Fruit-Growing Areas of South Australia: Australian Meteorological Magazine, No. 28, March 1960, pp. 13-29.

Whitten, H. T. (1964), Process-Response Models in Geology: Geological Soc. of Amer. Bull. V, 75, pp. 455-464, May 1964.

Williams, P. J. (1963), Suction and Its Effects in Unfrozen Water of Frozen Soils: Proc.: Permafrost International Conference, Nov. 1963, pp. 225-229, (also: Research Paper No. 297, Div. of Building Research/ Ottawa 1966 / NRC 9273.

Williams, P. J. (1966a), Pore Pressures at a Penetrating Frost Line and Their Prediction: Geotechnique, Vol. XVI, No. 3, Sept. 1966, pp. 187-208. (also Research Paper No. 299, Div. of Building Research, Ottawa/NRC 9305, Nov. 1966).

Williams, P. J. (1966b), Movement of Air Through Water in Partly Saturated Soils: Nature, Vol. 212, No. 5069, Dec. 1966. (also: Res. Paper No. 316, Div. Bldg. Research, Ottawa, May 1967/NRC 9574.

Williams, P. J. (1967), Replacement of Water by Air in Soil Pores: The Engineer, Vol. 223, No. 5796, 24 Feb. 1967. (also, Research Paper No. 311 of the Div. of Bldg. Research, Ottawa, April 1967, NRC 9533.

Williams, P. J. (1968), Properties and Behaviour of Freezing Soils: Norges Geotekniske Institutt, Publications NR72, 119 pp.

Yong, R. N. (1966), Warkentin, B. P., Introduction to Soil Behavior: Macmillan Series in Civil Engineering.

APPENDIX: MEASUREMENT

Temperature Measurement:

I. Thermistors

1. Probes: Y. S. I. "400" Series bead thermistors. Yellow Springs Instrument Co., Yellow Springs, Ohio.

2. Bridge: Wheatstone bridges with fixed arms of 7.5K ohms and variable arms (0-10K ohms and 0-100K ohms) were constructed. These bridges are calibrated by fixing the dial potentiometer and a decade resistance at 7355 ohms ($0^{o}C.$) and then adjusting a small potentiometer in the opposite arm of the circuit until no out of balance current was registered by the galvanometer. A 1K ohm resistor is placed in series with the bridge power source (a 1.5V. Dry Cell), when the units are used for continuous recording, to lessen the self heating of the probes. Manual out of balance measurements are made with a Simpson 25-0-25 μ A meter.

3. Recording: The bridge out of balance currents are placed across the galvanometer of Rustrak recorders (25-0-25 μ A and 0-50 μ A) and the deflection is calibrated by using a resistance decade in the place of the probe and the manufacturers resistance-temperature figures. The probe interchangeability is listed as $\pm$ $.2^{o}C.$ within the temperature range of concern.

4. Accuracy: Manual readings of the thermistor probes should be accurate to ± .05°C. when the probes have been ice bathed and careful attention is given to self heating effects of the probes.

Recordings are assumed to have an absolute accuracy in the realm of ± .3°C. over the calibrated range (15 to -15°C.). The rates of temperature change, however, have a much higher precision over limited temperature ranges.

5. Switching: It was possible to record the temperature at several levels in the soil when a small relaxation oscillator was used to trigger a twelve point stepping switch to which one side of the probe leads was connected.

II. Thermocouples

1. Probes: Copper-Constantan thermocouples.

2. Reading: The e.m.f. resulting from the temperature difference between a thermocouple in the soil and one in an ice water bath was read on a Leeds and Northrup Potentiometer.

3. Accuracy: The absolute accuracy of these readings is believed to be in the realm of ± .4°C., whereas the relative accuracy is assumed to be somewhat higher (± .2°C.).

4. Switching: Soil thermocouples were switched using an eleven position rotary switch (Cu). The copper junctions were soldered and the common constantan junction was wound. The entire switching unit was encased in a fiberglass jacket in an attempt to limit the magnitude of thermal gradients in the switch.

Radiation Measurement:

I. Net Radiation

A Thornthwaite Net Radiometer (unventilated) was used to monitor net radiation at approximately 1/2 meter above the soil surface to reduce problems of flux divergence (see Funk (1960, 1962)).

The signal from the radiometer was recorded on a Thornthwaite Net Radiation Recorder and later on a Thornthwaite Microvolt Recorder, which allowed use of nearly the full scale in the 300 μV. range.

II. Directional Radiation

A Stoll-Hardy Radiometer (Williamson Development Co.) with a red filter over the sensing cone was used to detect differences in thermal radiation levels. The "x" scale was calibrated to cover energy differences of 0-0.3 ly. min.$^{-1}$. It was hoped that this type of calibration would eliminate the errors encountered when the instrument is not used at its calibration temperature. The mean sky hemisphere temperature was computed using the nine directional shots with the sensing head, which has a 20^{o} field of view. The mean sky hemisphere energy difference was computed by multiplying the zenith reading, the mean of the four 45^{o} inclined readings taken at the four points of the compass, and the mean of four readings inclined approximately 10^{o} from the horizontal at the four points of the compass by geometric weighting factors. These factors were proportional to the portion of the total sky hemisphere which the readings represent. The boundaries of these zones measured from the horizontal were inclined horizontal (0-27.5^{o}), 45^{o} inclined (27.5^{o} -67.5^{o}) and zenith

(67.5^{o} -90^{o}). The appropriate weight factors were .46, .46 and .08. The sky hemisphere radiation temperature was then obtained by subtracting the mean energy difference from the black body function of the calibration cube temperature and consulting black body tables to evaluate the sky hemisphere radiant temperature. The same procedure was used in evaluating the radiant temperature of the soil surface. Net radiation values measured during the 15-17 Feb. 1968 series were on the average .02 ly. $min.^{-1}$, lower than the same item recorded by the Thornthwaite system. This discrepancy could arise through calibration drift, zero drift and sampling errors in either or both of the instrument systems. No attempt was made to further evaluate the source of this discrepancy which is obscured by the additional problem of comparing continuous with spot time measurements.

Accuracy: It is difficult to determine the absolute accuracy of these measurements. The information above indicates that it would be unwise to attach an absolute accuracy of greater than 20% to the range of nocturnal radiation flux values. However, due to the design of the Thornthwaite radiometer the zero value is quite reliable, if frequent checks are made of the zero calibration point on the recorder.

Soil Heat Flux Measurement:

Soil Heat Flux Discs and Recorders

Thornthwaite soil heat flux discs were used with the same manufacturer's soil heat flux recorder and microvolt recorders. The use of the latter in the study allowed the utilization of nearly the entire chart width when the 1000 μV. range was employed and provided a sensitive indicator of the sensor output time variations. This instrument system

has been the subject of much discussion, as its design and calibration contain several restrictive assumptions (Portman, D. et. al. in Lettau and Davidson (1957) p. 17-79).

A test was carried out in the Soil Physics Laboratory at the University of British Columbia to determine the effect of the heat flux disc on soil thermal conditions. A bead thermistor was placed at the same level (2 cm.) in the soil as a similar bead underlying a heat flux disc. The moisture tension in the soil sample from the needle ice study site was held constant by a 60 cm. hanging column of water and a heat pulse was delivered to the sample by means of two infrared lamps. The temperature rise and decline was always in agreement to $\pm$ .3°C. which is the realm of accuracy of the recording system. While this does not eliminate the problem, this result indicates that measured heat flux values may be expected to be in the correct realm.

During the 1967-68 measurement series, a disc was placed quite close to the soil surface (approx. 3 mm). As the heat flux value normally increases rapidly when the surface is approached from below, this sensor arrangement should have produced values near to the magnitude of the surface flux. At this stage it is impossible to evaluate the accuracy or even the precision of these measurements except within the rather narrow confines of design assumptions due to the perpetual variation of moisture and structural conditions in the soil near the surface (in fact the object under investigation). However, the measurements are of great value in detecting the times of ice nucleation, heat flux directional change, and sudden changes in heat flux rates that correlate with other observed phenomena.

Soil Heave Measurement:

I. The Freyman Meter (built by S. Freyman, former student in the Dept. of Plant Sci./U.B.C.)

This instrument can best be described as a mechanical thermograph-type drum on which the pen arm is attached vertically to the soil surface by a drinking straw.

The instrument has several deficiencies. (1) It shields the soil beneath it from a considerable portion of the coldest area of the night sky near zenith. (2) the heave-trace ratio is non-linear and difficult to evaluate due to leaning of the straw once heaving has begun. (3) There is sufficient drag on the pen to prevent the meltout of needle ice from being recorded. While these limitations do exist the unit does give a considerable amount of information at an extremely low cost. The limitations of this unit led to the construction of the unit described below.

II. The Schmitt Heave Meter (named for W. Schmitt, Civil Engineering Shop, U.B.C., who helped design and then built the instrument).

Essentially a resistance slide wire device with which the soil surface is directly linked mechanically to a wiper: The wiper slides along the resistance wire which was taken from a discarded variable potentiometer and straightened. Soil heave is directly translated to a resistance variation which is converted in a temperature measurement bridge to an out-of-balance current which is then recorded. The unit, as constructed, converts 5 cm. of vertical displacement to a full scale deflection of a 0-50μA Rustrak recorder and, thus, makes surface elevation variations

as small as 1 mm. easily detectable. The unit has almost no drag so the meltout is also recorded. A photo of the unit is included in Fig. A-1., where (1) is the wiper, (2) connection to the resistance wire, (3) linkage of wiper to heave arm, (4) top of heave arm, (5) foot which rides on soil surface.

Measurement of Water Tension:

The De Vries Tensiometer (as built by Dr. J. De Vries/ Dept. of Soil Sci./U.B.C.)

This instrument is essentially a mercury manometer which is in hydraulic contact with the soil water. In all respects, except the mode of this contact, it is similar to other units for water tension measurement. In this unit the contact between the soil water and the water in the tensiometer system, which is de-aired in the laboratory before the field installation, is maintained through a paste of 29 μ spherical glass beads placed in a plastic holder and connected to the manometer through a sheet of fine porus nylon (millipore membrane). The system has a low impedance and is useable to a tension of approximately 150 mm.Hg. which is the air intrusion value of the composite tensiometer membrane. The unit is shown in Figure A-2. where (1) is the manometer stem, (2) is the mercury reservoir, (3) is the point where the sensing head is buried in the soil centered on a depth of 5 cm. The glass bead holder is mounted vertically and has contact dimensions of approximately 2x2 cm. and, thus, gives a mean tension reading for the 3-5 cm. depth zone in the soil.

This basic unit can be made into a recording device by using the mercury as a sliding contact on a resistance wire in the same manner

Fig.A-1. The electrical heave meter.

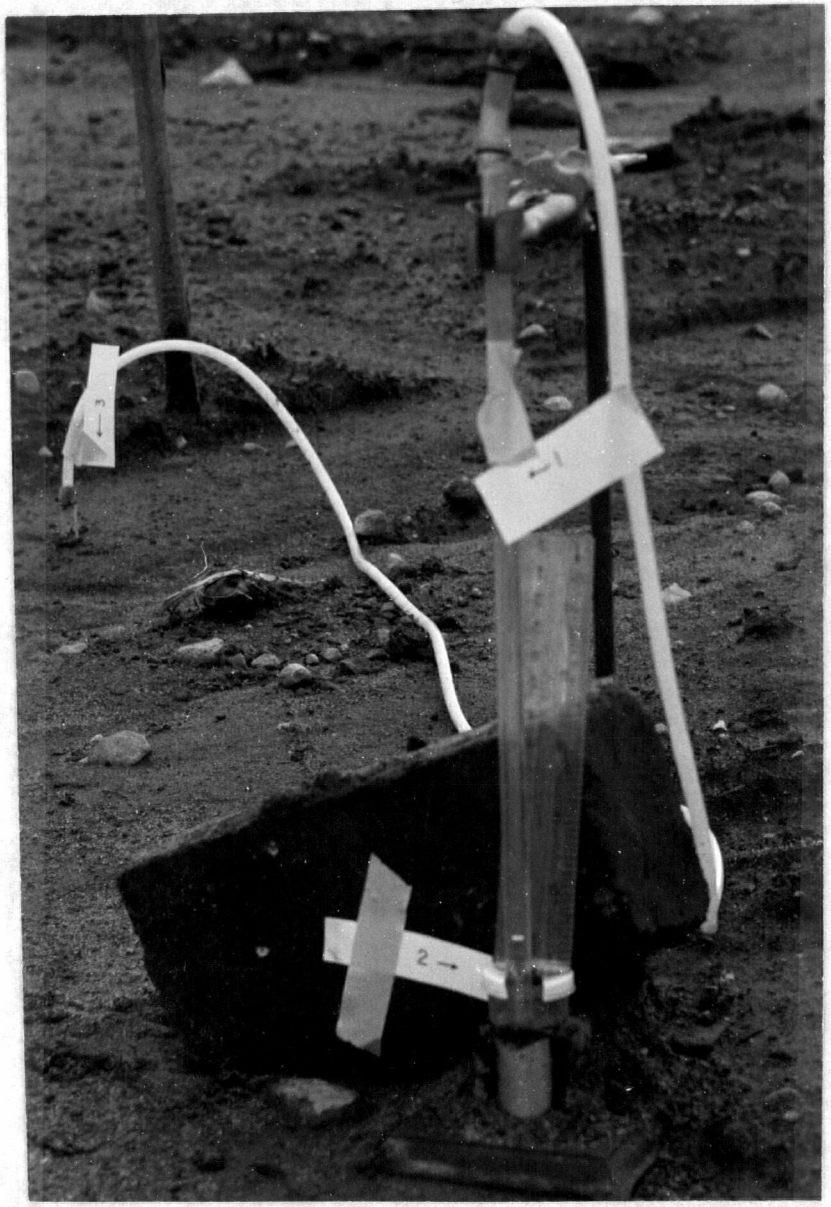

Fig.A-2. The soil water tensiometer.

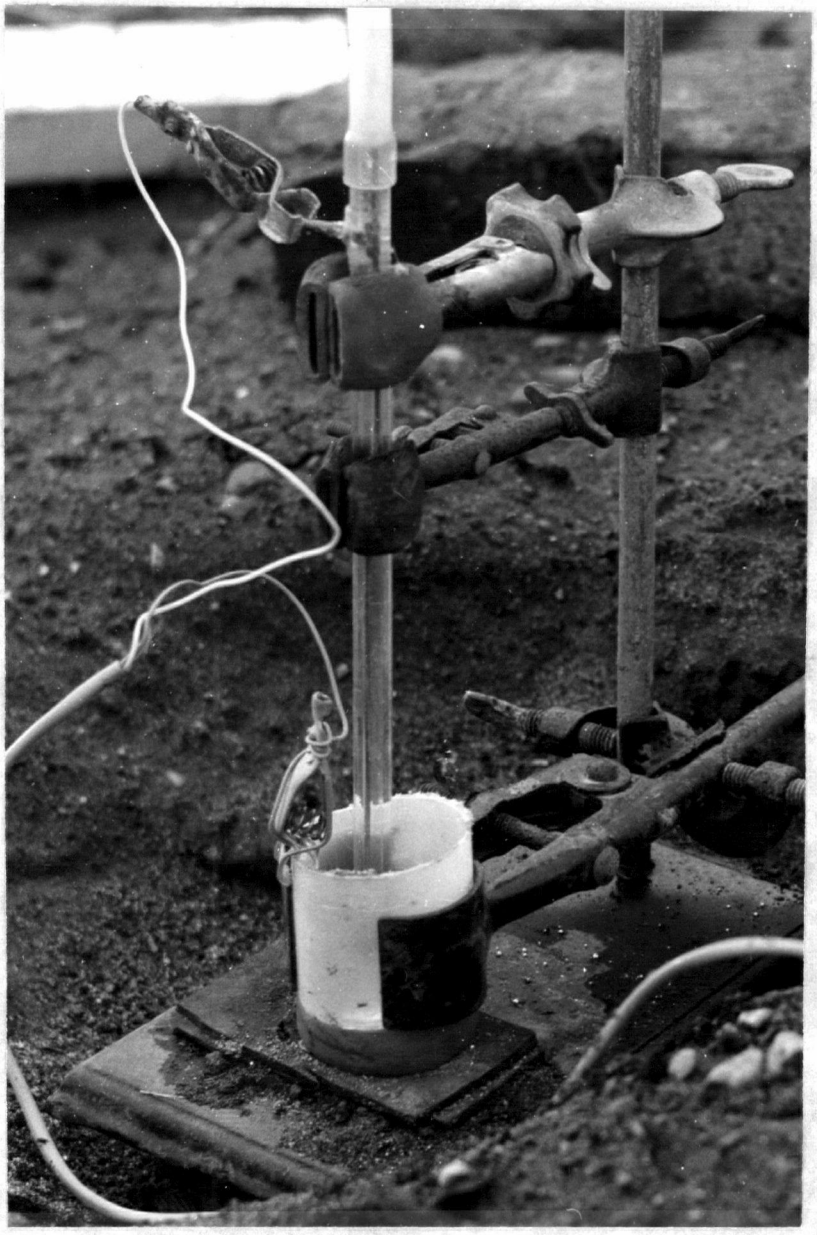

Fig.A-3. The slide wire addition to the tensiometer.

as the wiper on the Schmitt heave meter. This arrangement is illustrated in Fig. A-3. which shows the slide wire mounted inside the manometer stem and the two electrical clips which bring the bridge voltage into contact with both the mercury reservoir (lower clip) and the resistance slide wire by way of a bolt in the perspex manometer stem (upper clip). This variable resistance is made an arm of a wheatstone bridge, and as such, the out-of-balance current becomes a non-linear analog of soil water tension. The unit is calibrated by placing the sensing head in a water bath and lifting the mercury column to varied heights with corresponding notations of deflections of the Rustrak recorder.

The major difficulty with the unit is that at sub-freezing temperatures the water in the system freezes disturbing the trace and in fact may destroy the slide wire by frost action on the resistance wire windings. This happened in the installation during the latter part of February 1968. This deficiency could be removed in the future by burying the entire system in the soil or placing the above surface portion of the unit in an enclosure heated to just above the ice point.

Another problem was the gradual diffusion of air out of the soil water which moved into the system as a result of several wetting and drying cycles. This problem was eliminated by adding an air trap to the system. This modification should permit the use of the measurement system in remote sites where laboratory de-aired water is not available.

Humidity and Dew Point Measurements:

Air dew points were calculated from the wet bulb depression of aspirated wet and dry bulb mercury thermometers.